

Supported Ionic Liquid Phase (SILP) Catalysis for the Production of Acetic acid by Methanol Carbonylation

Hanning, Christopher William; Fehrmann, Rasmus; Riisager, Anders

Publication date:
2012

Document Version
Publisher's PDF, also known as Version of record

[Link back to DTU Orbit](#)

Citation (APA):

Hanning, C. W., Fehrmann, R., & Riisager, A. (2012). Supported Ionic Liquid Phase (SILP) Catalysis for the Production of Acetic acid by Methanol Carbonylation. Kgs.Lyngby: DTU Chemistry.

DTU Library

Technical Information Center of Denmark

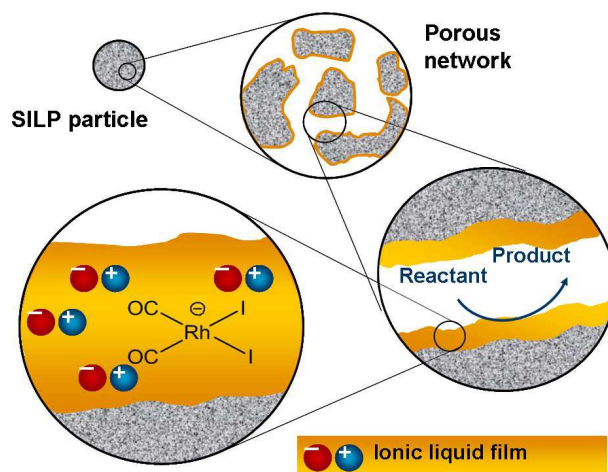
General rights

Copyright and moral rights for the publications made accessible in the public portal are retained by the authors and/or other copyright owners and it is a condition of accessing publications that users recognise and abide by the legal requirements associated with these rights.

- Users may download and print one copy of any publication from the public portal for the purpose of private study or research.
- You may not further distribute the material or use it for any profit-making activity or commercial gain
- You may freely distribute the URL identifying the publication in the public portal

If you believe that this document breaches copyright please contact us providing details, and we will remove access to the work immediately and investigate your claim.

Supported Ionic Liquid Phase (SILP) Catalysis for the Production of Acetic acid by Methanol Carbonylation



Christopher W. Hanning

Ph.D. Thesis

Technical University of Denmark

Centre for Catalysis and Sustainable Chemistry

Department of Chemistry

July 2012

Contents

1	Introduction	1
1.1	Acetic Acid	1
1.2	Production Methods for Acetic Acid	3
1.2.1	Biologically Derived Acetic Acid	3
1.2.2	Catalysed Acetic Acid Production	5
1.2.3	Carbonylation Reactions	8
1.3	Ionic Liquids	16
1.3.1	Supported Ionic Liquids	17
1.4	Commercial Acetic Acid Production/ Reactor Styles	20
2	Experimental Set-up	23
2.1	Introduction	23
2.2	Design and Construction	23
2.2.1	Pressure Testing	27
2.3	Corrosion	29
2.4	Flow Controllers	30
2.5	Back Pressure Regulating Valve	33
2.6	Heating	36
2.6.1	Ovens	36
2.6.2	Heating Control	37
2.7	Addition of MeI co-catalyst	41
2.7.1	Initial Cooling	41
2.7.2	Further MeI cooling	42
2.8	Major Alterations	43
2.8.1	Reactor Pressurisation	43
2.8.2	Removal of “Dead Space” after P Valve	44
2.9	Achieving a Suitable Back Pressure of the Pressure Regulating Valve	45
2.10	Product Isolation	45
2.11	Maintenance/“down-time”	46
2.12	Blocking of the GC valve inlet	48

2.13	Corrosion resistant materials	48
2.14	Final Incarnation of the Test-Rig	49
2.15	Wacker Chemie AG Pilot Plant	49
3	Analytic system	51
3.1	GC Configuration	51
3.1.1	H ₂ Detector TCD	52
3.1.2	FID Detector	53
3.1.3	Organics TCD Detector	53
3.2	Oven Ramp	55
3.3	Internal Standards	55
3.3.1	Methane as an Internal Standard	57
3.4	Calibration of components	57
4	Experimental results	58
4.1	Replication of Previous Results	58
4.2	Iodide dimer	60
4.3	Chloride precursor	64
4.4	Rhodium Sources	66
4.5	Cation variation	67
4.6	Anion variation	68
4.7	Iridium Catalysts	69
4.8	Products	70
4.9	Water addition	73
4.10	Gas solubility in IL	74
4.11	Intellectual Property	75
5	Catalysis analytical tools	76
5.1	TGA- Thermal gravimetric analysis.	76
5.1.1	Ionic Liquids/Molten Salts	76
5.1.2	Rh Source	77
5.1.3	SILP Catalysts	79
5.1.4	Slow Heating	79
5.2	DSC - Differential Scanning Calorimetry	82
5.3	BET- Brunauer-Emmett-Teller isotherm	82
5.4	FT-IR - Fourier Transform Infra Red Spectroscopy	83
6	Experimental	87
6.1	Reactors	87
6.2	Flow Controllers	88
6.3	Heating	88

6.4	Pressure	89
6.5	MeI Addition	90
6.6	Product Isolation	91
6.7	Methanol Tank	91
6.8	After a Reaction	92
6.9	GC Sequence	93
7	Conclusion	95
A	Experimental Synthesis	112
A.1	The basic procedure	112
A.2	Variations	113
A.3	Ionic Liquids	114
B	Components Listing	116
C	Evolution of the test rig over the course of the Project	119
D	Examples of Corrosion Experienced	125
E	Comparison of Various Steel Types	130
F	Exposure of a MeOH wetted, Bmim I/[Rh(CO)₂I₂]⁻ SILP to air over a period of 1 hour	131
G	Fresh and Used Examples of SILP Catalysts	135

List of Figures

1.1	Acetic Acid End Uses	2
1.2	Oxidation of Acetaldehyde	7
1.3	Co Catalytic Cycle	9
1.4	Ni Catalytic Cycle	10
1.5	Monsanto Catalytic Cycle	12
1.6	Cativa Catalytic Cycle	13
1.7	Standard Carbonylation Reactor	13
1.8	Complete Cativa Catalytic Cycle	15
1.9	Different types of SILP-style Catalysts	18
1.10	Process Diagram of a Methanol Carbonylation Plant	21
2.1	The Original Incarnation of the Test Rig	24
2.2	Initial Test Rig Design	25
2.3	Examples of corrosion	26
2.4	Reactor Cross Section and Bed	27
2.5	Reactor with Connections Labelled	28
2.6	Reactor Connection Fittings	29
2.7	Comparing Components Before and After the Reactor	30
2.8	CEM and MFCs	31
2.9	Flow Controllers and CEM	32
2.10	Control Box for Flow Controllers and CEM	32
2.11	Pressure Regulating Valve	33
2.12	Pressure Valve Actuator	33
2.13	Pressure Transducer	34
2.14	Corrosion around the Valve Pin	34
2.15	Comparison of the K_{vs} values	35
2.16	Surface of the Pin Seat Showing Black/Brown Condensate	35
2.17	Broken Valve Pin	35
2.18	Heating Cable used for Pressure Valve	36
2.19	Adaptor used to connect the Pressure Valve to the Swagelok Components in the rest of the System	36
2.20	Original Control Box for Oven Control	37

2.21	Labview Screen for Oven Control	38
2.22	CN616 controller	38
2.23	Simplified Wiring Diagram of CN616 controller	39
2.24	Broken Heating Tapes	40
2.25	Example of a Heating Cable	40
2.26	Haake EK20 for Cooling MeI	42
2.27	Julabo F12 used to Pump Cooling Water Around the System .	42
2.28	The Dead Space Previously Leading to the Reactor	44
2.29	System After the Removal of The Dead Space	44
2.30	Condenser Containing Condensate from System	46
2.31	Condenser from Above, Showing Inlet and Outlet to Condenser	46
2.32	Blockage of the GC Valve	48
2.33	HPLC reading just after automatic shutdown	49
2.34	The Final and Current Incarnation of the Test-Rig	50
3.1	Configuration of the GC collums and valves	52
3.2	Temperature Profile of GC Method	56
4.1	TOF for the initial Experiment	60
4.2	$[\text{Rh}(\text{CO})_2\text{I}]_2$ dimer	61
4.3	$[\text{Rh}(\text{CO})_2\text{I}]_2$ dimer under CO atmosphere	61
4.4	Freshly prepared SILP catalysts	61
4.5	Fresh SILP in Air	62
4.6	Discoloured SILP in Air	62
4.7	$[\text{Rh}(\text{CO})_2\text{Cl}]_2$ dimer Structure	65
4.8	$[\text{Rh}(\text{CO})_2\text{Cl}]_2$ dimer Crystals	65
5.1	(N-Methyl-N-phenylamino) Ph_3P I Degradation	77
5.2	Decomposition of $\text{RhCl}_3 \cdot x\text{H}_2\text{O}$	78
5.3	Decomposition of $[\text{Rh}(\text{CO})_2\text{Cl}]_2$	78
5.4	Fresh sample of Ph_3MePI at 250°C for 20 hours	80
5.5	Used sample of Ph_3MePI at 250°C for 20 hours	80
5.6	15 vol% Ph_3MeP I/ $[\text{Rh}(\text{CO})_2\text{Cl}]_2$ Stability at 250°C over 2 hours	81
5.7	Degradation of Ph_4PI at a heating rate of $1^\circ\text{C}/\text{minute}$	81
5.8	Samples used for FT-IR Study	84
5.9	Spectra of CO stretching in mixed I/Cl systems	85
5.10	The mixed chlorine/iodine complex formed	86
5.11	Loss of CO from the complex over time	86
6.1	Labview Screen for Oven Control	89
6.2	Pressure Valve Control Box	90

6.3 MeOH tank used	92
------------------------------	----

List of Tables

1.1	Components of Pyrolygneous Acid	4
1.2	Consumption of Acetaldehyde for the Production of Acetic Acid, 2006	8
1.3	Heterogeneous vs Homogeneous Catalysis	19
3.1	Retention time of Compounds on the FID detector	54
3.2	Retention time of compounds on the TCD detector	54
3.3	Oven Heating Programme	55
4.1	Results Summary	59
4.2	Comparison of published results and initial trials	60
4.3	Catalyst Wetting Trials	64
4.4	Variation of Rh loading	64
4.5	Comparison of Iodide and Chloride Rhodium Precursors	65
4.6	Alternative Rhodium Sources	66
4.7	Variation of Cation Used	68
4.8	Anion Variation	69
4.9	Rhodium vs. Iridium Catalysts	70
4.10	Main Product Distribution over Presented Reactions	71
5.1	Salt Degradation Ranges	77
5.2	Rh Complex Degradtion	78
5.3	Decomposition of SILP with Varied IL Loadings	79
5.4	Long Term TGA Experiments	81
5.5	Eutectic Points of 0.5:0.5 Mole ratio salt combinations	82
5.6	BET Measurements	83
5.7	Measured C=O Stretches	83
5.8	IR Experiments performed	84

Aknowledgements

All of the work carried out here was conducted at the Centre for Catalysis and Sustainable Chemistry (CSC), in the Department of Chemistry at the Technical University of Denmark in Lyngby. It was supervised by Rasmus Fehrmann and Anders Riisager and in collaboration with Wacker Chemie AG.

Special thanks go to Olivier Nguyen Van Buu for his help building and running of the test rig, Asbjørn Klerke for writing the LabView programme seen in Chapter 2, Bodil Holten for running the BET measurements and Anders Theilgaard Madsen for taking over the running of the test rig towards the end of the project.

Anyone that deserves a mention here knows who they are already. To the special few, you have my undying gratitude and I will forever be in your debt.

“Don’t Panic”

- Douglas Adams, “The Hitchhikers Guide to the Galaxy”

Christopher Hanning

Kongens Lyngby, July 2012

Abstract

The work presented here is focused on the development of a new reaction process. It applies Supported Ionic Liquid Phase (SILP) catalysis to a specific reaction. By reacting methanol and carbon monoxide over a rhodium catalyst, acetic acid can be formed. This reaction is important on a large scale industrially, with millions of tonnes of acetic acid being produced annually. Acetic acid is an important precursor for making adhesives, plastics and fabrics.

By using the SILP concept we are able to carry out the reaction in a continuous system, allowing a steady production of acetic acid without having to stop and re-start the reaction. This sort of continuous flow reaction is a subject of great research effort in recent years as it is more sustainable (and in some cases financially viable) than the current method of carrying out chemical reactions in large size batch reactions.

The project started right at the beginning with the construction of a suitable test reactor, then followed by the synthesis and testing of all the catalysts reported.

A variety of nitrogen based ionic liquids were initially tested, giving good results and stability in the system. Later a number of phosphonium based salts were tested (these were no longer classified as ionic liquids due to melting points above 100°C). The phosphonium salts showed even better activity in the system compared to the ionic liquids.

Overall the work has shown that this process for the manufacture of acetic acid is viable industrially. This is backed up by the construction and operation of a pilot plant by Wacker Chemie AG in Munich.

Dansk Resumé

Denne afhandling omhandler udviklingen af en ny kemisk proces. Ved at benytte et rhodium-kompleks i en supporteret ionisk væskefase (Supported Ionic Liquid Phase, "SILP") som katalysator for carbonyleringsreaktionen mellem methanol og kulilte kan eddikesyre fremstilles. Carbonyleringen af methanol bruges til industriel fremstilling af eddikesyre på megaton-skala, hvilket er et vigtigt udgangsstof for at lave plastik, fibre, tekstiler og bindere som f.eks. lim.

Ved at anvende SILP-båret katalysator kan reaktionen udføres i en kontinuert reaktor, hvilket tillader en konstant fremstilling af eddikesyre uden at skulle stoppe og genstarte reaktionen som i en batch-reaktor. Kontinuerte processer undersøges i stigende grad som erstatning for kemiindustrielle processer baseret på batch-reaktorer, idet kontinuerte systemer normalt tillader bedre kontrol med produktkvaliteten, er sikrere, mere bæredygtige og ofte mere økonomiske i storskala-produktion.

Projektet har omfattet opbygning af en passende opvarmet og tryksat reaktionsopstilling, efterfulgt af syntese og afprøvning af en række katalysatorer. Et antal forskellige kvælstof-baserede ioniske væsker er indledningsvis blevet testet som SILP-bærere for rhodium-katalysatoren. Efterfølgende er et antal phosphonium-baserede salte med smeltepunkter over 100°C (og dermed teknisk set ikke ioniske væsker) blevet testet som erstatning for de kvælstof-baserede ioniske væsker til SILP, og disse medførte højere katalytiske aktiviteter af de afprøvede SILP-katalysatorer .

Afhandlingen demonstrerer, at denne type proces er en lovende industriel metode til fremstilling af eddikesyre, hvilket understreges af Wacker Chemie AGs opbygning af et pilotanlæg i München baseret på teknologien.

Publications

International Conferences

EuropaCat IX: “Catalysis for a Sustainable World”, Salamanca, Spain, 30th August - 4th September 2009

- Poster: “Carbonylation Reactions using Supported Ionic Liquid Phase (SILP) Catalyst Technology”

Nordic Symposium on Catalysis, Helsingør, Denmark 29th - 31st August 2010

- Poster: “Monsanto Carbonylation by Supported Ionic Liquid (SILP) Catalysis”, Winner of Poster Prize Day 1

Green Solvents for Synthesis: “Alternative Fluids in Science and Application”, Berchtesgaden, Germany, 10th - 13th October 2010

- Poster: “Application of Supported Ionic Liquid Phase (SILP) Catalysis to Monsanto Carbonylation Reactions”

EuropaCat X: “Catalysis across the disciplines”, Glasgow, UK, 28th August 2011 - 2nd September 2011

- Poster: “SILP Catalysis: The future of large scale ionic liquid catalysis?”

Local Presentations

DTU Chemistry PhD Symposium 2010

- Poster “SILP Carbonylation”

DTU Chemistry PhD Symposium 2011

- Poster “SILP Carbonylation”

Aarhus University, OChem Autumn School, 28th - 30th October 2010

- Poster: “Methanol Carbonylation via SILP”

Peer Reviewed Publications

- Yury Y. Gorbanev, Søren Kegsnæs, Christopher W. Hanning, Thomas W. Hansen and Anders Riisager, “Acetic Acid Formation by Selective Aerobic Oxidation of Aqueous Ethanol over Heterogeneous Ruthenium Catalysts”, *ACS Catalysis*, **2** (4), 604-612, 2012
- Christopher W. Hanning, Anders T. Madsen, Rasmus Fehrmann, Anders Riisager, “Acetic Acid Production: A mini-review” - In Preparation
- Christopher W. Hanning, Rasmus Fehrmann, Anders Riisager, “Application of SILP techniques to the carbonylation of Methanol” - In Preparation.

Patents

- Verfahren zur befüllung eines reaktors mit einem katalysator. C.W. Hanning, A. Riisager, R. Fehrmann, A. Zipp, C. Rüdinger, DE 10 2012 202 621.5, filed 21. February 2012 (Wacker Chemie AG)

- Katalysator zur carbonylierung carbonylierbarer verbindungen in der gasphase. C.W. Hanning, A. Riisager, R. Fehrmann, A. Zipp, C. Rüdinger, DE 10 2012 202 622.3, filed 21. February 2012 (Wacker Chemie AG)

Abbreviations:

316SS: Standard grade stainless steel

AAB: Acetic Acid Bacteria

AcH: Acetaldehyde (Ethanal)

AcOH: Acetic Acid (Ethanoic Acid)

BDmim: Butyl DiMethyl Imidazolium

Bmim: 1-butyl-3-methylimidazolium

Bu: Butyl C₄H₉-

DME/MeOMe: Dimethyl Ether

DTU: Technical University of Denmark/Danmarks Tekniske Universitet

FID: Flame Ionisation Detector

GC: Gas chromatography

HPLC: High Performance Liquid Chromatography

IL: Ionic Liquid

MeI: Methyl iodide (Iodomethane)

MeOH: Methanol

Ph: Phenyl C₆H₅-

Pr: Propyl C₃H₇-

Pyr: Pyridinium

SILP: Supported Ionic Liquid Phase

STY: Space Time Yield

TCD: Thermal Conductivity Detector

TMG: Tetra Methyl Guanidinium

TOF: Turn Over Frequency

TON: Turn Over Number

vol%: Volume percent

WGS: Water Gas Shift

wt%: Weight percent

Conversions

1psi = 0.07 bar

1 inch = 2.54 cm

1 atm = 1.01 bar

1 MPa = 10 bar

Chapter 1

Introduction

1.1 Acetic Acid

Acetic acid (AcOH) as a chemical has been known for thousands of years, but large scale synthetic production has only become important since the late 20th Century. AcOH (Also known by the IUPAC name of ethanoic acid, or if in aqueous solution often colloquially referred to as vinegar¹) is an important second level bulk chemical produced on a scale of millions of tonnes annually.²⁻⁵

In general AcOH is rarely used in its pure form, functioning, as it does, largely as a precursor molecule for higher value chemicals, Fig 1.1. The largest usage of acetic acid worldwide is in the production of vinyl acetate monomer accounting for over 30% of worldwide AcOH usage,^{3,6} but AcOH finds other usages as a precursor to various other chemicals.

Vinyl acetate monomer is the precursor molecule for poly(vinyl acetate), a widely used polymer used in a variety of fields ranging from floor tiles to safety glass.^{7,8}

Vinyl acetate monomer(VAM) is generally combined with other polymers in order to obtain further polymer or co-polymers.⁹ By far the largest use is in the manufacture of poly(vinyl) acetate accounting for over three quarters of vinyl acetate usage.^{8,10}

By itself VAM is used as an emulsifier in water based paints, adhesives,

coatings and textile coatings. It is also used to synthesise ethylene vinyl acetate polymers used as adhesives and coatings.

AcOH is an important starting point for the manufacture of terephthalic acid which in turn is the precursor to polyethylene terephthalate (PET), which is a common and important plastic used in the majority of plastic bottles today.¹⁰

Usage of acetate esters as solvents is primarily limited to the printing industry, they are popular solvents for paint and ink thinners. This preference is linked to their high volatility.

The manufacture of acetic anhydride is an important use of AcOH within the chemical industry. Acetic anhydride is an important reagent in the synthesis of a large number of other chemicals. Industrially one of its main (and growing) uses is in the synthesis of cellulose acetate used in fabric applications¹¹ and, a large growth area, cigarette filters.¹²

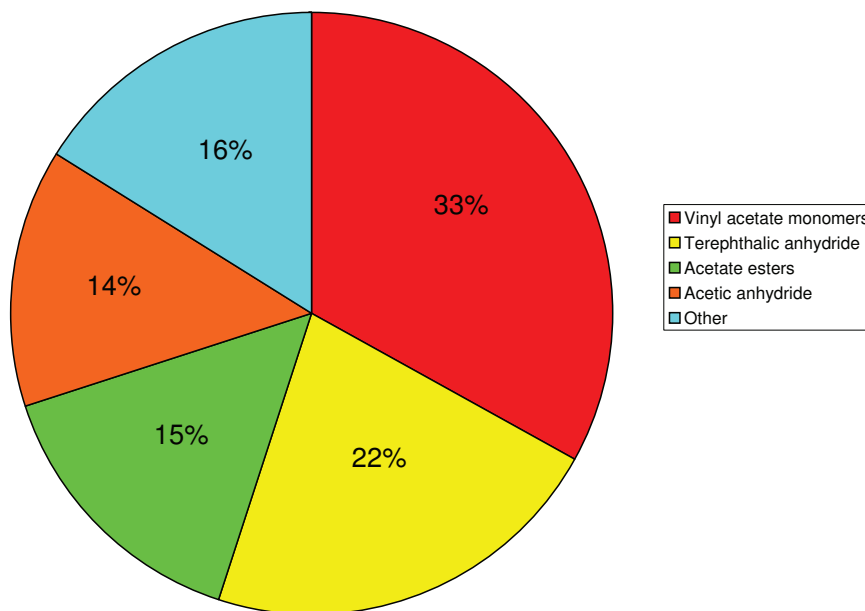


Figure 1.1: Acetic Acid End Uses

1.2 Production Methods for Acetic Acid

1.2.1 Biologically Derived Acetic Acid

AcOH has been produced for thousands of years. Prior to the introduction of synthetically derived AcOH beginning in the 19th Century, all AcOH was produced by fermentation of organic matter. The original AcOH “production” was as a result of the spontaneous fermentation of alcohols (notably in wine.) This production from wine is the original source of the name “vinegar” in English, coming from the french “vinaigre” which translated means “sour wine.”¹³

All such AcOH production occurs in aqueous solution and is facilitated by acetic acid bacteria (AAB.) AAB is not a single organism but is a whole family of bacteria i.e. they are polymorphous.¹⁴ Nowadays, the term “vinegar” describes an aqueous solution of AcOH obtained by fermentation as laid out by the United States Federal Food and Drug Act, 1906.¹⁵

Vinegar production relies on a substrate of ethanol and an air atmosphere. Traditionally this ethanol was present in the solution already, such as in wine. Nowadays, this ethanol is generally derived from sugars in the organic matter before undergoing the final oxidation to AcOH.⁶ Although such a process seems old fashioned and time consuming, it remains a very important one, accounting for approximately 1900×10^6 L of 10% vinegar in 2000⁶, used mainly in food production. There is a legal requirement that any AcOH (in this case always as a vinegar solution), must be obtained from biomass sources¹⁶

Industrially used AAB strains Interestingly, despite the volume of information on AAB, the application of this knowledge to industrial production has been limited. This is linked to the difficulty in isolating and growing the strains used in the industrial reactors.⁶

The most common method industrially for vinegar production is via a Frings acetator. In 1993, Frings acetators had a production capacity of 1354×10^6 L of 10% AcOH.¹⁴ They manufacture plants capable of vinegar concentrations of 12, 15 or 20%. The secret to the system is the use of a Frings

aerator to disperse the air evenly throughout the fermentation medium, but the downside of this is the excess of foam produced at the top of the reactor, this can, however, be mechanically removed easily.¹⁷

Prior to industrialisation of acetic acid production, the only route to high concentration AcOH or glacial acetic acid, was by fermentation to vinegar followed by distillation to remove water from the product. This was a both energy and time consuming and so was rare until the beginning of the 20th Century when industrial methods began to be developed.

Wood Vinegar

The first large scale industrial route to AcOH, was via “wood vinegar.” This form of AcOH was obtained from waste water produced during wood processing. This liquor is a black mixture containing a wide variety of compounds, Table 1.1, with the two largest ones being AcOH and MeOH each making up approximately 20% of the mix.¹⁸ The mixture can also be referred to as pyroligenous acid¹⁹ due to the method of obtaining it by destructive distillation of biomass. In order to purify the AcOH extensive distillation is required, which is why this process is no longer industrially viable. However, during the period from the 1920’s - 1950’s this was a viable industrial process for the production of AcOH.²⁰ Since the introduction of catalysed AcOH production, beginning with acetaldehyde oxidations in the 1950’s, the level of wood vinegar production has decreased. Wood vinegar is still produced today, but it is primarily used as fertiliser.²¹

Table 1.1: Components of Pyroligenous Acid¹⁸

Yield per 1000kg of air dry wood	
Acetic Acid	50kg
Methanol	16kg
Acetone and Methyl Acetone	8kg
Soluble Tars	190kg
Insoluble Tars	50kg

1.2.2 Catalysed Acetic Acid Production

Zeolites

Zeolites are microporous crystalline solids with well-defined structures.²² They can be used in a huge variety of reactions, including the production of AcOH. By constraining Rh compounds in zeolites, it is possible to carry out carbonylation reactions on MeOH.^{23–25} By starting with a Rh(III) source, active carbonyl clusters of the form $\text{Rh}_6(\text{CO})_{16}$ can be formed. These clusters are then able to carbonylate MeOH in the vapour phase in the presence of MeI.^{26,27} The zeolite structure acts as a form of ligand for the Rh centre, stabilising the charge density at the Rh centre.^{27,28} The Rh is incorporated into the structure via ion exchange and an even concentration of Rh throughout the zeolite takes time, otherwise there will be a higher concentration of the Rh near the surface of the zeolite. Typically the Rh carbonyl clusters are then formed calcining under a CO atmosphere. Addition of H_2O to the system reduces the CO conversion over NaY zeolite.^{25,28} It is thought that addition of H_2O to the system removes some of the CO ligands from the Rh centre.

Syngas

Direct synthesis of AcOH from syngas is also a possibility. This has been shown with a ruthenium-cobalt bimetallic catalyst, of the form $\text{RuO}_2\text{—Co}_2(\text{CO})_8\text{—Bu}_4\text{PBr}$. At 200°C with a Brønsted acid promoter it is possible to achieve high selectivities to AcOH from a MeOH feed.²⁹ It has also been shown that Rh dispersed on SiO_2 is able to catalytically form AcOH via CO hydrogenation. The Rh is initially derived from RhCl_3 which is then put into microemulsion with SiO_2 .^{30,31} Addition of manganese, lithium and iron producing supported Rh-Mn-Li-Fe was shown to increase the activity of the system, and favour AcOH formation.^{32,33} Perhaps the most important factor for all of these reactions that they are carried out under iodine free conditions. This is in contrast to all the carbonylation reactions used industrially which require the addition of iodine for the reactions to proceed.

Naphthalene Oxidation

One of the older routes to AcOH production is by the air oxidation of short chain alkanes and alkenes, generally of lengths C_4-C_6 . This oxidation can be carried out using cobalt^{34,35} and vanadium.^{36,37}

A precise mechanism for these reactions has not been completely determined yet. By using butane and Co(III) acetate in acetic acid, it is possible to form AcOH with 83% selectivity at temperatures between 100-125°C.³⁸ For a VO_x catalyst, supporting on TiO_2 gives good activity, but water also seems to play an important part in the reaction.³⁹

C_2 Oxidation

Following on from the traditional fermentation of alcohol, there has also been research into the utilisation of other C_2 sources.^{20,40} A more “traditional” route is the direct oxidation of ethanol. A large body of work has been carried out within our group on such ethanol oxidations⁴¹, most notable using supported gold catalysts.⁴² These processes have been shown to work well under aqueous conditions, and it is this factor that makes them highly unlikely for commercialisation. The hygroscopic nature of AcOH means that as far as possible water in the system is kept to a minimum due to the high purification and separation costs. It has also been shown that ethane can be directly oxidised to AcOH over a palladium based catalyst, of the form $Mo_{1-x}V_{0.25}Nb_{0.12}Pd_{0.0005}O_x$, although this only results in low selectivities to AcOH with CO_x species forming the major reaction products.⁴³

Acetaldehyde Oxidation

Oxidation of acetaldehyde is one of the major industrial routes for production of industrial scale AcOH. Prior to the large scale adoption of the Monsanto process and latterly the Cativa process, acetaldehyde oxidation dominated commercial AcOH production. Since the late 1960’s with the adoption of carbonylation reactions, acetaldehyde based manufacturing capacity has been gradually reducing globally as plants come to the end of their life-span, although they still account for 20% of global production.^{2,3,5}

This process makes use of dioxygen as an oxidant and one of a number of metal catalysts including, manganese, cobalt, copper, vanadium, iron, chromium or nickel. In general the preferred catalyst is manganese as it shows the best selectivity to AcOH.^{3,44} The acetaldehyde itself is obtained via another oxidation reaction, commonly known as the “wacker oxidation.”⁴⁵ In general this process for AcOH manufacture is a joint process combining a wacker oxidation reaction of a suitable C₂ feed stock, before further oxidation of the acetaldehyde to give AcOH.

The reaction is a two step one. In the initial stage, dioxygen reacts with the acetaldehyde to form peracetic acid. This is followed by a Baeyer-Villiger type⁴⁶ oxidation of the peracid with another acetaldehyde molecule. This internal oxidation results in two molecules being oxidised to AcOH, Fig 1.2, only one of which proceeds via the peracetic acid.⁴⁷ It is in order to avoid high concentrations of the peracetic acid in the reaction mix and a run away reaction, the catalyst also functions as a free radical inhibitor.

The catalyst for the process is a metal acetate, typically chosen from manganese, cobalt, copper, iron, chromium or nickel. The most common being manganese, this is due to the major product from all the other metals is acetic anhydride.

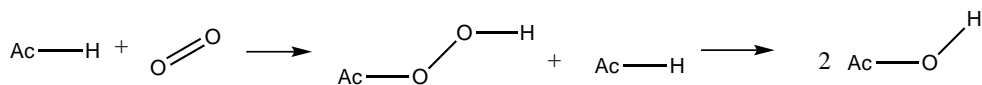


Figure 1.2: Oxidation of Acetaldehyde

Most plants using acetaldehyde oxidation are those designed before the industrialisation of methanol carbonylation dating from the late 1960’s and are now gradually being phased out as they reach the end of their industrial lifetime. The oxidation of acetaldehyde is no longer used (as of 2006) for the production of AcOH in the USA, Table 1.2.

The use of a catalyst increases rate of reaction to a degree that it becomes “oxygen starved” due to the high activity of the catalyst and instead of AcOH, decomposition product begin to be formed. The most important thing to remember about the catalytic oxidation of acetaldehyde is that the

presence of a catalysts act as both a reaction promoter and a reaction inhibitor so the correct level of catalyst usage should be carefully considered when carrying out the reaction industrially^{48,49} as a shortage of dioxygen at the reaction site leads to the formation of unwanted byproducts.⁵⁰

Table 1.2: Consumption of Acetaldehyde for the Production of Acetic Acid 2006⁵¹

Country	Tonnes 10 ³
USA	0
Mexico	11
W Europe	89
Japan	47
Total	147

1.2.3 Carbonylation Reactions

Currently, the most widely used process for the manufacture of AcOH is by the carbonylation of MeOH, making up 60% of all AcOH manufacturing annually.⁵² MeOH and CO are reacted under pressure (30 - 600 bar) and temperature (180 - 250°C) forming AcOH with high selectivity and producing low levels of byproducts.

Cobalt and Nickel

The original MeOH carbonylation reaction for the production of AcOH was patented by BASF.^{53,54} The original patent in 1913 showed that CO could be reacted with MeOH at high pressures and temperatures over group VIII metals to produce AcOH. Work at BASF found that the highest reactivity was obtained by cobalt based catalysts, with the active catalytic species $\text{HCo}(\text{CO})_4$.⁵⁴

BASF first commercialised the carbonylation process in 1960 with an iodine promoted Co catalyst running at 600atm and 230°C. Later, small amounts of H_2 introduced into the mixture were shown to enhance activity.⁵⁵ The catalytic cycle, Fig 1.3, shows that the initial step is the addition of MeI to the catalytic centre as is the standard for the carbonylation reactions. The

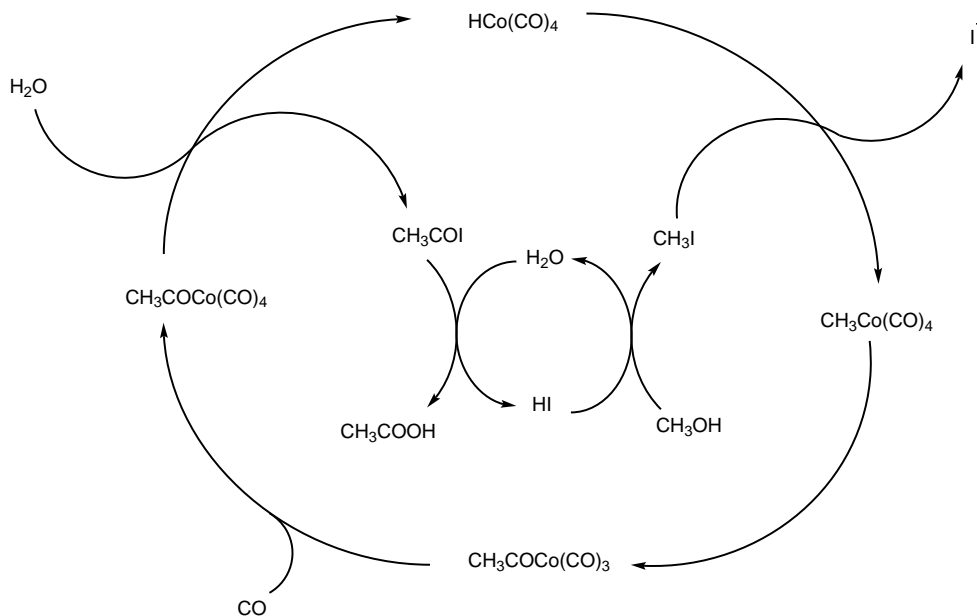


Figure 1.3: Co Catalytic Cycle

reaction is rate dependant on pressure, but this pressure dependency can be reduced by the addition of activators to the system

Ni is also active as $\text{Ni}(\text{CO})_4$ formed from NiI_2 . Although this system uses similar conditions to the Co system, it is possible to carry out the reaction at milder conditions (35 bar and 150°C) if $\text{Ni}(\text{OAc})_2 \cdot 4\text{H}_2\text{O}$ is used with a Ph_4Sn promoter.⁵⁵ As with the Co system, the activity can also be improved by the addition of stabilisers to the system.⁵⁵ With careful control, it is possible to create highly active Ni based catalysts, but the high volatility and toxicity of $\text{Ni}(\text{CO})_4$ has meant the system has not been adopted industrially.

In general, the addition of water was required in order to shift the equilibrium from MeOAc to AcOH .

Unfortunately the process is also highly corrosive. As with other processes forming acetic acid, the use of a standard stainless steel reaction vessel is not suitable. In general in circumstances where a reaction in a corrosive medium is being carried out, it is common to try either titanium or tantalum based materials. Unfortunately, even they do not provide sufficient protection from corrosion. It was due to this problem that the development of the system

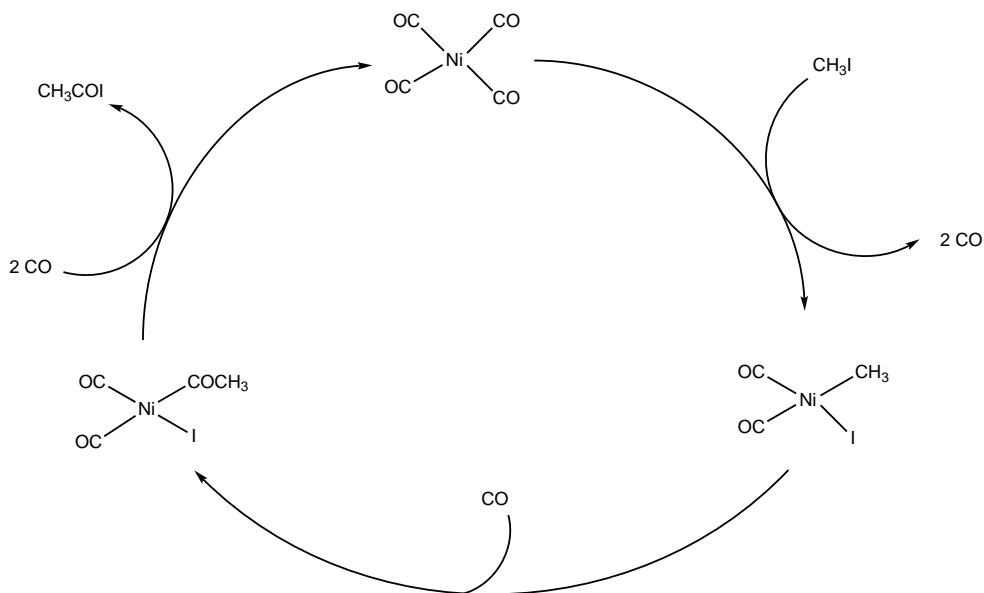


Figure 1.4: Ni Catalytic Cycle

by BASF was delayed. Eventually the alloy hastelloy C* was found to be suitably resistant to begin commercialisation of the process in the 1960's.⁵⁴

Compared to previous methods, the BASF system was capable of producing high yields of AcOH of up to 90%. The major byproducts of the system were CH₄, yielding 3.5% and assorted liquid byproducts, (mainly propionic acid) yielding 3.5%. Compared to the previous methods of creating high purity AcOH this system was very advantageous.⁵⁶

Already it can be seen via the catalytic cycles the importance of MeI and HI in industrial carbonylation reactions. It is also seen that corrosion is a major issue in the process. This requirement to use iodide containing compounds coupled with high levels of corrosion are issues that remain problematic to this reaction even to this day.

Rhodium and Iridium

Currently the two major carbonylation processes are based on Rh and Ir as originally described by Paulik and Roth in 1968.⁵⁷

*See appendix E for a comparison of steel types

Initially the research focus was on the Rh based systems as they showed a higher activity for the reaction. As a result of these there has been a large body of research work into the Rh based systems. The Rh catalysed carbonylation reaction, Fig 1.5, is referred to as the “Monsanto Process”, after the company that first commercialised it.⁵⁸ Although their work was building on that already carried out with Co and Ni based catalysts by BASF.⁵⁴ For the Ir catalysed process (Basic catalytic cycle, Fig 1.6) this was initially commercialised by BP Chemicals, but is generally referred to as the “Cativa Process”. The Cativa process is significantly newer and was first used on a commercial scale in 2000 at a BP plant in Malaysia.⁵⁹ Both of these processes, and their resulting refinements, are currently running industrially and combined make up 60% of global AcOH production.

Both of the processes are carried out in similarly designed reactors, in a batch-wise process with subsequent product purification by distillation. As is shown in Fig 1.7.

As in the BASF process (see Section 1.2.3), both reactions require the use MeI as a co-catalyst. This part of the catalytic cycle is highly important as it leads to the Me- ligand binding to the Rh centre which in turn results in the formation of the AcI intermediate. The resulting HI formed during the catalytic cycle is also particularly important in the termination of the catalytic cycle.

In both systems, the biggest problem is preventing the precipitation of the inactive iodides of the metal centres, RhI_3 and IrI_3 .⁵² In order to limit this precipitation, the original Monsanto system required high levels of water to stabilise the catalyst centre. The presence of water also influences the formation of HI, promoting the termination of the catalytic cycle.

The rate limiting steps between the processes differs slightly. In the Monsanto process the rate limiting step is the oxidative addition of the MeI to the Rh centre, for the Cativa process it is the migratory insertion of the CO ligand.⁶¹

Unfortunately, HI is involved in the catalytic cycle. This is one of the strongest aqueous acids and highly corrosive. This requires the reactors to be built of expensive, corrosion resistant materials. A substantial cost on top

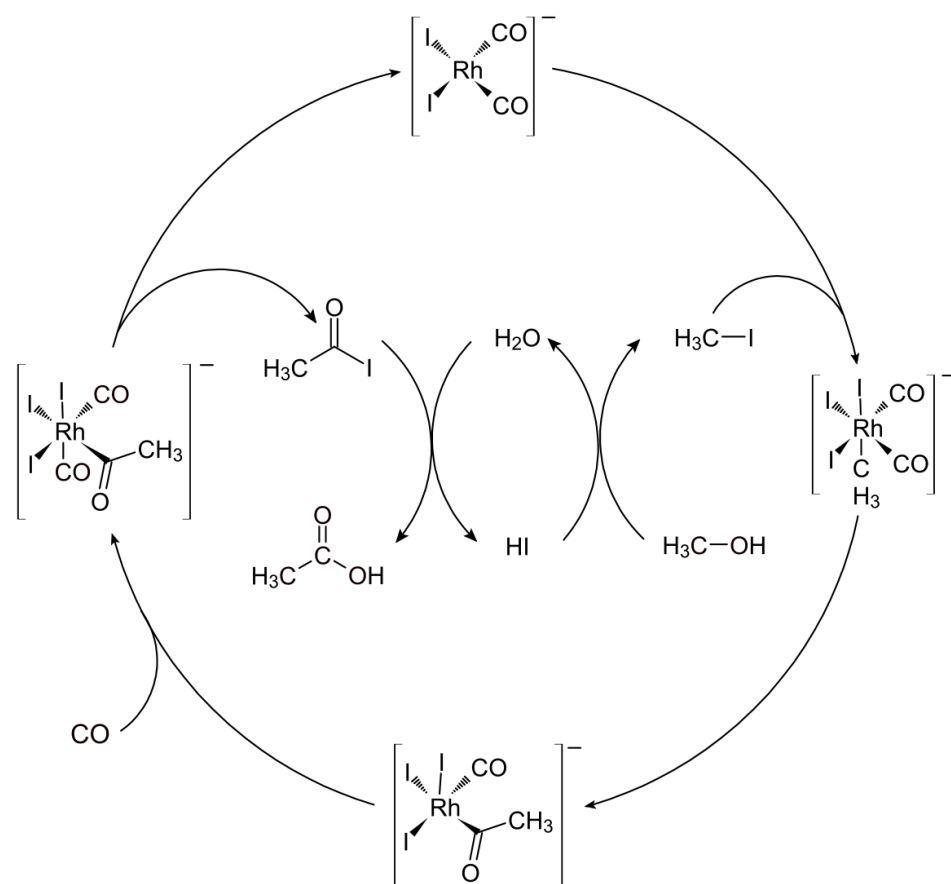


Figure 1.5: Monsanto Catalytic Cycle

of the already expensive catalyst. This nature of this corrosive atmosphere is something that will become more apparent later in this work.

Overall, the two processes are very similar with comparable mechanisms and reaction conditions. Although the Rh based Monsanto process initially was favoured due to higher activity, nowadays due to economic issues related to the high cost of rhodium, the iridium based Cativa process is favoured.

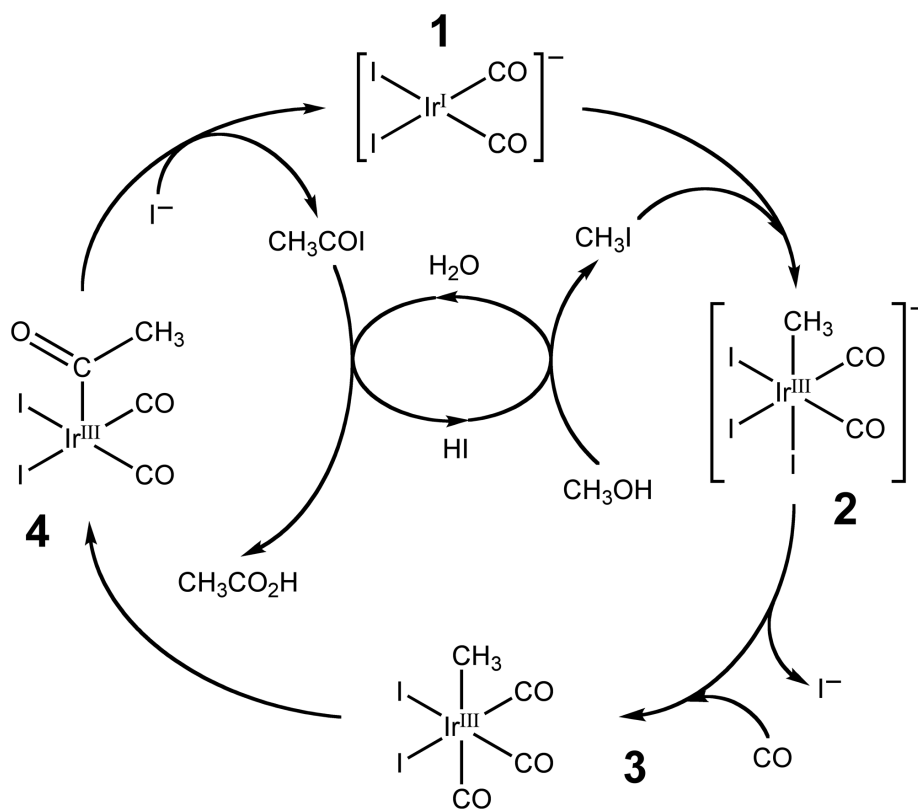


Figure 1.6: Cativa Catalytic Cycle

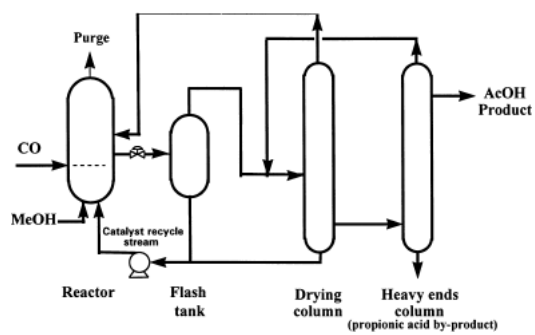


Figure 1.7: Standard Carbonylation Reactor⁶⁰

Monsanto Process Development Due to the age of the Monsanto process, there have been research into improving the effectiveness of the system.

Up to 15wt% water is required for the process⁶² and this is linked with the formation of HI in the system. This H₂O-HI equilibrium is particularly important as it is the acid catalysed hydrolysis of AcOI that is critical for the liberation of AcOH.

The first major derivative of the Monsanto process was developed by Hoechst-Celanese.⁶³ This was known as the Celanese Acid Optimisation (AO Plus).^{4,64} By the addition of metal iodide salts to the system, the level of water required could be significantly reduced as well as an improvement in catalyst stability under such low water conditions. Addition of LiI in particular, results in rates similar to that Monsanto process, but with a greatly reduced water level. In the normal process, reduction of the water level would lead to a rate reduction, but the addition of LiI seems to avoid this problem. The usage of such metal iodide salts seems to promote the oxidative addition of MeI to the Rh centre, which otherwise is the rate determining step, although the precise mechanism is not yet fully understood.⁶⁵

The presence of water in the system is very important for catalyst stability, especially when the CO partial pressure is low.⁶⁶ Unfortunately, high water means that more distillation columns are required to purify the final product. From a cost perspective such a large amount of distillation columns is unfavourable due to their high energy requirements, combined with the hygroscopic nature of AcOH.⁶⁷ Of the metal iodide salts trialled, only LiI and NaI remained in solution in the reaction mixture at room temperature. In general catalyst more stable at high CO pressures, LiI can increase rate via formation of LiOAc species which acts as a promoter and decreases HI concentration, giving a higher equilibrium concentration of Rh(I).⁶⁶

Addition of phosphine ligands to Rh centre, has been a field of a large amount of study and is best covered by Thomas and Süß-Fink in their review article.⁶⁸ It's not clear how many of these phosphine modifications have made it from the lab into industry. In general this work with phosphine ligands is not largely focused on MeOH carbonylation on industrial scales, but rather other reactions focused on similar Rh catalytic centres.

Ir Catalysis Ir carbonylation also referred to in the original letter describing Rh carbonylation.⁵⁷ Ir is currently cheaper than Rh⁶⁹ since the vast majority of Rh is used in the manufacture of catalytic converters for cars. In 2000, the Rh demand for catalytic converters was 6 million ton/year⁵⁹ severely limiting the availability of Rh for use as a catalyst. In 1996 the Cativa process began to be commercialised.⁵⁹ Ir works well in low H₂O conditions and seemed to be stable in conditions not suited to Rh. It is also more soluble in medium than Rh allowing for high catalyst concentrations. The mechanism for the reaction is complex,^{70,71} Fig 1.8. Promoters can also be used to improve the efficiency of the reaction. These promoter fall into two categories carbonyl or halocarbonyl complexes of W, Re, Ru, Os, or simple iodides of Zn, Cd, Hg, Ga and In. There are two Ir catalytic cycles, one with neutral Ir(I) complex and the other with anionic Ir(III) complex, Fig 1.8. Due to the rate determining step, it is hard to isolate the $[\text{Ir}(\text{CO})_2\text{I}_2]^-$ complex⁷² to study the cycles in depth.

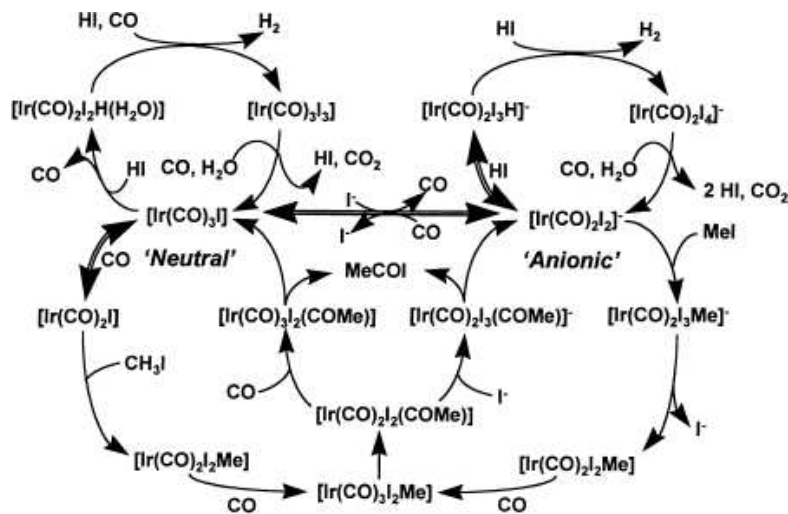


Figure 1.8: Complete Cativa Catalytic Cycle showing “neutral” and “anionic” routes⁶⁰

1.3 Ionic Liquids

Ionic liquids (ILs) have been well documented over the last 15 years.^{73,74} The generally accepted definition of an IL is “a substance composed of 2 distinct ions that is liquid below 100°C.”⁷⁵ As a comparison, table salt (NaCl) has a melting point of 801°C. A subcategory of ILs is the Room Temperature Ionic Liquid (RTIL) where a melting point below 25°C is used.⁷⁶ At various points over the last 10 years, ILs have been described as green,⁷⁷ designer⁷⁸ or “ferarri”⁷⁹ solvents. Recently the “green” label is not used as often as previously as there have been increasing numbers of toxicology studies carried out on ILs showing their biodegradability and toxicity, particularly to aquatic lifeforms.^{80–85}

The wide variety of ILs available (10^{23} binary combinations according to calculations by Plechkova and Seddon⁷³), combined with the ability to functionalise the ions meant that initially a large number of people viewed ILs as a modern alkahest, or universal solvent. Now the honeymoon period has past and the limitations of ILs has been recognised, but has resulted in the more serious studies of ILs is being carried out⁸⁶ particularly in the field of catalysis.^{87–93}

Despite the large body of research in the field. Large scale adoption of ILs into industrial processes remains limited, not least due to the high capital cost of ILs in comparison to normal solvents and the industry preference of “race to be second”, especially with such new technologies.

Overall little details or companies investing in and using ILs is available and the most complete picture is presented in a review by Plechkova and Sheldon in 2008.⁷³ The most vocal company about utilising ILs is BASF, who have widely promoted their usage of ILs in the BASIL (Biphasic Acid Scavenging utilising Ionic Liquids) process. This process was first publicly revealed in 2002 and has been in use since then. The process is used downstream to scavenge the undesired acidic byproduct of a reaction.⁹⁴

Eastman has little publicly acknowledged interest in any processes using ILs, although *did* run an isomerisation plant from 1996 - 2004 utilising some IL based technologies. The plan was eventually shut down due to lack of de-

mand for the product. More interestingly it has filed a number of patents and published details of carbonylation reactions using ILs.⁹⁵ Their work focuses on a bulk phase IL containing the catalyst while the reagents and products are in the gas phase. They found that $\text{PR}_4 \text{I}$ salts were more efficient than other ILs.⁹⁶

Both BP and Exxon-Mobil have large patent holdings regarding ILs, but currently have made little public announcements regarding their usage of ILs.

Other companies that are known to be involved in using ILs include: IFP (Institut Français du Pétrole), Degussa, Air products, Sasol, PetroChina's "ionikylation" alkylation plant and Scionix

1.3.1 Supported Ionic Liquids

The concept of supporting liquids for catalysis is not a new one, with a wealth of research. Initial work was in the field of Supported Liquid Phase (SLP).⁹⁷ The more modern branch where ILs are supported is far newer. The first reference to supported ionic liquids the author can find is a patent from Akzo Nobel in 1999.⁹⁸ The patent discloses a procedure for the alkylation of aromatic compounds using a "supported ionic liquid catalyst." The IL referred to is based on a chloro-aluminate anion and the support is a standard large surface area solid. It is not clear if this patent found any commercial use.

The first mention of supported ionic liquids in the academic literature was published by Mehnert *et. al.* in 2002.⁹⁹ Their paper describes the concept described as Supported Ionic Liquid Catalysis (SILC). A monolayer of IL is covalently bound to the surface of a porous solid and further addition of IL results in layers of free IL on the support. The bound IL layer acts as an anchor for the subsequent layers of IL. The result of this SILC material was to "immobilise" a catalytic metal centre in the IL via electrostatic interaction, but during the reaction, the fluid nature of the IL gave a homogeneous reaction site. Further work looked at supporting catalytic ILs on a charcoal support for Friedel-Crafts acylation reactions.¹⁰⁰

In 2003, the concept of supported ILs was expanded again with the report

of a Supported Ionic Liquid Phase (SILP) system, by Riisager *et. al.*¹⁰¹ This concept is similar to that shown by Mehnert, but with SILP the IL is not covalently bound to the support and bound to the support purely by electrostatic and capillary forces.

Since then a number of systems based on supporting ILs have emerged, creating a complicated system of acronyms. Some of the more common ones are: (g-)SILLP - (gel-) Supported Ionic Liquid Like Phase;¹⁰²⁻¹⁰⁴ SCILL - Supported Catalyst with Ionic Liquid Layers;^{105,106} SILM - Supported Ionic Liquid Membranes;^{107,108} SILC(A) - Supported Ionic Liquid CAtalysts.¹⁰⁹⁻¹¹¹

Unfortunately, there doesn't appear to be any conventions when naming these systems. This is often the result of multiple "discoveries" of a similar concept. This problem is further compounded by making it unclear the differences between the various systems and difficult to easily search the relevant literature. One of the few papers that distinguishes between some of these different labels is Van Doorslaer *et. al.*¹¹² Fig 1.9. They define four types of catalyst-ionic liquid systems, but don't cover the breadth of all the names.

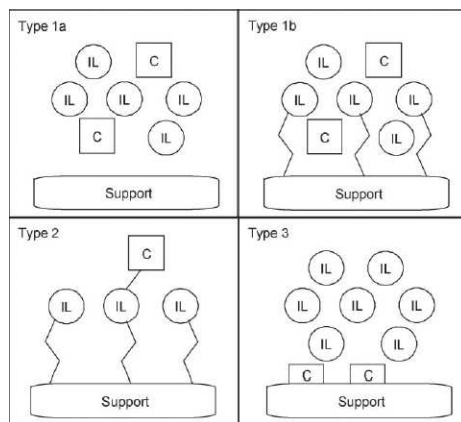


Figure 1.9: Different types of SILP-style Catalysts¹¹²

Type 1a and 1b both represent true SILP materials as in both cases the catalyst and some degree of the IL are not bound to the support material. Type 2 is often referred to as SILC as both the IL and catalyst are bound to the support. Type 3 is a SCIL type system where only the IL is not

bound to the support. For these support-IL systems, the main benefit is the combination of both homogeneous and heterogeneous aspects of catalysis in one system. With the current trend to heterogeneous catalysis, it is often difficult to obtain similar selectivities, Table 1.3.

Table 1.3: Heterogeneous vs Homogeneous Catalysis

	Heterogeneous	Homogeneous
Catalyst Form	Solid, often metal or metal oxide	Metal Complex
Mode of Use	Fixed bed or slurry	Dissolved in Reaction Medium
Solvent	Usually not required	Usually required - can produce byproducts
Selectivity	Usually Poor	Can be tuned
Stability	Stable to High Temperature	Often Decomposes at less than 100°C
Recyclability	Easy	Can be Difficult
Special Reactions	Haber Process, exhaust clean up, etc.	Hydroformylation of alkenes, methanol carbonylation, asymmetric synthesis, etc.

The SILP principle of type 1a is the focus of the body of this work. The actual catalyst material is presented outwardly as a solid material, but the active catalytic site and solvent are both homogeneous in the ionic liquid phase.

The majority of work on the SILP concept remains academic, but Süd-Chemie seems to be showing an interest in the field with a number of publications (in collaboration with the Wasserscheid group at Erlangen-Nürnberg.)¹¹³⁻¹¹⁵ More relevant to this thesis is the interest of Wacker Chemie AG in SILP technology for acetic acid manufacture. This reaction was initially demonstrated here at DTU,¹¹⁶ but since then a successful pilot plant has been constructed at their research site in Munich, Germany. The success of the pilot plant makes it likely that the work will be further scaled up to a medium-sized pilot plant to determine the overall industrial feasibility of the SILP process for such a reaction.

Although the choice of support material is variable, currently silica is the support of choice, with its large surface areas and the ability to form it into shaped pellets. The choice of IL is much more varied and is often tied to the reaction that it is to be used for. The ability to functionalise ILs mean that it is possible to tune the ILs used for each reaction to achieve the desired results.

In order to prevent leaching of the IL and catalyst, SILP type reactions are typically carried out in the gas or slurry phase. The concept of SILP can be and has been applied to a number of different reactions such as, oxidation of primary alcohols,¹¹⁷ isopropylation,¹¹⁸ very low temperature WGS,¹¹³ hydroformylation,^{101,119,120} hydrogenation,¹²¹ Grubbs metathesis,¹¹⁴ Friedel-Crafts acylation,¹⁰⁰ and de-sulphurisation.¹²²

1.4 Commercial Acetic Acid Production/ Reactor Styles

Currently all large scale industrial production of AcOH is carried out in large batch reactors. Both acetaldehyde oxidation, naphthalene oxidations and carbonylation reactions are all carried out in solution in batch reactors, with purification carried out by distillation. All of the reactions are carried out under pressure either of CO or O₂ and the corrosive nature of the reagents and products require that suitable corrosion resistant materials are required for the plant construction.

Carbonylation reactions are carried out in AcOH solution with the catalyst dissolved in it. The system is pressurised under CO so that the solution becomes saturated in CO before MeOH and MeI are fed into the reaction mix.

The overall process has three sections: reaction, purification and off-gas treatment, Fig 1.10.⁷² The reactor is a continuous stirred tank with a MeOH feed, CO feed and recycle feed coming from the purification stream. Product removal from the reactor is carried out via a flash valve. This allows for separation of the “lights” i.e. MeOAc, AcOH, MeI and allows

for the remainder to be recycled back into the reactor. The purification of the product initially involves the separation of unwanted byproducts and reagents before a final distillation to obtain a suitably pure form of AcOH. The purification is usually carried out by three columns although this number depends on the contamination of the product feed and the purity of the AcOH required. The first column splits off MeOAc and MeI for return to reactor, the second column dries the AcOH and the third column removes any remaining “heavies” from the product stream. Running in parallel to this purification is treatment of the off gas from the system. This removes any product or undesired chemicals before the stream is vented to a flare.^{72,123}

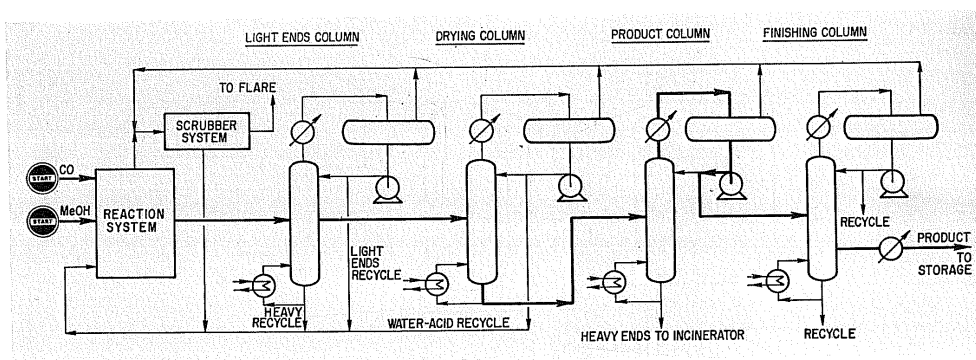


Figure 1.10: Process Diagram of a Methanol Carbonylation Plant¹²³

A vapour phase system has been attempted before by Monsanto. They showed that Rh on activated carbon was possible, but didn't carry through the work to industrialisation.¹²⁴

Standard Industrial Reactors

Currently all industrial scale manufacture of AcOH is carried out batchwise. This is based on the tradition method of carrying out large scale chemical synthesis by “scaling up” reactions from a lab scale round bottomed flask to a large industrial sized equivalent. Large stirred tank reactors are used. The typical solvent used in the reaction is AcOH as all reagents and products are soluble in it. The reaction mixture is then flushed with the reagent gas to the required reaction pressure, this allows for the reaction medium to become

saturated in the reagent gas.

The major energy costs associated with the production of AcOH is the final purification of the product. AcOH is hygroscopic and so it becomes increasingly difficult to remove the last vestiges of water from the final product.

In recent years there has been some movement away from batch reactors, to continuous flow systems as illustrated by Eastman with their IL containing bubble column¹²⁵ and Wacker Chemie AG with their use of SILP as currently demonstrated in their pilot plant in Munich.

Chapter 2

Experimental Set-up

2.1 Introduction

This project required that (in order to carry out catalyst testing) a completely new test-rig had to be constructed. This construction was carried out completely “in house” at DTU Chemistry. The original test-rig is shown in Fig 2.1.

The initial construction was originally envisioned as approximately a three month process, but in reality it required substantially more time alongside the requirement of regular maintenance to retain a continuing operational capability. The test-rig has been one of the most important factors linked to the catalyst testing frequency and abilities during the course of the project.

All electrical wiring of the supplied components was carried out by the author. These included the heating tapes and cable, the temperature measurement and control equipment and the pressure regulating valve.

For specific details of all the components used, see Appendix B.

2.2 Design and Construction

The original design for the test rig was based on a technical diagram shown in Fig 2.2. Since then the test-rig has gone through a large number of iter-

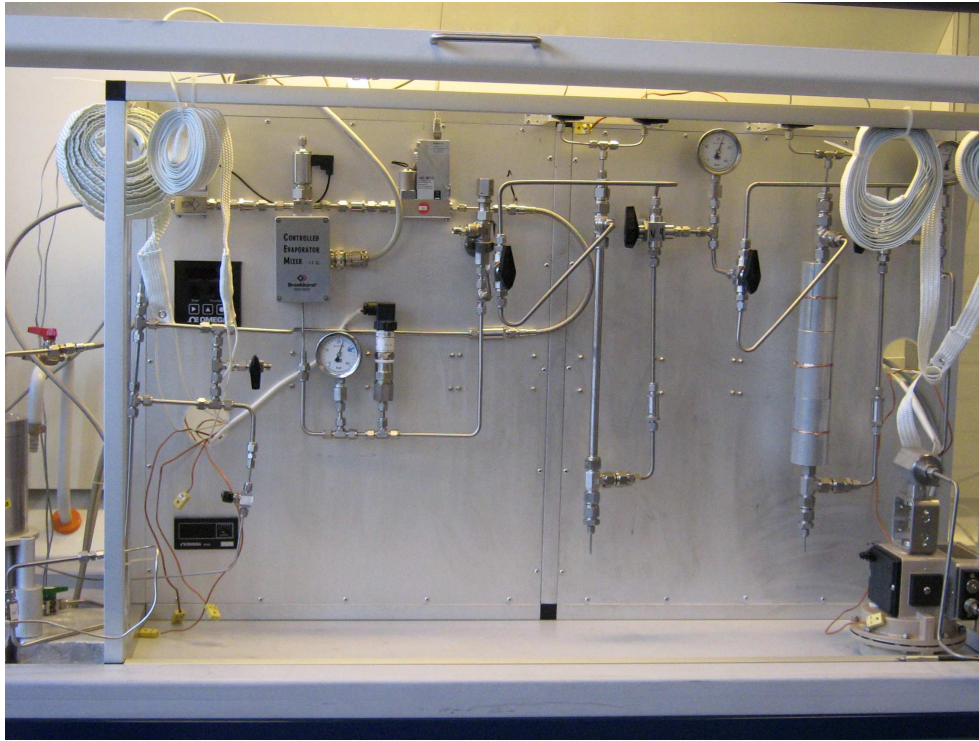


Figure 2.1: The Original Incarnation of the Test Rig

ations, both from necessity to retain its ability to continue operating and as continuing “improvements” on the original design.

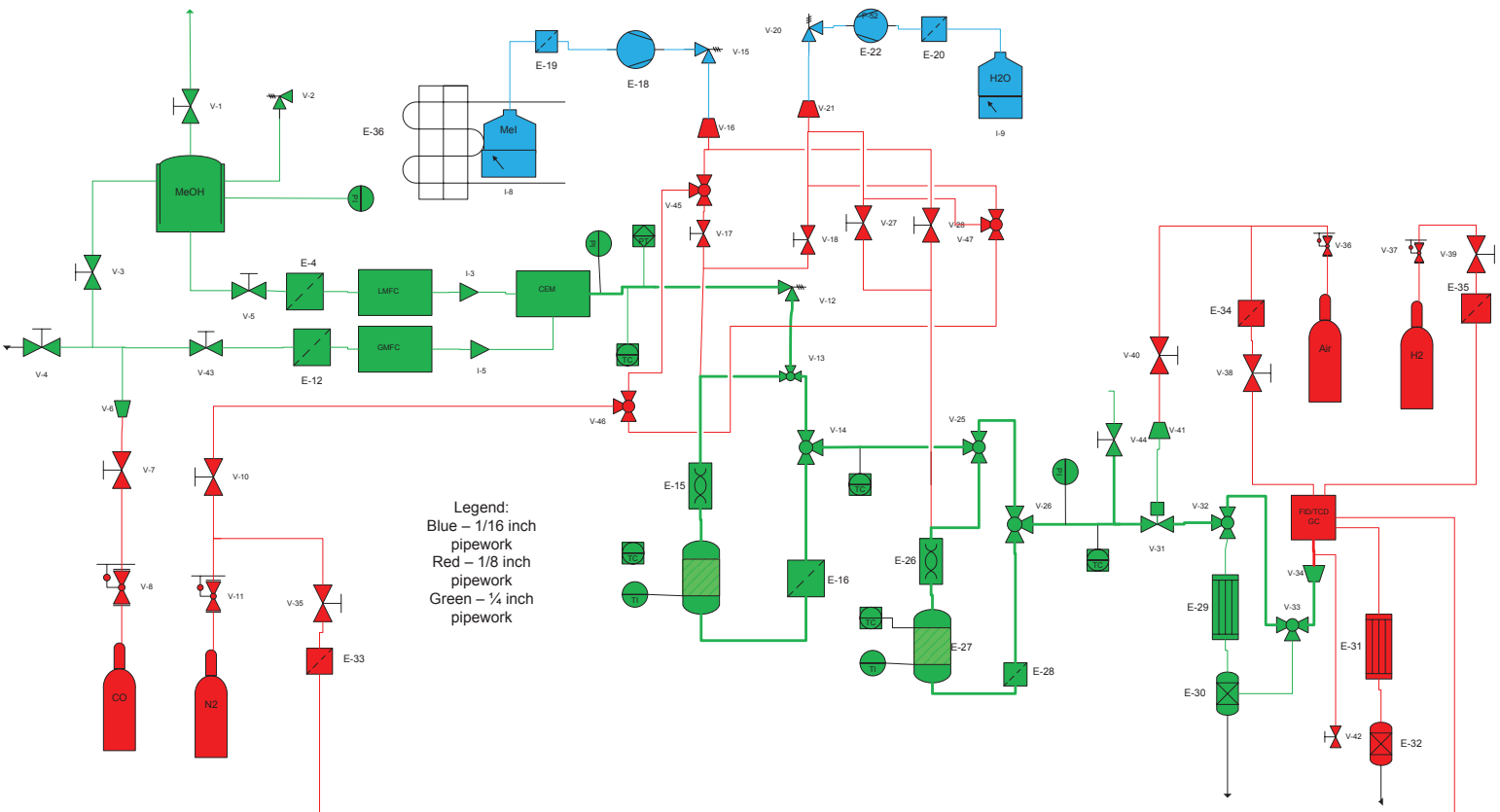


Figure 2.2: Initial Test Rig Design

Using the original diagram as a starting point for initial practical thoughts on pipe/valve placement. An initial “outline” sketch was drawn onto the aluminium frame that would form the backbone holding the test-rig. This sketch outline allowed for easier visualisation of the final product and allowed us to see where we were likely to run into difficulties during the construction. Using these two designs as a basis, the required fittings and components were ordered to begin the construction.

The system is primarily composed of 316SS stainless steel fittings. The pipes are a mixture of both 316SS and 316Ti stainless steels*. The usage of 316Ti is in order to try and reduce corrosion issues after the reactor linked to the corrosive atmosphere of the system. Unfortunately we very quickly discovered that corrosion of even 316Ti was unfortunately inevitable, Fig 2.3. Components were either 1/4" size or 1/8" size and due to the availability of the fittings, it was required that the majority of joints, filters, manometers were 316SS. All the fittings used were Swagelok brand† where available, otherwise they were bought with appropriate adaptors to Swagelok fittings.

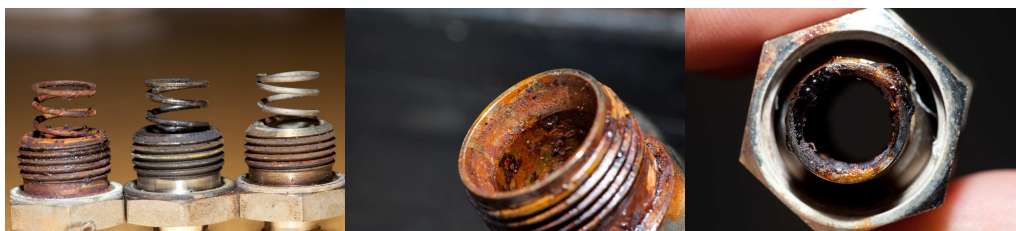


Figure 2.3: Examples of corrosion

*See appendix E for a comparison of steel types

†<http://swagelok.com/>

This usage of 316SS made the issue of corrosion endemic but by having a supply of spare components, we quickly became adept at replacing/repairing corroded components quickly and efficiently. All of the reactors were constructed “in-house” by the DTU Chemistry workshop. These were designed in 1/2" diameter in order to create a suitable reactor volume. They were of a fixed-bed design, formed by the fusing of two halves together creating a fretted steel bed half way down the reactor. The selection of a suitable thickness of fretted steel, combined with the fusing together of the two reactor halves proved tricky, resulting in the reactors not being available to incorporate into the system until towards the end of the construction process.



Figure 2.4: Reactor Cross Section and Bed

2.2.1 Pressure Testing

Following construction and before the introduction of CO into the system, a primary pressure test was carried out. This initial test allowed for the early detection of any loose joints in the system and its ability to maintain initial low levels of pressure ~ 5 bars of N_2 . This introduced the problem of detecting leaks in the system, since N_2 is not a gas detected easily. After using the N_2 to identify the major leaks in the system, via manometer readings, in order to allow us to detect any further leaks it was decided to switch to CO. This decision was based on the ease of detection combined with the large availability of CO alarms but introduced other safety concerns when carrying

out the work. Using CO and gradual increases in total pressure, we were able to get the system pressure tight to just over 20 bars at room temperature. Unfortunately, we didn't realise at the time than after the heating of the system, there was a very real possibility of further leaks becoming apparent. After an initial heating of the system to test the heating tapes, we found that a large number of "new" leaks had become apparent in the system. After this initial heating, we then had to remove all of the newly attached heating tapes to allow access to the leaking fittings, this proved to be quite a time consuming process. This formation of leaks due to the heating and cooling of the system is something that we cannot avoid. As a result of this we try and keep the system at a constant temperature even when not in use. By doing this we seem to have limited the developments of new leaks resulting from any expansion/contraction in the system.

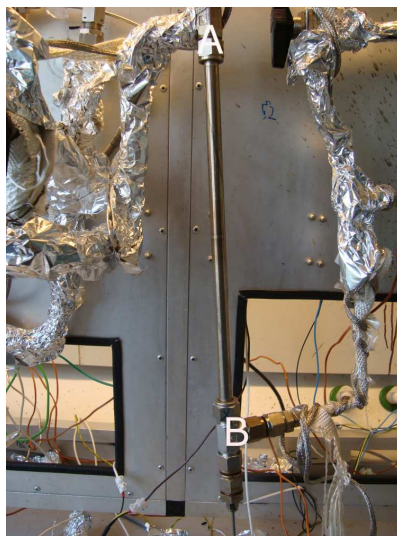


Figure 2.5: Reactor with Connections Labelled

Some of the issues linked to leaks in the system can be linked to the frequent removal/fitting of new components (in particular the reactors). Swagelok components are designed to provide a seal tight enough to withstand very high pressures, unfortunately this is only the case for the first connection of the joints. As soon as the joints need removed and/or replaced, it is impossible to achieve a "perfect" seal. This issue had to be beared in

mind during any maintenance and/or cleaning work on the system. This problem is most pronounced for the reactor as it is the component that is removed and reattached the most often. To try and limit the problem, only two specific fittings were used to remove and reattach the reactor, Fig 2.5 and 2.6.



(a) A- Fitting used at the Top of the Reactor (b) B- Fitting used at the Bottom of the Reactor

Figure 2.6: Reactor Connection Fittings

2.3 Corrosion

The high degree of corrosion that is observed in the system is important to remember when construction and/or replacement of components is undertaken. The corrosion is as a result of the presence of HI in the system. The HI can be present in either the gas phase or due to heating failures or cold spots in solution. By itself HI is not a corrosive substance, but once in the presence of water it forms a very strong acid ($pK_a = -9.5$). As a result of this highly corrosive atmosphere, all components of the system, particularly from the reactor onwards, are subject to heavy corrosion, Fig 2.7. The problem is so pronounced that in general most components had a lifetime of approxi-

mately 9 months of continuous usage. In order to alleviate this problem, we attempted to slow down the rate of corrosion by using titanium supported stainless steel for certain components and pipework, but even this enhanced steel was subject to corrosion over extended periods of time. Due to the scale of the test rig, components in Ti supported steel were not available for all of the components and so we had to use the 316SS parts available. As a result, it was often these parts that caused the most problems in the system. Unfortunately their replacement required complete shutdown of the system and the removal of all the heating tapes from the system. The amount of time required to carry this out is not insignificant and so in some cases it made more sense to carry on with a component that was functioning, albeit not perfectly, until there were enough problems with the system to justify a shutdown and reparation period.



Figure 2.7: Comparing Components Before and After the Reactor

See Appendix D for a fuller selection of pictures detailing the corrosion.

2.4 Flow Controllers

Outside of the main reactor system were a number of other important components.

Addition of CO and MeOH into the system was controlled by a system of flow controllers and a mixing unit, Fig 2.8. The Liquid Mass Flow Controller (LMFC), Fig 2.9a, was calibrated directly for use with MeOH liquid. The Gas Mass Flow Controller (GMFC), Fig 2.9b, was calibrated directly for usage with CO gas. Both of the MFCs fed into a Controlled Evaporator Mixer



Figure 2.8: CEM and MFCs

(CEM) unit, Fig 2.9c, before entering the reactor system. The CEM is used to combine the separate flows of gas and liquid as well as heating them up to the same temperature as the rest of the system to stop condensation of the MeOH as it is added to the system. Perhaps most importantly the CEM has a check valve, so it is impossible for any of the iodide containing substances in the system to damage any of the components. All three components were controlled automatically by a control box, also from Bronkhorst, Fig 2.10. Since both of the MFCs are calibrated for their respective chemical, this means that the control box allows for real-time alteration and monitoring of the flow rates. In order for the flow controllers to function well, it is important to have a slight back pressure. This is obtained by maintaining a pressure in the system prior to the flow controllers of between 25-30 bar.

All of these components proved to be generally reliable over the course of the work, for the most requiring only minor repairs at irregular intervals. Unfortunately when any servicing *was* required, it was necessary for the components to be sent to the Netherlands for repair, as the supplier did not have a service partner located in Denmark. The results of this was an extended period of time from us sending a component until we received it back again. On a couple of occasions this delay was aggravated by communication issues between us, our contact in Denmark and Bronkhorst. In each case we had



Figure 2.9: Flow Controllers and CEM

to endure extended periods where we were not able to conduct experiments due to the MFCs and CEM being integral to the process.



Figure 2.10: Control Box for Flow Controllers and CEM

2.5 Back Pressure Regulating Valve

We required a back pressure regulating valve to regulate the pressure in the reactor system and allow pressure reduction prior to the GC. For our test-rig we use a Samson back pressure valve, Fig 2.11 and 2.12, to decrease the pressure in the reactor (20 bar) to close to atmospheric pressure in order to analyse the products via the on-line GC. This pressure regulating valve is an industrial scale component, but we were able to adapt it for usage on our small scale system. The valve regulates the pressure in the system via a pneumatically operated pin, which is raised or lowered according to the pressure of the system measured via a transducer, Fig 2.13 . The transducer is located just after the CEM and next to a manometer so we have a “failsafe” measure of the pressure at that point in the system.

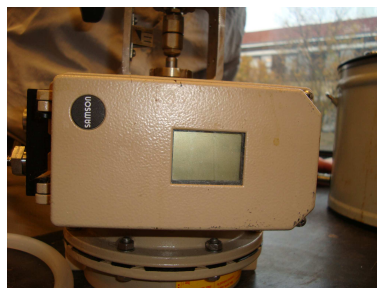


Figure 2.11: Pressure Regulating Valve Figure 2.12: Pressure Valve Actuator

Over the course of the project, corrosion at other points in the system had a significant knock on effect on the valve, Fig 2.14. Due to the scale of the test rig, the original regulator pin used ($K_{vs} = 0.001$)* proved unsuitable. We then changed the pin so that it was the smallest possible ($K_{vs} = 0.00063$), Fig 2.15. This small K_{vs} means that the presence of any foreign bodies condensing around the pin would be enough to jam it and stop it regulating the pressure correctly even breaking the valve pin itself, Fig 2.17. Since, the

*The K_{vs} value expresses the amount of flow in a regulating valve at a fully open position and a pressure differential of 1 bar



Figure 2.13: Pressure Transducer



Figure 2.14: Corrosion around the Valve Pin

reaction mixture after the reactor beds is so varied it is impossible to say exactly what may condensate around the regulator pin. One of the most apparent substances is iodine as can be witnessed by the dark brown/black colour of any solvent used to clean the valve as well as the presence of black crystals on the surface, Fig 2.16.



Figure 2.15: Comparison of the K_{vs} values. Left: 0.001 Right: 0.00063



Figure 2.16: Surface of the Pin Seat Showing Black/Brown Condensate



Figure 2.17: Broken Valve Pin

In order to try and limit the condensation of any substances, we implemented an auxiliary heating cable solely used to heat the valve seating, Fig 2.18. This cable was set to heat to maximum temperature to try and ensure that any high boiling substances entering the valve would also be evaporated.

Since the pressure regulating valve is an industrial component, this meant we had to use adaptors for converting unusual thread sizes to swagelok standard, Fig 2.19. This conversion from one thread type to another did not give a perfectly tight seal and initially we tried using o-rings to ensure a better fit. Unfortunately we discovered that the rubber quickly perished in the chemical environment and thereafter we began to use teflon tape in order to achieve a suitably tight seal which proved more successful.



Figure 2.18: Heating Cable used for Pressure Valve



Figure 2.19: Adaptor used to connect the Pressure Valve to the Swagelok Components in the rest of the System

2.6 Heating

2.6.1 Ovens

Heating of the reactor was carried out by heating jackets, made by Horst to our specific requirements. Initially control of the ovens was manual, the desired temperature was set on the control box, Fig 2.20, and the actual temperature measured by the heating jacket's own internal thermocouple. Initial use of the ovens this way required some fine tuning. A thermocouple, connected to a temperature readout, was inserted into the bottom of the reactor and is used to determine (as close as possible) the actual temperature of the reactor. Since the reactor was not directly heated by the heating jacket, but was surrounded by aluminium blocks to improve heat capacity, there was a substantial time lag between the temperature of the jacket and the measured temperature of the reactor. As a result, the set point of the oven would need to be checked and altered periodically to maintain a stable temperature in the reactor.

We were able to automate the oven control via a labview programme, Fig 2.21. This programme automatically monitored the reactor temperature and compared it with the set temperature then controlling the oven as required.



Figure 2.20: Original Control Box for Oven Control

As shown in Fig 2.21, the labview display is remarkably simple. It also enabled detailed logging of reactor temperature over time.

2.6.2 Heating Control

The heating of the whole test-rig is split into a number of “sections” and controlled via six-zone PID temperature controller, Fig 2.22. Our system is set up so that each “section” corresponds to one heating cable. Although control of six separate “sections” is possible, only four are currently used in isothermal conditions. Our design has split the four sections into two separate groups. The first group, wired on one circuit, is set at 180°C to heat the test-rig and consists of three heating cables. The second group is wired on an independent circuit so as to reduce the chances of power failure. The group consists of a single heating cable, that is used to ensure the back pressure valve is constantly heated. This is very important to avoid the possibility of condensation, or the results become apparent as was seen in Fig 2.14. This heating tape is set to 200°C , but the valve box does not reach this temperature due to the difficulty in wrapping the heating cable tightly enough around the valve, as shown in Fig 2.18.

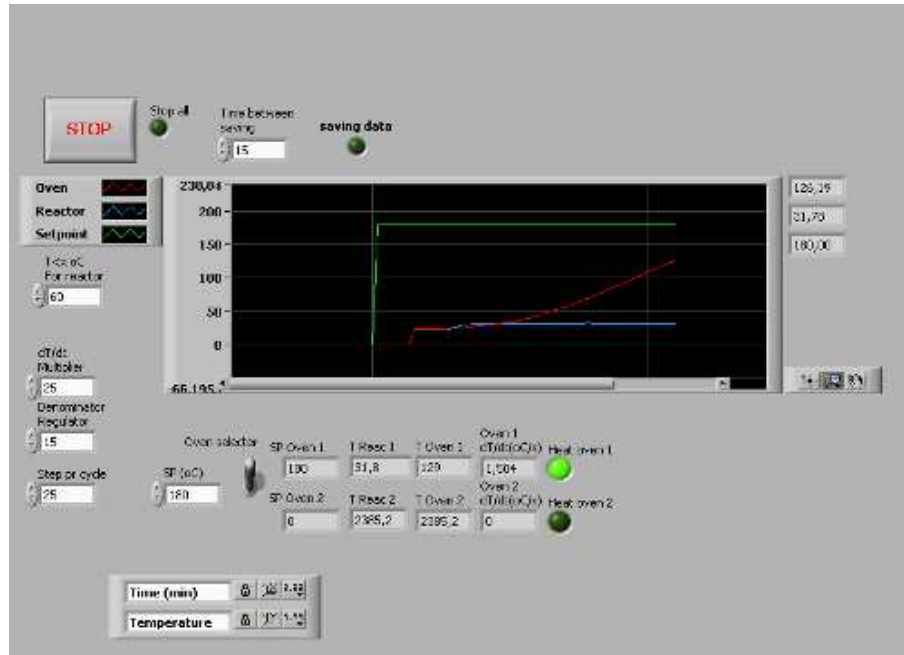


Figure 2.21: Labview Screen for Oven Control



Figure 2.22: CN616 controller

The wiring for the system involves the use of relays in order to control the current to the heating cables and thus the heating gradient. This required that all of the heating cables had to be wired correctly in order to function as desired. All the heating cables are used in conjunction with a thermocouple. The feedback from this thermocouple is then processed by the temperature controller, which in turn regulates the heating of the cables via the relays positioned on the back of the test-rig. A simplified schematic of the electrical wiring is shown in Fig 2.23

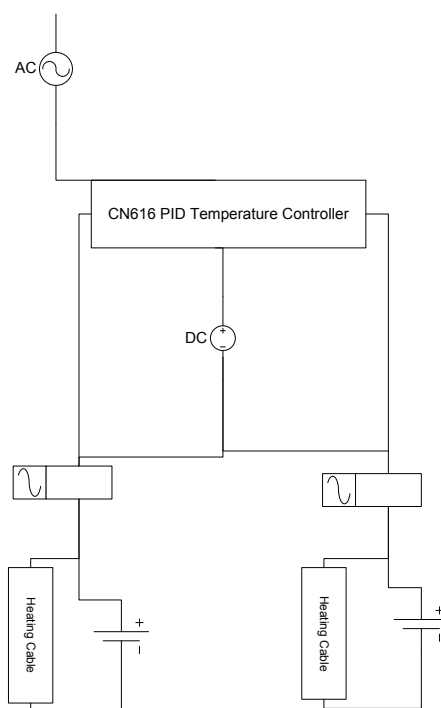


Figure 2.23: Simplified Wiring Diagram of CN616 controller

Heating Problems

During the initial construction of the system, Isopad brand heating tapes were used to heat the test-rig. Very quickly problems with the heating tapes became apparent, particularly regarding both short circuiting and uncontrolled heating of the system. This resulted in breaking a large number of these brand heating tapes, Fig 2.24. Following some discussion with col-

leagues we decided to change our heating *tapes* to heating *cables* (HSTD-type, Horst GmbH, Fig 2.25).

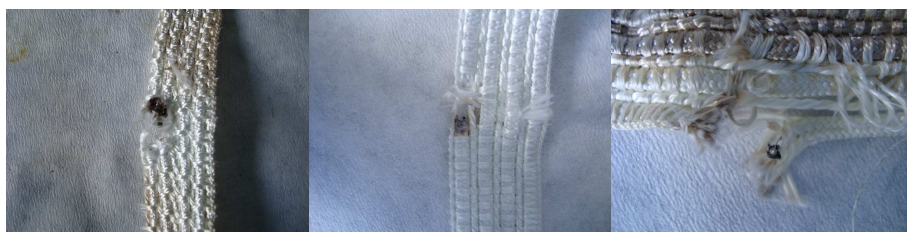


Figure 2.24: Broken Heating Tapes

These cables are of a very different construction from the original heating tapes. The original heating *tapes* were composed of metal heating bands covered in glass fibre. Each tape was constructed of four such bands all of which were coated in a further layer of glass fibre. This glass fibre coating makes the tapes tricky to work with, leaving residues behind whenever the tape is manipulated. Unfortunately manipulation of certain sections of the heating tapes was required (mainly around the reactor fittings). This repeated manipulation is also likely to have been the source of some of the failures observed. The major benefit of these heating tapes was the ability to completely cover the surface of the tubing in the test rig.



Figure 2.25: Example of a Heating Cable

The construction of the heating *cables* is of a simple heating core, insulated and then covered with a metal sheath. The construction of the cables

makes them more flexible and easier to manipulate, without any glass fibre involved in the construction the assorted issues such as dust and difficulties in handling. One of the initial concerns with switching to the heating cables was the formation of cold spots or cold fingers within the system, due to the cables inability to prove a constant temperature gradient around all parts of the pipes. After trialling the cables, this was not observed based on monitoring the flow of MeOH in and out of the system.

2.7 Addition of MeI co-catalyst

The addition of the MeI co-catalyst to the system proved more difficult than originally planned. The very high vapour pressure (53.32 kPa at 25.3°C), combined with low boiling point (42°C) and high density (2.28 g/ml) resulted in a number of issues in maintaining a steady flow rate of MeI into the system.

Initially there were issues with the HPLC pump at the start of the system. The MeI was by necessity kept outside of the fumehood and so fitted a carbon filter and pumped into the reactor via a 1/8 inch diameter length of tubing. The high density of the MeI (combined with high vapour pressure resulted in large bubbles visibly forming in the tubing leading from the bottle to the HPLC pump. Initial attempts to stop this involved using high flows of MeI through the pump, but this resulted in negative effects on the system, not least an increase in corrosion.

2.7.1 Initial Cooling

In order to try and reduce the vapour pressure of the MeI, it was decided to cool the bottle before it was pumped through the HPLC pump. This was achieved by the use of a Haake EK20 cryostat, Fig 2.26, available to us that was capable of cooling to -20°C in a propylene glycol bath (MeI melting point = -66.45°C). The introduction of cooling proved sufficient to remove air bubble in the feed leaving only MeIs high density to be dealt with.

The high density of MeI results in a large discrepancy between the “set” flow rate on the pump compared with the “actual” flow rate. Unfortunately

due to the method used for cooling of the MeI bottle, accurate weighing of the bottle was not possible and so a “correction” of MeI flow was only capable during data analysis. By trial it was possible to find an “accurate” flow that results in 0% conversion of MeI. This “correction” carries the important error that it was unable to account for HI presence in the product stream, nor for any sublimation of elemental I₂ in the system (the presence of I₂ is something that is observed during cleaning of the system)



Figure 2.26: Haake EK20 for Cooling MeI



Figure 2.27: Julabo F12 used to Pump Cooling Water Around the System

2.7.2 Further MeI cooling

At one point there was some doubt on the accuracy of the LMFC's measurement of MeOH flow into the system resulting in a large discrepancy between MeOH conversion and product formation. This made it seem like some MeOH was “disappearing” in the system. In order to try and correct this it was decided to measure an actual feed of MeOH by using a balance and a second HPLC pump, this was fed directly into the reactor via the second inlet originally designed for (and initially used for) addition of H₂O into the system. This addition of a second liquid feed meeting the MeI at the introduction into the reactor also resulted in “bubble” formation in the MeI

feed. The exact reason for this is not known. In order to try and combat this second “vapourisation” issue, it was decided to try and introduce a second cooling system for the MeI feed just prior to its entry into the reactor system. This was achieved by the adaptation of a second cryostat, Fig 2.27 attached to a water bath capable of pumping the cooled liquid round a loop. In the interests of safety and as an initial test, we chose water as the cooling fluid, cooled as low as possible by the water bath (setpoint ca. 1°C, but the cooling capability of the bath seems closely linked to the ambient temperature varying between 3°C - 7°C depending on the daily temperature and humidity.) Whilst only envisioned as a short term trial, this second cooling system proved so successful that it has now been adopted more permanently into the system and even looped with one of the product condensers after the GC allowing collection of liquid samples from the system (something previously impossible, or only via other external cooling of the condenser (typically with liquid N₂ which led to an issue of “backwash” from the gas bubbler used to monitor the gas flowing through the system.)

2.8 Major Alterations

2.8.1 Reactor Pressurisation

One of the most significant alterations to the system that allowed us to increase catalyst testing frequency was the introduction of a secondary gas inlet to the first reactor. This feed was taken directly from the CO inlet to the system and allowed independent pressurisation of the reactor and catalyst without requiring the use of the GMFC. Prior to the implementation of this we first required a stabilisation period of MeOH via the reactor bypass, the MeOH feed would then be stopped to pressurise the reactor (and test for leaks), before finally the MeOH feed was restarted. This process was very time consuming and could sometimes require several hours from the interruption of the MeOH feed until a stable level was obtained once again. This alteration significantly reduced the time from loading of a catalyst to a reaction ready system to approximately 20 minutes.

2.8.2 Removal of “Dead Space” after P Valve

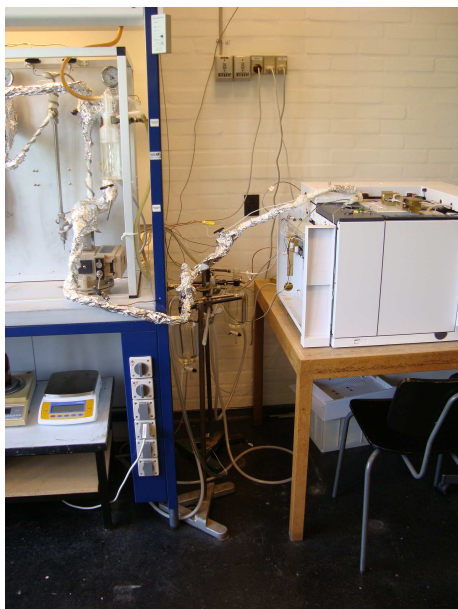


Figure 2.28: The Dead Space Previously Leading to the Reactor

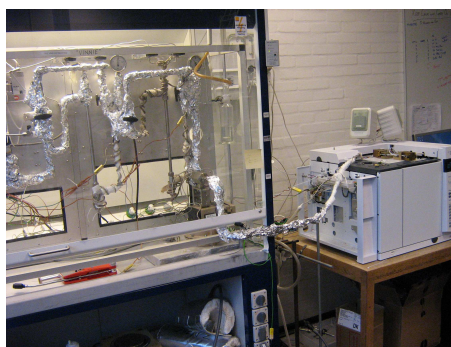


Figure 2.29: System After the Removal of The Dead Space

On the original plan for the system, Fig 2.2, two product recovery options were possible. These comprised of two condensers to isolate liquid products, Fig 2.28. One was placed between the pressure valve outlet and the second attached to the GC outlet. Unfortunately, in order to fit the condenser before the GC inlet this required a large volume of pipework. The major problem with this large volume was that the pressure at this point was close to 1 bar. This resulted in a low flow rate through this part of the system giving a large volume of “dead space.” The dead space resulted in a significant time lag between the product stream leaving the pressure regulating valve and reaching the GC inlet valve. At times up to three hours were required before any change in the reactor system was observed on the GC. Obviously the duration of the GC method is a factor in this delay, but such a delay was too long for us to monitor accurately any changes in the system. In order to resolve this, we removed the first condenser from the system entirely. By removing this condenser from the system, Fig 2.29, it allowed us to reposition

a significant volume of pipework resulting in a dramatic reduction in the volume from the pressure valve to the GC valve inlet. By doing this we dramatically decreased the “lag” from the system to the analytical system. The most significant knock-on effect of this was a dramatic reduction in catalyst testing times. Prior to this, it could take up to one week to obtain meaningful results from each catalyst as it was impossible to easily gauge the effects of changes to the system. By a reduction of this delay from three hours to approximately 30 minutes meant that the testing time for a catalyst was reduced to just over one day.

The issue of dead space also became apparent at other points during the course of the work, linked to alterations/removal of other components. As work went on we also tried to streamline the system whilst maintaining operational capacity.

See Appendix C for a full selection process flow diagrams.

2.9 Achieving a Suitable Back Pressure of the Pressure Regulating Valve

After some time of running the system, we eventually noticed the pressure valve was having problems in successfully regulating pressure. The valve pin was only recently replaced and the engineer was also puzzled by this problem. A solution was found by increasing the back pressure to the valve via a needle valve positioned just after the pressure valve outlet. At the same time a manometer was placed between the needle valve and the GC valve inlet to allow us to see how well the valve was regulating the pressure of the system. With this addition the problem seemed to resolve itself.

2.10 Product Isolation

Initially condensation was attempted at room temperature, but quickly this was shown to be impractical. It was then decided to introduce water cooling, via the mains water supply. Unfortunately this quickly ran into problems,

when it resulted in a flooding of the lab. The second solution was to make use of a cryostat to cool and pump a fixed volume of water through the system. This proved much more successful allowing easy collection of liquid product from the system. The condenser is shown in Fig 2.30 and 2.31



Figure 2.30: Condenser Containing Condensate from System



Figure 2.31: Condenser from Above, Showing Inlet and Outlet to Condenser

2.11 Maintenance/“down-time”

During any periods linked to maintenance on the test-rig there was a resulting “down-time” for catalyst screening. Although to try and limit this, component replacement/cleaning was generally carried out semi-regularly. This pre-emptive work was an attempt to reduce the chances of more serious breakdowns that would have required substantially more time to resolve. Unfortunately, by fixing one problem you often end up creating another, and as such on many occasions what seemed like a small issue quickly became much larger. One of the more general observations during the course of the work was that extended periods of “down time” was caused by interruption of electricity supply; shutdown of ventilation systems; holiday periods; other external maintenance often resulted in increased incidences of problems with the system. To combat this we have attempted to maintain the system in a

“stand-by” state whenever possible. This generally involves continuous heating combined with a constant flow of CO into the system. The process of bringing the system back up to operational capability after a shutdown also has to be a slow and gradual process, whereby any problems encountered may be fixed as they appear, in particular leaks. If this is not observed it was often the case that we very quickly ran into larger problems. This slow restart process was also used to save time. In order to repair/replace any components, it was required to remove the heating tape followed by the insulation from the specific part of the system. If this joint was half-way down a length of heating tape, the whole heating tape needed to be removed, the fitting replaced, then the heating tape re-attached. This process was very time consuming making it highly preferable that the problems were addressed before the heating tapes were in place.

Changes in the heating/cooling of the system could be linked to the creation of leaks within the system as the joints expand and contract accordingly. Swagelok components only create a “perfect” seal the first time they are used subsequently the seal formed is never quite as tight. The actions required to maintain the system such as the removal, replacement and altering of the various joints can reasonably be expected to contribute to the creation of leaks due such maintenance.

Each time the system has to be stopped and shutdown it is the case that for reasons of safety all pressure has to be released from the system. This process can never remove all traces of compounds from the system as a result these will remain and will condense out onto the internal surfaces. Most likely the continued presence of MeI within the system (and thus by extension HI) contribute significantly to corrosion of the system during any down time. By maintaining heating and a residual flow of CO in “stand-by” we are able to limit this condensation of the system and by extension some of the corrosion observed.

2.12 Blocking of the GC valve inlet

Towards the end of the project, it was observed that the pressure valve seemed to have difficulty regulating the pressure of the system. On further inspection the problem was isolated to the GC valve. On inspecting the valve was blocked by a hard black solid material, Fig 2.32. To try and clear the blockage, solvent was pumped through the valve using an HPLC pump. Initially acetone was used and it proved very difficult to pump the solvent through the blockage, with the pressure on the HPLC building up to 300 bar and triggering the automatic shutdown of the pump, Fig 2.33. Eventually after a number of days, we managed to get the solvent to flow through the valve, but still under high pressures. We chose to switch the solvent to AcOH to see if this would be more successful. The blockage proved to be slightly more soluble in AcOH, but it still proved difficult to dissolve. Finally, it was decided to replace the tubing leading up to the valve, removing the problem entirely.

2.13 Corrosion resistant materials

In an attempt to reduce corrosion affecting specific components in the system we attempted to replace some of the 316SS components with those composed of the more resistant Monel alloy-400*. Unfortunately these components also proved susceptible to corrosion under our reaction conditions and in

*See appendix E for a comparison of steel types

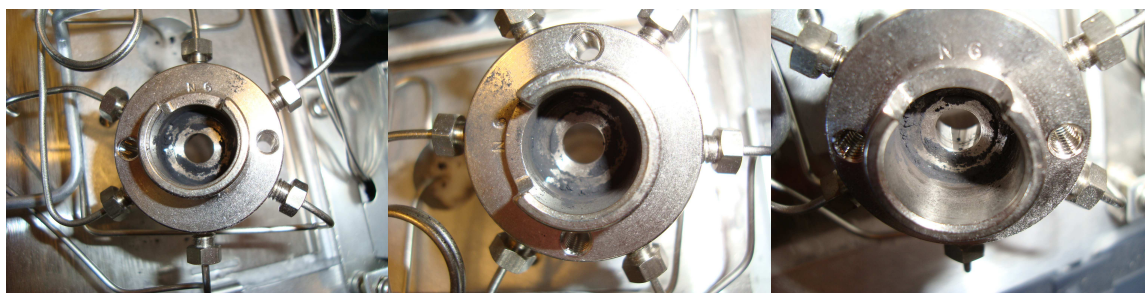


Figure 2.32: Blockage of the GC Valve



Figure 2.33: HPLC reading just after automatic shutdown

the interests of costs, convenience and interchangeability, we decided that it would be simpler to discontinue their use. Instead we carried on using 316SS components, but replacing them with 316Ti where possible, in order to try and reduce the corrosion of the 316SS components. Continuing redesign of the system still takes place alongside modifications to try and remove or limit the number of fittings in the system subject to corrosive conditions.

For a comparison of all the materials used see Appendix B

2.14 Final Incarnation of the Test-Rig

After various alterations and changes, the current form of the test-rig is shown in Fig 2.34.

2.15 Wacker Chemie AG Pilot Plant

Following on from the successes at DTU, a pilot scale plant was designed and build by Wacker Chemie AG at their site in Munich. In a departure from the results obtained at DTU, the major product was observed to be AcOH of a high purity level. Also in a departure from the DTU result, the major byproduct was methane, mainly observed during the start up period of the plant.

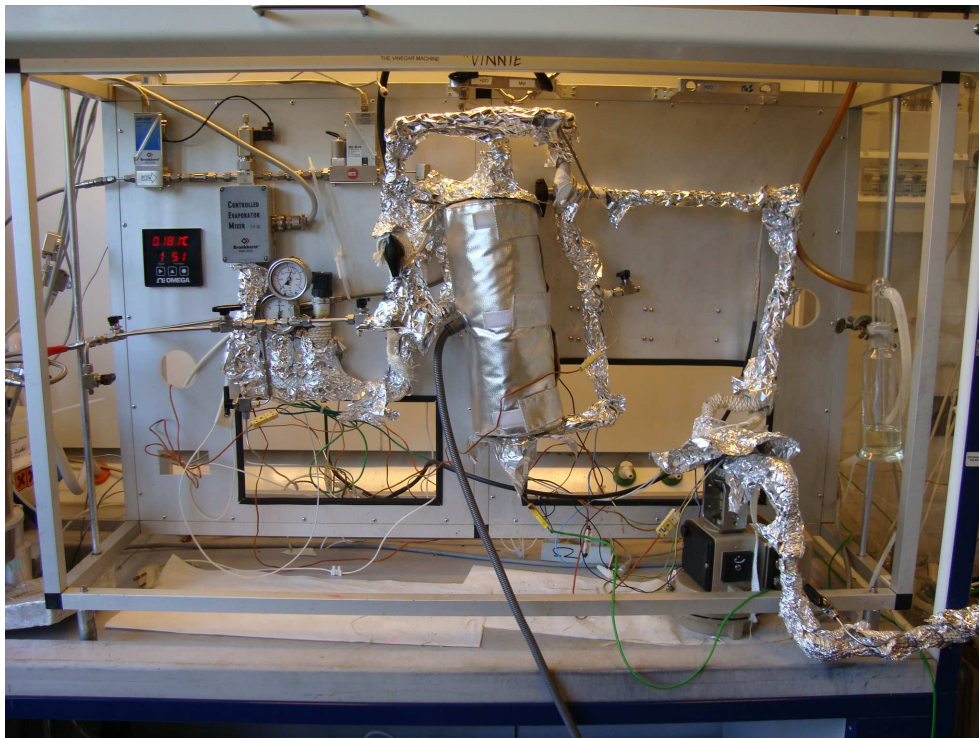


Figure 2.34: The Final and Current Incarnation of the Test-Rig

Chapter 3

Analytic system

The majority of chemical analysis was carried out via online Gas Chromatography (GC).

As a result of this a large body of analytical data resulted during the course of the project. Whilst for many cases a large excess of data is preferred, in this case it resulted in too much data to be completely analysed. Unfortunately for most of the project we had no way of easily processing the volume of data generated due to software “incompatibilities” requiring manual data entry for the majority of catalyst tests. As a result of this large amounts of time during the first two years of the project were spent on data entry. This can in part be related to the general complexity of the GC system, designed with three separate detectors to enable the complete detection of all likely byproducts.

3.1 GC Configuration

At the start of the project an Agilent 7890A GC was purchased. The model used is a three-module, on-line detector GC consisting of a packed-column channel (PCM-C) and a capillary-column channel (PCM-B+EPC), that is connected in series via a 10-port valve and a 6-port valve. The packed-column channel uses a TCD detector (N_2 carrier) for analysis of H_2 , while the capillary-column channel uses the combined FID/TCD detectors (He carrier)

for analysis of all organics, acids and H₂O, Fig 3.1. Although complex, this design, agreed on with the help of Agilent experts, allows an all-in-one analytical system for almost all possible products and byproducts of the system.

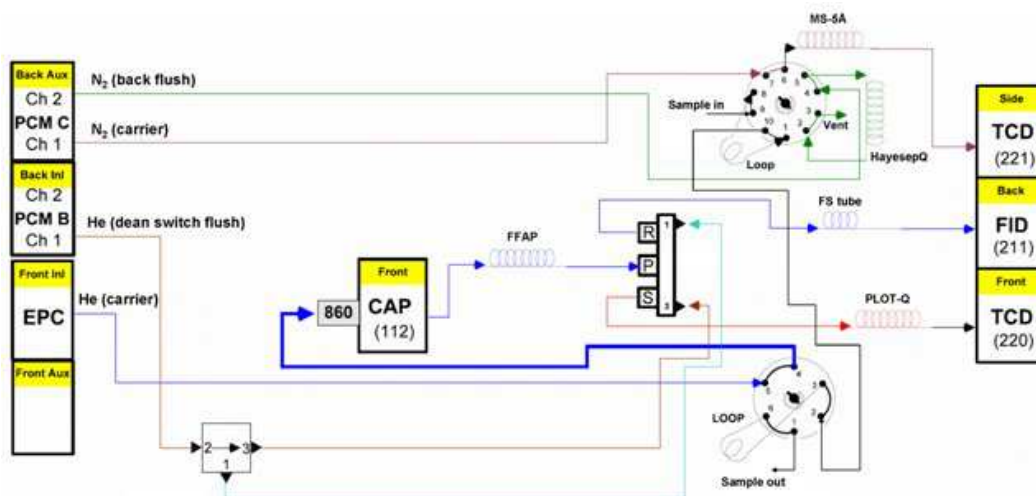


Figure 3.1: Configuration of the GC collums and valves

From the sample loop of the 10-port valve the sample is injected into a pre-column (HayesepQ) from where H₂ passes to a mol-sieve column (MS5) for separation followed by TCD detection. A back-flush of the pre-column allows all other retained components to be vented out. From the sample loop of the 6-port valve, the sample is passed into the capillary injection port (via a heated line) before injection into a capillary column (FFAP) where the heavier organic products are separated. After the capillary column the gas stream is split by a dean switch to allow the light components MeOH, MeI, MeOMe and H₂O to be separated on a Poraplot Q column (PLOT-Q) for detection by TCD, while the heavier organic products AcOH and AcOMe are sent to the FID detector via an empty column (FS tube).

3.1.1 H₂ Detector TCD

N₂ is used as a carrier gas through the molecular sieve column (MS5) at 30 mL/min with a pressure of 30 psi set on PCM-C channel 2 to enable

backflushing to prevent contamination of the column. (As hydrogen has a negative thermal conductivity relative to nitrogen, to obtain a positive peak on the chromatograph it is required to reverse the polarity of the detector.) Prior to injection, valve 1 is held in the “off” position (load), allowing the sample to flow through the loop filling it with the analyte. At time 0 mins, the valve is moved into position “on” (inject) allowing the contents of the loop to pass into the initial HayesepQ column. At time 0.4 mins, the valve is returned to the “off” position allowing back flushing of the remaining compounds resident in the precolumn (HayesepQ). By opening and closing the valve at these set points, we allowed only H₂ gas through to the molecular sieve column and onto the detector. Otherwise we would have contamination of the column with all of the other present compounds. The retention time of H₂ on the detector was found to be 0.79 min.

3.1.2 FID Detector

He is used as a carrier gas. The gas flow to this detector is limited by a deans switch, the switch is controlled via valve 3. Since the deans switch connects the columns leading to the FID and second TCD detector, it is not possible to set the flows of the empty column (FS tube) and the plot Q column independently of each other. In the empty column leading to the FID detector, the flow rate is set to 0.60 ml/min. The FID detector is used to detect all of the carbon containing compounds, with the exception of CO, the retention time of which are given in Table 3.1.

3.1.3 Organics TCD Detector

A carrier gas of He is used. Described above, this detector is linked with the FID via the deans switch. This requires a flow rate linked with that in the empty column (FS tube). To this end a pressure of 9.0 psi is used. The main use of this TCD is for the detection of water, however it is also possible to separate out a number of the other components allowing them to be detected via this TCD instead of the the FID. Unfortunately for AcOH, AcOMe and similar compounds, the choice of column results in large peak tails, making it

Table 3.1: Retention time of Compounds on the FID detector

Compound	Retention time (min)
Dimethyl ether (Me ₂ O)	2.24
Diethyl ether (Et ₂ O)	2.42
Methyl iodide (MeI)	3.41
Methyl acetate (AcOMe)	3.76
Ethyl Iodide (EtI)	4.16
Methanol (MeOH)	4.73
Ethanol (EtOH)	4.97
Propanol (PrOH)	5.76
Acetic acid (AcOH)	7.73

problematic to separate these components when they have similar retention times. A list of the retention times is given in Table 3.2.

Table 3.2: Retention time of compounds on the TCD detector

Compound	Retention time (min)
Dimethyl ether (Me ₂ O)	5.77
Diethyl ether (Et ₂ O)	7.75
Carbon monoxide (CO)	2.60
Acetic acid (AcOH)	9.87
Methyl acetate (AcOMe)	7.75
Methanol (MeOH)	6.09
Ethanol (EtOH)	7.22
Propanol (PrOH)	8.45
Water (H ₂ O)	6.51

Hydrogen Iodide Detection During the start of the project, construction of the system and design of the GC analytics was very much a hand-in-hand process. The complexity of the GC required many trial and error tests to find a suitable method program allowing for the separation and detection of all the important components from the reactor. In particular detection of HI (a key component in the reaction) has proved to be highly tricky. Literature searches have confirmed this difficulty, with very few published reports on GC detection of the compound. One of the results of this has been a significant imbalance between the iodine_{in} - iodine_{out} balance for the system.

3.2 Oven Ramp

The flows in all columns are maintained at a constant flow throughout the GC method. Separation of the components is therefore primarily controlled by variation of the oven temperature. Due to the similar size and chemistry of the compounds to be detected a temperature range from 35°C - 200°C is used with four different holding temperatures throughout the method. The oven heating is given in Table 3.3 represented graphically in Fig 3.2

Table 3.3: Oven Heating Programme

Rate	Set Temp	Hold time (min)	Run time (min)
-	35	2	2
13	60	0	39.231
50	150	1	67.231
50	200	3	10.723

3.3 Internal Standards

As a result of the complicated method programme developed to separate all the required components, there was also difficulty in finding a suitable internal standard for the system. Initially we focused on a liquid standard,

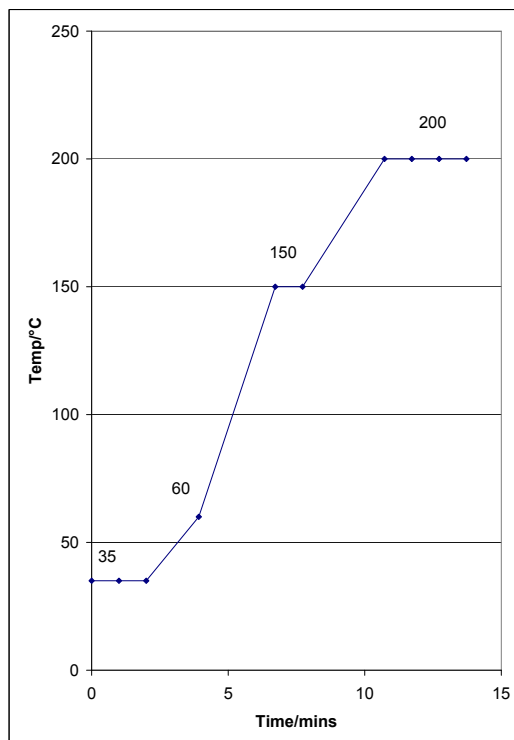


Figure 3.2: Temperature Profile of GC Method

but this was difficult to find. The standard was required to be soluble in methanol, unreactive under the conditions used and we had to be able to resolve it. Initially it seemed like a suitable compound was 2-methoxyethanol, but unfortunately after a few trials in the reactor system it was found to react.

As a result of all of this, we switched to relating conversion to MeOH based on the previous calibration curves.

After this, we decided to try some inert gases as standards. Since we were already using both N_2 and He for the GC detectors, we would have to try and find some other gas. Initial trials involved both Ar and CO_2 , but it was very difficult to separate these gases from the CO peak on the TCD. One possibility was to try and alter the GC method to allow for separation, but

since it had taken so long to find a method that gave adequate separation of all the other compounds, we decided to leave this as it was. A chance suggestion from a colleague led us to try methane as a standard.

3.3.1 Methane as an Internal Standard

Methane is a highly stable compound and generally unreactive towards other chemicals. After some initial tests, we could show that methane could be easily separated and detected on both the FID and TCD. Unfortunately, Rh is a very good water-gas shift ($\text{CO} + \text{H}_2\text{O} \rightarrow \text{CO}_2 + \text{H}_2$) and methanation catalyst ($\text{CO} + 3 \text{H}_2 \rightarrow \text{CH}_4 + \text{H}_2\text{O}$). If these reactions were occurring the internal standard would no longer be accurate giving us lower yields. Fortunately both of the reactions result in or consume H_2 which we were able to detect this via a TCD detector on the GC. Based on the previous experiments using a liquid internal standard, we didn't observe the formation of any methane in the system nor of H_2). Once we switched to CH_4 as our internal standard, we were still unable to observe any H_2 formation, making it highly unlikely that there was any water-gas shift or methanation reactions occurring after adding CH_4 to our system.

3.4 Calibration of components

Calibration of all the standard MeOH carbonylation byproducts was carried out, mainly by direct injections to the GC, although once we switched to online usage of the system, the retention times observed during calibration remained within acceptable levels of deviation. This method has remained unchanged during the course of the project.

Initial calibration was done with reference to MeOH, the response factors obtained were then used to relate to, initially, 2-methoxyethanol and then methane internal standards.

Chapter 4

Experimental results

Table 4.1 presents an overview of all the experiments carried out during the course of this work. It outlines the rhodium source, IL used and highlights the TOF and STY for each reaction.

4.1 Replication of Previous Results

Initial catalyst testing focused on the replication of the original results achieved by Riisager *et. al.*¹¹⁶ using the newly constructed test rig. The system as described is based on a $[\text{Rh}(\text{CO})_2\text{I}]^-$ catalytic anion, dissolved in BmimI ionic liquid and supported on commercially available silica.

After some initial tests to find the best flows and temperatures for the reactor, we were very quickly able to achieve similar results to those published i.e. TOF = 100, Table 4.2. All of the catalysts used in these initial tests were synthesised using chemicals available in the lab and with standard schlenk techniques under an Ar atmosphere, as laid out in the original paper. Specific details of the procedure are laid out in Appendix A

Experiment	Metal source	IL	Rh loading (wt%)	IL loading (vol%)	TOF (nor- malised)	STY (nor- malised)
1	[Rh(CO) ₂ I] ₂	Bmim I	0.65	42	---	---
2	[Rh(CO) ₂ I] ₂	Bmim I	0.65	42	---	---
4	[Rh(CO) ₂ I] ₂	Bmim I	2.45	42	--	+
5	[Rh(CO) ₂ I] ₂	Bmim I	3.56	42	---	-
6	[Rh(CO) ₂ I] ₂	Bmim I	2.45	42	+	+
7	[Rh(CO) ₂ I] ₂	Bmim I	2.45	42	++	+++
8	[Rh(CO) ₂ Cl] ₂	Bmim I	2.45	42	++	+++
9	[Rh(CO) ₂ I] ₂	Bmim I	2.45	42	+++	++++
10	[Rh(CO) ₂ Cl] ₂	Bmim Cl	2.56	47	---	--
11	[Rh(CO) ₂ Cl] ₂	PBu ₃ Me I	2.31	56	+++	+++
12	RhCl ₃	Bmim I	4.6	43	--	++
13	IrI ₄	Bmim I	4.4	54	--	--
14	[Rh(CO) ₂ Cl] ₂	Bmim I	2.58	42	--	--
15	[Rh(CO) ₂ Cl] ₂	Bmim I	2.42	45	-	--
16	[Rh(CO) ₂ Cl] ₂	PBu ₃ Me I	2.6	47	o	o
17	[Rh(CO) ₂ Cl] ₂	BDmim I	2.47	44	+	o
18	[Rh(CO) ₂ Cl] ₂	Bu-Pyr I	2.54	43	--	--
19	[Rh(CO) ₂ Cl] ₂	TMGH I	3.28	46	o	+++
20	[Rh(CO) ₂ Cl] ₂	BmimSO ₃ H I	3.3	7.27	+	+
21	[Rh(CO) ₂ Cl] ₂	BmimSO ₃ H I	2.52	41.43	-	-
22	[Rh(Acac) · 2 CO	BmimI	4.67	42.47	--	---
23	[Rh(CO) ₂ Cl] ₂	Bu ₃ MeP Br	2.34	42	--	---
24	[Rh(CO) ₂ Cl] ₂	PyrH I	2.35	41.96	----	----
25	[Rh(CO) ₂ Cl] ₂	Mim-C ₄ H ₈ COOH I	2.61	43	----	--
26	[Rh(CO) ₂ Cl] ₂	Bmim I	2.61	43	o	-
27	[Rh(CO) ₂ Cl] ₂	Ph ₃ MeP I	2.2	49.1	+++	+++
28	[Rh(CO) ₂ Cl] ₂	Ph ₃ MeP I	2.17	33.5	++++	+++
29	[Rh(CO) ₂ Cl] ₂	Bmim OH	2.2	49.1	----	--
30	[Rh(CO) ₂ Cl] ₂	No IL	3.03	0	----	----
31	[Rh(CO) ₂ Cl] ₂	Ph ₃ MeP I	2.5	16.23	---	---
32	[Rh(CO) ₂ Cl] ₂	Ph ₃ MeP I	2.72	8.34	--	---
33	[Rh(CO) ₂ Cl] ₂	Bmim I	3.04	41.52	-	+

Table 4.1: Results Summary

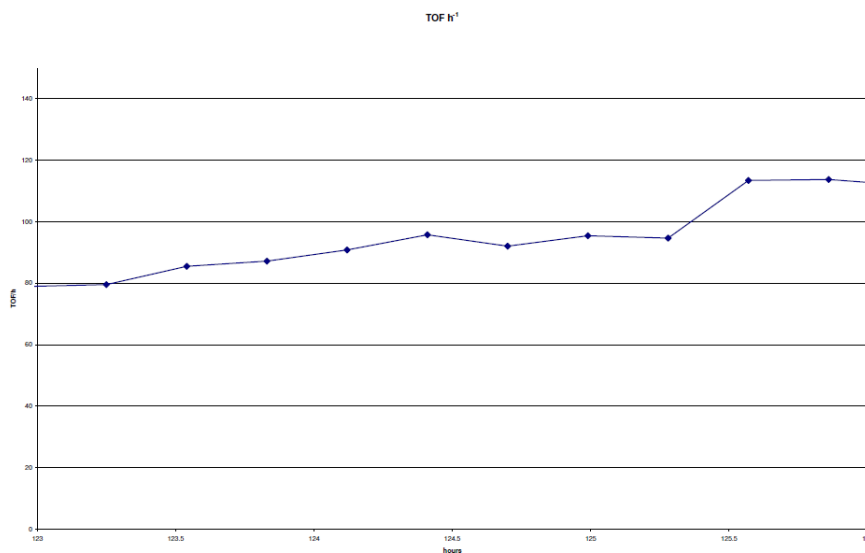


Figure 4.1: TOF for the initial Experiment

Table 4.2: Comparison of published results and initial trials

Experiment	Metal source	IL	Rh loading (wt%)	IL loading (vol%)	MeOH conversion (%)	TOF (normalised)
Original Results	[Rh(CO) ₂ I] ₂	Bmim I	0.65	42	99	- - -
2	[Rh(CO) ₂ I] ₂	Bmim I	0.65	42	25	- - -

4.2 Iodide dimer

Synthesis

Schlenk techniques were used to limit atmospheric exposure of the air sensitive [Rh(CO)₂I]₂ catalyst precursor, Fig 4.2. With our preparation, complete isolation from atmosphere is impossible. The preparation requires usage of an accurate balance and the result of this is that the precursor must be exposed to air for some time during weighing and transfer to the schlenk tube used for synthesis. Since an accurate weight is necessary to calculate the activity of the catalyst in the system, it is impossible to relate this exposure to atmosphere to any deactivation of the catalyst.

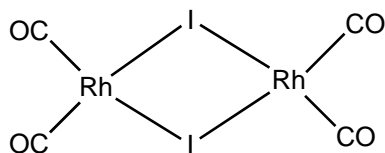


Figure 4.2: $[\text{Rh}(\text{CO})_2\text{I}]_2$ dimer

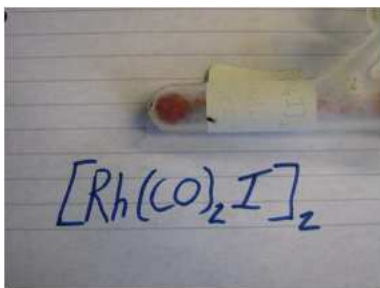


Figure 4.3: $[\text{Rh}(\text{CO})_2\text{I}]_2$ dimer under CO atmosphere



Figure 4.4: Freshly prepared SILP catalysts

Appearance

The $[\text{Rh}(\text{CO})_2\text{I}]_2$ catalyst precursor is in the form of dark red crystals, Fig 4.3. If the precursor is left exposed to air for an extended period an obvious change can be noticed as the originally bright orange crystals will slowly darken until they form a black powder, the air stable but catalytically inactive RhI_3 .

After synthesis the resultant SILP catalyst takes the form of a fine brown powder, Fig 4.4 . Once the catalyst is exposed to air during loading into the reactor a subtle colour change is observed. Once the catalyst is exposed to air an almost immediate darkening of the catalyst is observed. This darkening to a “medium” brown occurs within 1–1½ minutes after initial exposure to air, Fig 4.5 . If the catalyst is left for an extended period it will darken even further to a very dark brown or black colour, Fig 4.6. The most obvious explanation for such a colour change is air oxidation of the Rh(I) present in $[\text{Rh}(\text{CO})_2\text{I}]_2$ to the Rh(III) in RhI_3 also liberating the loosely bound CO ligands. The most important implication of this is that the ionic liquid alone does not provide a sufficient protecting layer to prevent oxidation of the air sensitive Rh centre. See Appendix F for the complete series of pictures.



Figure 4.5: Fresh SILP in Air



Figure 4.6: Discoloured SILP in Air

Synthesis under CO atmosphere

The visible discolouration of the catalyst when exposed to air indicates that actual catalyst being loaded into the reactor is not identical to that synthesised under an inert atmosphere. Any deactivation occurring could be removing a large part of the catalytic activity before the catalyst was loaded into the reactor and pressurised under a CO atmosphere. Our assumption is that both times the rhodium-iodide complex is exposed to air (during synthesis and loading), there must be some degree of deactivation occurring. This is supported by the colour change observed between exposing the SILP to air for the first time until it is loaded into the reactor. The initial exposure during the synthesis was unavoidable but could be limited by carrying out the transfer of the SILP precursors quickly. A further idea attempted was to replace the Ar atmosphere during synthesis with a CO atmosphere. It was hoped that this excess of CO would “reverse” any CO loss that may have occurred during the transfer of $[\text{Rh}(\text{CO})_2\text{I}]_2$ to the schlenk tube. An added benefit of this was the ability to control the atmosphere during drying. If the catalyst losing CO ligands and deactivating under a normal atmosphere it was hypothesised that drying of the SILP catalyst under vacuum was also likely to result in the loss of CO ligands. This small alteration was successful and showed an improvement in the catalyst activity. However, the distinct colour change observed during the loading procedure was still evident, suggesting that there remained loss of CO during the period the catalyst was

exposed to air.

Usage on Industrial Scale

This observed discolouration of the catalyst could be a significant issue if the process were scaled up to industrial scales, particularly due to the inability to successfully measure how much of the expensive Rh based catalyst was active and how much was deactivated. Trying to keep the catalyst under a CO atmosphere during loading was also impossible, as catalyst loading would be carried out by workers “emptying bags of the catalyst into the reactor,” thus leading to insurmountable health and safety issues. The common factor between both of these syntheses seemed to be the problem of having to expose the catalyst to an air atmosphere during the loading procedure. This seemed to be resulting in either oxygen dissolving into the ionic liquid and quickly oxidising the Rh centre or weak bonded CO ligands (due to the large excess of I⁻ anions available) being released from the Rh centre. This commonality of gas diffusion seemed to form the basis of the problem. The solution decided on to try and remove this issue was via incomplete drying of the SILP during synthesis or by “wetting” of the SILP after synthesis. In each case the volume of solvent remaining would have to be sufficient to fill the remainder of the pore volume not already occupied by the ionic liquid and metal complex and coat the entirety of the surface of the catalyst. This was easy to determine visually in the post-synthesis wetting procedure, but was not so easy to judge via the incomplete drying procedure. Both of the procedures were attempted using two different solvents, MeOH and AcOH. In all cases where the [Rh(CO)₂I]₂ precursor was used in combination with this procedure an increase in activity was observed, Table 4.3. In particular the case using AcOH wetting resulted in one of the few occasions of the test rig producing AcOH. These inherent difficulties in the synthesis of catalysts mean that a large period of time was having to be used in their synthesis, approximately two days. It also proved difficult to accurately judge the mass of catalyst being loaded into the reactor due to the additional mass of the solvent contained within the pores.

Table 4.3: Catalyst Wetting Trials

Experi- ment	Metal source	IL	Protec- tion	Atmos phere	Rh loading (wt%)	IL loading (vol%)	TOF (nor- malised)	STY (nor- malised)
2	[Rh(CO) ₂ I] ₂	Bmim I	X	Argon	0.65	42	---	---
4	[Rh(CO) ₂ I] ₂	Bmim I	X	Argon	2.45	42	--	+
5	[Rh(CO) ₂ I] ₂	Bmim I	X	Argon	3.56	42	---	-
6	[Rh(CO) ₂ I] ₂	Bmim I	MeOH	CO	2.45	42	+	+
7	[Rh(CO) ₂ I] ₂	Bmim I	MeOH	CO	2.45	42	++	+++
9	[Rh(CO) ₂ I] ₂	Bmim I	AcOH	CO	2.45	42	+++	++++

Rh Loading

Initial experiments looked at optimising the loading of Rh that would provide the best catalytic activity. We saw that by increasing the initial loading of Rh by a factor of 4, a saw significant increase in the catalytic activity was observed. In order to try and improve this even more, we increased the Rh loading 5 time from the original to 3.56 wt%, but this did not lead to a corresponding increase in activity. In fact we saw a decrease in activity, Table 4.4, implying that the loading of Rh was too high to fully utilise all of the metal present. As a result of this, we began to use a 4x loading of Rh, equivalent to 2.45 wt%.

Table 4.4: Variation of Rh loading

Experi- ment	Metal source	IL	Rh loading (wt%)	Il loading (vol%)	TOF (normalised)	STY (nor- malised)
2	[Rh(CO)2I] ₂	Bmim I	0.65	42	---	---
4	[Rh(CO)2I] ₂	Bmim I	2.45	42	--	+
5	[Rh(CO)2I] ₂	Bmim I	3.56	42	---	+

4.3 Chloride precursor

As the availability of our [Rh(CO)₂I]₂ source was declining, instead of carrying out further synthesis involving further work under a CO atmosphere, we decided to try and synthesis a SILP using the [Rh(CO)₂Cl]₂ precursor complex, Fig 4.7 and 4.8, available cheaper and in larger quantities as well as

being more air and temperature stable than the iodide precursor, Table 4.5. Initial trials using this alternative precursor in Bmim I showed that it too possessed a high catalytic activity for the reaction, although not as high as the previous iodide precursor. Importantly, there was no immediately visible colour change on exposure to air. The reduction in activity of approximately 5-10 % combined with the requirement to have a slightly higher MeI flow were considered, alongside the issues associated with the synthesis of the iodide precursor catalyst. Considering these factors, it was decided to attempt the use of the chloride complex in some other ionic liquids already screened for the iodide catalyst. In each case the chloride showed a slightly lower activity, but appeared to be significantly more stable during the synthesis and loading procedures.

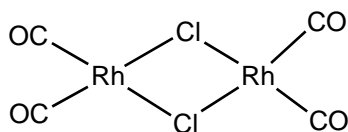


Figure 4.7: $[\text{Rh}(\text{CO})_2\text{Cl}]_2$ dimer Structure

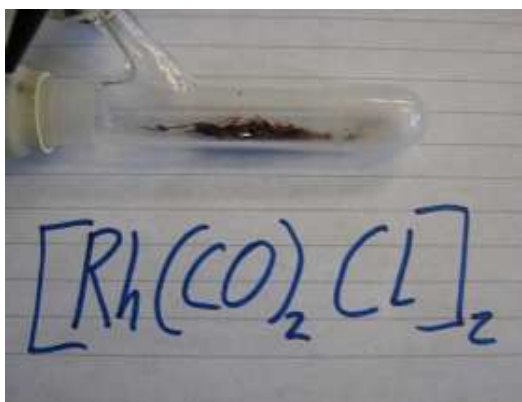


Figure 4.8: $[\text{Rh}(\text{CO})_2\text{Cl}]_2$ dimer Crystals

Table 4.5: Comparison of Iodide and Chloride Rhodium Precursors

Experiment	Metal source	IL	Protection	Atmosphere	Rh loading (wt%)	IL loading (vol%)	TOF (normalised)	STY (normalised)
4	$[\text{Rh}(\text{CO})_2\text{I}]_2$	Bmim I	X	Argon	2.45	42	--	+
9	$[\text{Rh}(\text{CO})_2\text{I}]_2$	Bmim I	AcOH	CO	2.45	42	+++	++++
8	$[\text{Rh}(\text{CO})_2\text{Cl}]_2$	Bmim I	X	Argon	2.45	42	++	+++
14	$[\text{Rh}(\text{CO})_2\text{Cl}]_2$	Bmim I	X	Argon	2.58	42	--	--
15	$[\text{Rh}(\text{CO})_2\text{Cl}]_2$	Bmim I	AcOH	CO	2.42	45	-	--

4.4 Rh Sources

Having begun with the industrial Rh source and then moved on to its air stable chloride analogue, we decided to explore other Rh sources to see how their activity compared. The most obvious starting point was the precursor used in both the synthesis of $[\text{Rh}(\text{CO})_2\text{Cl}]_2$ and $[\text{Rh}(\text{CO})_2\text{I}]_2$, $\text{RhCl}_3 \cdot x\text{H}_2\text{O}$. A miscalculation during the synthesis resulted in a Rh loading twice as much as normal. Despite $\text{RhCl}_3 \cdot x\text{H}_2\text{O}$ being a non-catalytic compound in the standard industrial reaction, we were able to observe a degree of catalytic activity. The activity was, in some cases, comparable to that observed for the iodide and chloride sources.

Further exploring this route we also decided to test $\text{Rh}(\text{acac}) \cdot 2\text{CO}$ as a source of Rh. This Rh source is the one used in the formulation of a hydroformylation catalyst. Again, a minor miscalculation resulted in a high Rh loading for the catalyst. Despite this high Rh loading, the activity observed was low. The reasoning for the difference in activity between $\text{RhCl}_3 \cdot x\text{H}_2\text{O}$ and $\text{Rh}(\text{acac}) \cdot 2\text{CO}$ is not easy to determine.

It should be noted, that neither compound is known to be catalytically active for carbonylation reactions. In industrial batch reactions, it is important to avoid the triiodide analogue RhI_3 as it is the unreactive deactivation product formed by the system. Despite this, both of the compound show some degree of catalytic ability when used in a SILP System, Table 4.6. Under the conditions we utilise with an environment saturated in I^- anions and with a high CO pressure seems to be sufficient to generate some sort of catalytic system suitable for carbonylation reactions.

Table 4.6: Alternative Rhodium Sources

Experiment	Metal source	IL	Rh loading (wt%)	IL loading (vol%)	TOF (normalised)	STY (normalised)
4	$[\text{Rh}(\text{CO})_2\text{I}]_2$	Bmim I	2.45	42	--	+
8	$[\text{Rh}(\text{CO})_2\text{Cl}]_2$	Bmim I	2.45	42	++	+++
22	$[\text{Rh}(\text{Acac}) \cdot 2\text{CO}]$	BmimI	4.67	42.47	--	---
12	$\text{RhCl}_3 \cdot x\text{H}_2\text{O}$	Bmim I	4.6	43	--	++

4.5 Cation variation

All cation variation experiments were carried out on the $[\text{Rh}(\text{CO})_2\text{Cl}]_2$ precursor complex.

Initially N- based ILs based on imidazolium, pyridinium and guanidinium cations were studied. The results achieved do not appear to show any general trend regarding size or functionality of the cation. Bmim I remains the most effective IL with only TMGH I comparing in activity, Table 4.7. Interesting the two cases where it was attempted to functionalise the IL did not result in an improved reactivity, nor a significant change in the product distribution, Table 4.10 All of the N- based compounds were ILs and so by definition liquids below 100°C . This low melting may have a distinct effect on their nature at the reaction temperature of 190°C , particularly if hot spots exist at the reaction surface.

The original patent covers the use of phosphorous based ILs alongside nitrogen based ones, so it was decided to try a phosphonium iodide based IL with the system. Our initial trial on $\text{PBU}_3\text{Me I}$ seemed to be very successful. The initial test giving results better than any of the N- based ILs so far. The reason as to why there should be a significant increase in activity with a phosphorous based salt is not something immediately apparent.

All of the salts studied were classified as ionic liquids. After this screening of N- based cations, it seemed that the effect, if any, of cation variation was insignificant compared to that of not using an iodide anion in the system. A switch of cation to P- based molecules, led to much more significant effect on the achieved results.

All of the phosphonium salts studied, showed higher activity compared to the imidazolium based ILs. All of the phosphonium salts had higher melting points compared to the imidazolium with a number being molten salts due to having melting points above 100°C . The improved activity of $\text{PR}_4 \text{ I}$ salts is not easy to explain. It can be speculated that the improvement is linked to the well documented effects of phosphonium ligands on the standard homogeneous rhodium catalyst. This is hard to verify. The limiting factor of these phosphonium salts is the upper temperature of the reactor. As all

experiments were carried out at 190°C meaning that this was the upper limit for the salt’s melting point. In order to explore further avenues using the phosphonium salts it was decided to explore eutectic mixtures in the hope generating a suitably low melting combination to try in the system. The salts used were those easily obtained commercially and mixtures of 0.5:0.5 mol mixtures were used

Table 4.7: Variation of Cation Used

Experi- ment	Metal source	IL	Rh load- ing (wt%)	IL load- ing (vol%)	TOF (nor- malised)	STY (nor- malised)
4	[Rh(CO) ₂ I] ₂	Bmim I	2.45	42	--	+
8	[Rh(CO) ₂ Cl] ₂	Bmim I	2.45	42	++	+++
11	[Rh(CO) ₂ Cl] ₂	PR ₄ I	2.31	56	+++	+++
16	[Rh(CO) ₂ Cl] ₂	PR ₄ I	2.6	47	o	o
17	[Rh(CO) ₂ Cl] ₂	BDmim I	2.47	44	+	o
18	[Rh(CO) ₂ Cl] ₂	Bu-Pyr I	2.54	43	--	--
19	[Rh(CO) ₂ Cl] ₂	TMGH I	3.28	46	o	+++
21	[Rh(CO) ₂ Cl] ₂	BmimSO ₃ H I	2.52	41.43	-	-
23	[Rh(CO) ₂ Cl] ₂	Bu ₃ P Br	2.34	42	--	---
24	[Rh(CO) ₂ Cl] ₂	PyrH I	2.35	41.96	----	----
25	[Rh(CO) ₂ Cl] ₂	Mim-C ₄ H ₈ COOH I	2.61	43	----	--
27	[Rh(CO) ₂ Cl] ₂	Ph ₃ MeP I	2.2	49.1	+++	+++
30	[Rh(CO) ₂ Cl] ₂	No IL	3.03	0	----	----

4.6 Anion variation

If altering the cation has an effect, then what would happen if we altered the anion. To find this out, we tested a selection of alternative anions as well as a heterogeneous system containing no IL. In all cases activity is lower than systems with I⁻, the implication of this being that I⁻ is important in the system, Table 4.8

In order to investigate this further, it was decided to look into the effects of altering the anion in the ionic liquid. ILs with iodide anions are not commonly available commercially and the the synthesis of most of such ILs is carried out by ion exchange from the chloride. This made the logical first

step to be a switch to the closest chloride equivalent of Bmim Cl. This trial was initially carried out on the $[\text{Rh}(\text{CO})_2\text{I}]_2$ complex due to its standard as the “base” catalyst. In this case whilst activity was seen, it was lower than that seen in the “standard” tests. The next test involved switching to the $[\text{Rh}(\text{CO})_2\text{Cl}]_2$ complex, also with Bmim Cl. This trial showed a significant drop in observed activity, to approximately 1/2 of that seen when the iodide IL is used.

Table 4.8: Anion Variation

Experi- ment	Metal source	IL	Rh loading (wt%)	IL loading (vol%)	TOF (nor- malised)	STY (nor- malised)
4	$[\text{Rh}(\text{CO})_2\text{I}]_2$	Bmim I	2.45	42	--	+
8	$[\text{Rh}(\text{CO})_2\text{Cl}]_2$	Bmim I	2.45	42	++	+++
10	$[\text{Rh}(\text{CO})_2\text{Cl}]_2$	Bmim Cl	2.56	47	---	--
23	$[\text{Rh}(\text{CO})_2\text{Cl}]_2$	Bu ₃ P Br	2.34	42	--	---
29	$[\text{Rh}(\text{CO})_2\text{Cl}]_2$	Bmim OH	2.2	49.1	----	--
30	$[\text{Rh}(\text{CO})_2\text{Cl}]_2$	No IL	3.03	0	----	----

4.7 Iridium Catalysts

Iridium is also catalytically active for the carbonylation of methanol. This is particularly emphasised by the commercialisation of the Cativa process. It was decided to try and apply the SILP concept to an Ir based system. Our first problem with any such trials was to obtain a suitable Ir source. After some searching we were able to locate a supply of IrI_4 , which we dully used. The oxidation state of +4 also proved rather interesting for an iodide complex of Ir. We succeeded in synthesising an Ir based SILP using Bmim I. Unfortunately the Ir SILP catalyst produced was not particularly active, as is shown in Table 4.9. As this experiment was tried with an “unusual” Ir source, we attempted to synthesise some further Ir based SILPs, but this proved surprisingly difficult. We obtained a sample of $\text{IrCl}_3 \cdot \text{H}_2\text{O}$, the iridium analogue of our rhodium source. Following procedures outlined in literature we tried to synthesise and isolate the suitable Ir catalyst for the carbonylation reaction. In each case we were unable to isolate any Ir containing complex

and thus create a usable SILP catalyst.

Table 4.9: Rhodium vs. Iridium Catalysts

Experi- ment	Metal source	IL	Metal loading (wt%)	IL loading (vol%)	TOF (nor- malised)	STY (nor- malised)
4	$[\text{Rh}(\text{CO})_2\text{I}]_2$	Bmim I	2.45	42	--	+
8	$[\text{Rh}(\text{CO})_2\text{Cl}]_2$	Bmim I	2.45	42	++	+++
13	IrI_4	Bmim I	4.4	54	--	--

4.8 Products

The major reaction product in all of our experiments is methyl acetate. This represents a significant difference compared to most reported Monsanto style reaction systems where the majority product is always AcOH. We only succeeded in forming AcOH as a reaction product in only three occasions, Table 4.10. Our major reaction byproduct was DME, with a yield typically of less than 5% and no propionic acid nor other standard byproducts were observed. These results seem at odds with the general mechanism of the Monsanto process, but this mechanism has been well established and studied. However, the mechanism has only ever been studied for reactions carried out batchwise and not as a continuous flow reaction, such as ours. A continuous flow system such as the SILP one seems to introduce variation to the eventual product distribution. This may be linked to the fact that the SILP principle results in a very different diffusion profile compared to that of the batch process.

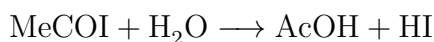
Table 4.10: Main Product Distribution over Presented Reactions

Experi- ment	MeI yield (%)	MeOH conv (%)	MeOAc (%)	AcOH (%)	DME (%)	STY (nor- malised)
1		60	20	1.5	5	
2	9	25	12	0	0.6	---
4	8	49-58	17-27	0	0.5	+
5	10	30-60	30-60	0	10 to 5	-
6	9-17	50	40	0-5	1	+
7	20	70	60	0	1	+++
8	18	60	50	0	2	+++
9	16	80	60	9-10	1.5	++++
10	24	40-60	20-25	0	10	--
11	20-30	60-80	60-70	0	2-3	+++
12	20	70	50	0	2	++
13	25	40-60	15-20	0	2-3	--
14	20	30	30	0	2-3	--
15	40	50	25	0	5	--
16	23	80	40	0	1.5-4	o
17	20	70	40	0	1-6	o
18	21	60	20-30	0	4	--
19	23	40-70	30-40	0	3	+++
20	24	60-65	30-45	0	2-2.5	+
21	20	40-50	17-23	0	2-2.3	-
22	20-22	35-40	13-20	0		---
23	15	55-60	14-17	0	1.3	---
24	20	13-50	16-38	0	1.7-2.5	----
25	20	62-75	27-31	0	1.5-1.9	--
26	17-19	62-70	28-30	0	1.5-1.8	-
27	22-41	87-92	57-66	0	1-2.1	+++
28	21-24	65-76	53-66	0	5.3-7.4	+++
29	2-17	24-37	20-30	0	1-7	--
30	4-27	0.6-30	0.2-7	0	2.3-12	----
31	6-17	30-65	7-22	0	1-5	---
32	28-35	68-71	15-24	0	4.7-7	---
33	27-40	50-75	10-35	0	1.5-7	+

In a SILP system, the active catalytic site is constrained in the IL layer, making the diffusion of the reagents into the IL bulk particularly important under the reaction conditions. It is known that the solubility of CO in ILs is limited,^{126–129} whilst the solubility of MeOH is very high.¹³⁰ The nature of our system, especially the high pressures used, make it difficult to estimate the solubility of the CO in comparison to MeOH. If we assume a similar behaviour to that at lower temperatures and pressures, a result of this would be a significant excess of MeOH dissolved in the IL in relation to CO. It may be that in the final stage of the catalytic cycle, there is a high excess of MeOH present at the catalyst site once the dissociation of the acetyl iodide occurs. This MeOH excess seems to present a more suitable target and so undergoes esterification with the acetyl species resulting in a final product of MeOAc. Another possibility is that the high polarity of the AcOH formed results in much slower diffusion out of the IL allowing time for an esterification reaction to occur before it diffuses back into the system. The role of HI in these processes is unclear, and the inability to detect it via the GC means we cannot draw any conclusions on its role in the process. This accumulation of the acid at the reaction site may also be linked to its polarity of the acid compared to the ester

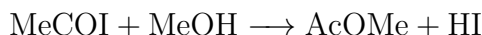
Within the system, the following reactions can be derived from the catalytic cycle:

AcOH Formation:



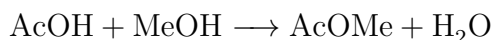
This is the normal termination of the catalytic cycle

MeOAc Formation:



It is a possibility that the excess of the MeOH in the IL leads to the termination of the catalytic cycle via the formation of MeOAc directly.

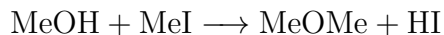
Ester Condensation:



The formation of AcOMe is possible via condensation of AcOH produced via the catalytic cycle and the excess MeOH in the IL. As the side product of this reaction is H₂O and the fact we are able to detect an H₂O peak on the

GC, this implies that this route is the preferred one for AcOMe formation.

DME Formation:



This is the only observed side product and does not appear to have any significant effect on the overall product distribution.

It should be noted that water is formed by the esterification of AcOH with MeOH. This production of water can be detected and measured by GC analysis. Over the course of the reaction the amount of detected water slowly increases after the introduction of MeI into the system until it reaches a steady state. This implies that the MeOAc is formed via esterification of the AcOH and not directly from the MeCOI, or at least until some form of equilibrium is reached.

4.9 Water addition

Under industrial carbonylation conditions, addition of water to the system is a very important requirement.

One of the most important uses of water in the reaction is to try and prevent precipitation of the insoluble and inactive RhI_3 and IrI_3 . Since water is present in the catalytic cycle, particularly linked to HI formation, we thought that by introducing water into the system we could facilitate the hydrolysis of the MeOAc to AcOH. (HI is formed from the reaction of MeI with H_2O and since HI is critical in the termination of the reaction to AcOH, it seemed reasonable to assume that by addition of excess H_2O to the system would result in formation of AcOH.)

Despite this we were still unable to produce AcOH in the system. However, what we did observe was an increase in corrosion. The only noticeable catalytic effect of water addition was a minor increase in the AcOMe yield, that lasted only for a short period. Our reasoning for this is that, since we don't have much contact time with the HI in the system, due to the small catalyst bed. This limited contact time appears to result in a modification of the catalytic cycle. It seems like the concentration of HI in the system is not high enough to result in the hydrolysis of the MeOAc. This could also

be linked to the distribution of the assorted compounds throughout the IL.

4.10 Gas solubility in IL

The solubilities of components in ILs are not always clear. This is particularly important with regard to both water and gases. Inevitably small volumes of water and gases remain dissolved within ILs after they have been synthesised, this has been established.¹³¹ Solubilities of gasses in ILs is something that is currently a field of very active study, both theoretical and practical.^{126,127,132} Typically, the diffusion co-efficient is 2-3 orders of magnitude lower than traditional solvents.¹³³

In our system we are looking at a variety of compounds dissolved in our IL layer, the largest component being CO. It is generally agreed that CO has only a limited solubility in ionic liquids, although these measurements have only been conducted at relatively low pressures. In our system with a partial pressure of CO close to 20 bar, the solubility should be increased.

MeOH is very soluble in the IL, as is witnessed during the synthesis of a SILP catalyst. This also becomes apparent when a MeOH flow is introduced to a SILP catalyst in the reactor, where the observed MeOH peak on the GC decreases until the IL becomes saturated with MeOH.

The solubilities of the other compounds is hard to determine. Once MeI begins being added to the system, then the whole mixture of compounds is observed by the GC. The only way to try and interpret relative solubilities of compounds is via the “like dissolves like” principle. This means that the more polar compounds will dissolve the most in the IL layer.

If this is the case it leads to the possibility of re-coordination of any lost CO ligands during either synthesis or loading. However, if this were the case it would be expected that all of the SILPs utilising the $[\text{Rh}(\text{CO})_2\text{I}]_2$ precursor should be able to re-coordinate CO ligands once loaded into the reactor and put under 20 bars of pressure. Any further conclusions from the results achieved are hard to draw due to the limited volume of information available. This highlights one of the major issues in SILP research at the current moment. There is very few in-situ measurements currently possible,

the vast majority of SILP measurements are all conducted ex situ on either fresh or used catalysts. The most common “test” for a SILP is to load it into a reactor and observe the end products. Whilst this may be of more interest to industrial research, it is rather limiting from a scientific point of view. This lack of in-situ measuring abilities make it particularly difficult to study the role of the ionic liquid in the containment of the catalyst as well as any gas/reagent/product solubility problems. Such studies could inform on the efficiency and effects of the SILP synthesis procedure in its current form. As a result of this almost all studies of SILP reactions tends to rely on the principle of empiricism to drawn any significant results from the reactions.

4.11 Intellectual Property

Since this project has been financed by Wacker, there has been a desire to capitalise on the result of the work conducted. At the time of writing, patentable results have been filed with the German patent office.

Chapter 5

Catalysis analytical tools

In order to categorise the SILP catalysts a selection of techniques were used.

5.1 TGA- Thermal gravimetric analysis.

TGA is a procedure that follows the mass loss of a sample as it is heated in a furnace. This is typically carried out from room temperature to hundreds of degrees.

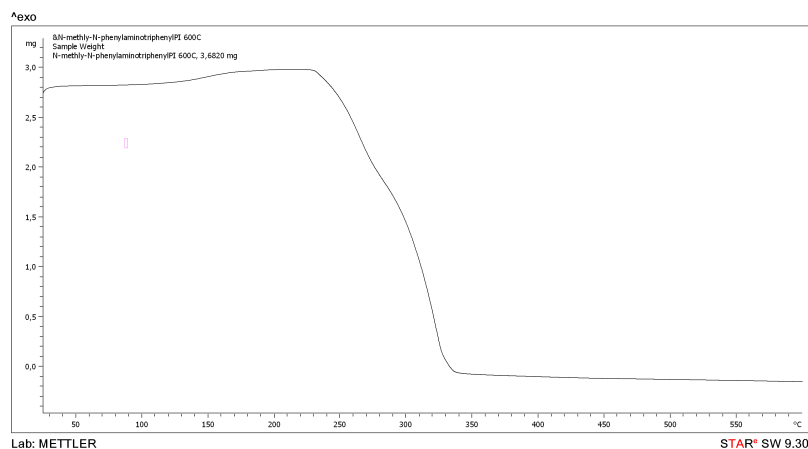
5.1.1 Ionic Liquids/Molten Salts

This technique was initially used to follow the degradation of the ionic liquids and molten salts used in the catalyst tests, Table 5.1.

Quick screening of the samples allowed for us to see if all of the imidazolium ILs used were suitable for testing at 190°C in the reactor and were not breaking down under reaction conditions. All of the PR_4 I salts were also tested and the result of these initial screenings showed that the phosphorus based molten salts had higher degradation temperatures than the imidazolium based ILs. It is likely that this difference is linked to their higher melting point. N-Methyl-N-phenylamino Ph_3P I seems to behave oddly compared to the other phosphonium salts, it gains a small amount of weight before beginning to degrade and the degradations seem to occur in two stages as shown in Fig 5.1.

Table 5.1: Salt Degradation Ranges

Salt	Decomposition Range °C
Bmim I	240 - 330
EtPh ₃ P I	270 - 380
(N-Methyl-N-phenylamino)Ph ₃ P I	230 - 345
Pr ₃ MeP I	340 - 445
Bu ₄ P I	320 - 420
Ph ₄ P I	360 - 480
i-PrPh ₃ P I	270 - 360
Ph ₃ MeP I	270 - 395

Figure 5.1: (N-Methyl-N-phenylamino)Ph₃P I Degradation

5.1.2 Rh Source

This method was also used on both of the Rh precursor complexes to show their individual stability at the reaction temperatures. The initial RhCl₃ · xH₂O precursor shows unusual behaviour *gaining* mass before degrading. After gaining mass, a degradation seem to occur between 50°C - 90°C, before the sample then gradually loses mass until 600°C, Fig 5.2. It should be noted, that the initial mass loss observed is due to liberation of the CO ligands. These results show the importance of a solvent in the reaction, so protect the Rh centre.

Table 5.2: Rh Complex Degradation

Rh Source	Decomposition Range °C
$\text{RhCl}_3 \cdot x\text{H}_2\text{O}$	50 - 90
$[\text{Rh}(\text{CO})_2\text{Cl}]_2$	70 - 135

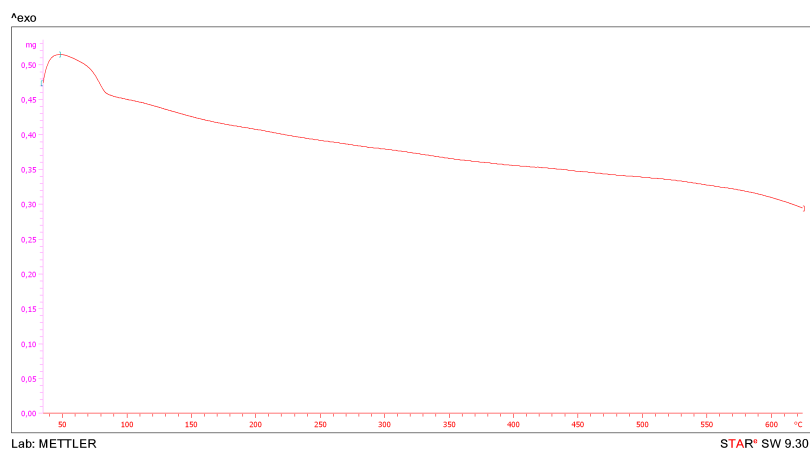


Figure 5.2: Decomposition of $\text{RhCl}_3 \cdot x\text{H}_2\text{O}$

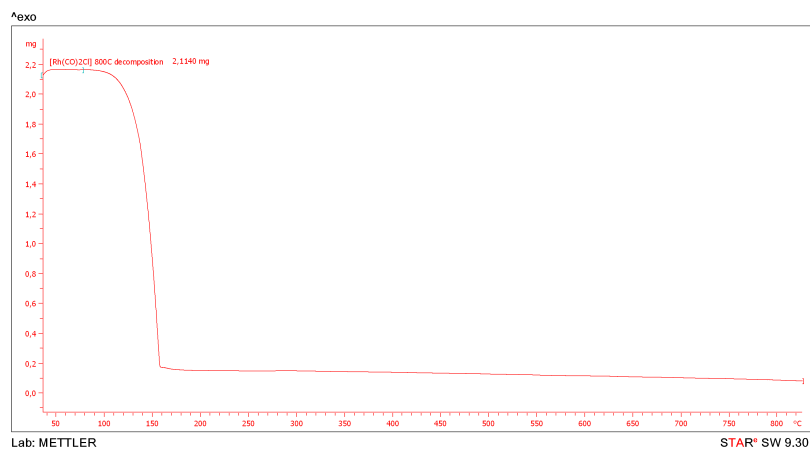


Figure 5.3: Decomposition of $[\text{Rh}(\text{CO})_2\text{Cl}]_2$

5.1.3 SILP Catalysts

After screening the ILs and molten salts, measurements of actual SILP catalysts were conducted. At the time of analysis, we already had a large selection of catalysts, but they were used and had been left exposed to air for an extended period. Because of this, it was decided to conduct the first measurement with a fresh catalyst, both unused and direct from out of the reactor. Comparison of the two samples showed little difference in decomposition temperature between the fresh and used SILP catalysts with decomposition temperatures similar to that of the ILs in the initial screenings.

Table 5.3: Decomposition of SILP with Varied IL Loadings

Sample	Decomposition Temp (°C)
[Rh(CO) ₂ Cl] ₂ / 30vol% Bmim I	200-300
[Rh(CO) ₂ Cl] ₂ / 15vol% Bmim I	200-300

5.1.4 Slow Heating

The complete picture of the decomposition, however, is hard to draw due to the high heating rate used (10°C/minute) to screen the salts. This rapid heating rate is likely to result in an “incorrect” decomposition temperature, linked to the heat transfer delay between the furnace, sample and detector. In order to study this in some more detail, a number of slower heating experiments were also carried out with a heating rate of 1°C/minute. These measurements allow for a more accurate picture of the onset temperature of degradation in the samples. This is particularly relevant for the SILP samples where heat transfer in the sample is also restricted due to the silica support limiting effective heat transfer from the outside of the sample to the inner IL containing pores. This delay in heat transfer in the sample is likely to be the reason for the small difference in degradation onset seen during the quick screening samples. Unfortunately using such a slow heating ramp made it almost impossible to find a decomposition temperature as the decomposition was slow and gradual and not sudden and sharp. Interestingly

it was the used sample that lost more mass, a possible indication of products remaining in the IL Even after reaction.

Two samples were also looked at under isothermal conditions for 20 hours. A fresh and used sample of $[\text{Rh}(\text{CO})_2\text{Cl}]_2/30 \text{ vol}\% \text{ Ph}_3\text{MeP I}$ were held at 200°C for 20 hours and the mass loss observed. In both cases there was a drop in mass over the course of the study, with the fresh sample losing more mass than the used one, Table 5.4

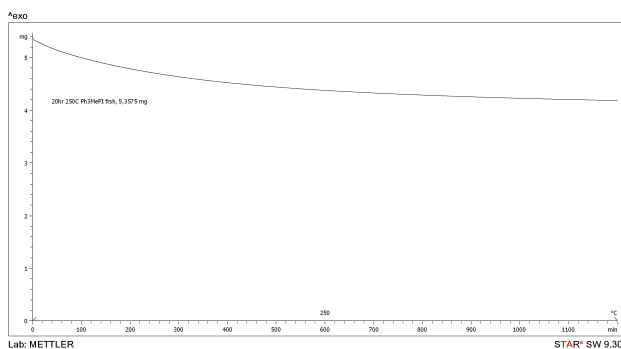


Figure 5.4: Fresh sample of Ph_3MePI at 250°C for 20 hours

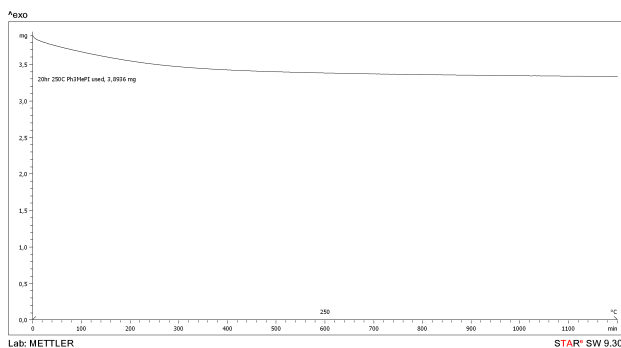


Figure 5.5: Used sample of Ph_3MePI at 250°C for 20 hours

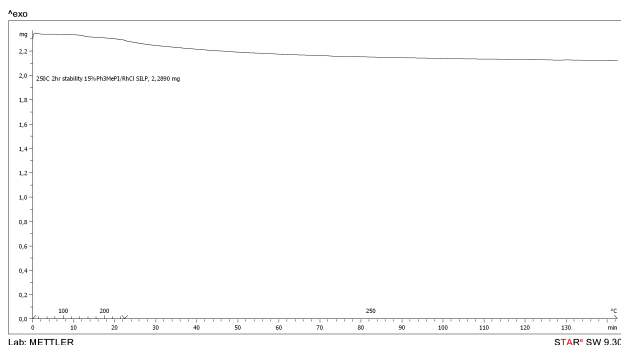


Figure 5.6: 15 vol% Ph₃MeP I/ [Rh(CO)₂Cl]₂ Stability at 250°C over 2 hours

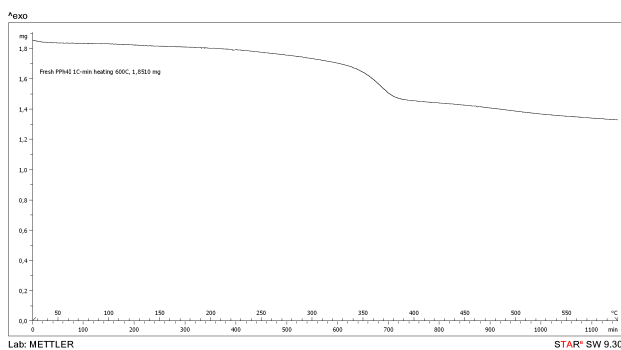


Figure 5.7: Degradation of Ph₄PI at a heating rate of 1°C/minute

Table 5.4: Long Term TGA Experiments

No	Sample	Final Temp (°C)	Heating Rate (°C/min)	Time (hours)	Mass Loss (mg)
1	[Rh(CO) ₂ Cl] ₂ / Ph ₃ MeP I (fresh)	600	1	-	0.54
2	[Rh(CO) ₂ Cl] ₂ / Ph ₃ MeP I (fresh)	250	-	20	1.1
3	[Rh(CO) ₂ Cl] ₂ / Ph ₃ MeP I (used)	600	1	-	0.95
4	[Rh(CO) ₂ Cl] ₂ / Ph ₃ MeP I (used)	250	-	20	0.54

5.2 DSC - Differential Scanning Calorimetry

DSC is a technique used to measure the phase transition temperature of a sample. For ILs it is mainly used to determine the onset of the liquid phase and “decomposition”. Such measurements are particularly useful for the phosphonium salts obtained as the literature values and accuracy of the melting point reported for the salts varies considerably. The use of DSC also allows for the determination of the eutectic point when two or more salts are mixed together. This measurement of the eutectic point was particularly important as if the salt was not molten at the reactor temperature of 190°C it would be useless.

Table 5.5: Eutectic Points of 0.5:0.5 Mole ratio salt combinations

Salt 1	Salt 2	Eutectic Point °C
Pr ₃ MeP I	Bu ₄ P I	155
Pr ₃ MeP I	n-methyl-n-phenyl-aminoPh ₃ P I	182
iPrPh ₃ P I	Bu ₄ P I	97
MePh ₃ P I	Bu ₄ P I	No obvious eutectic point
Pr ₃ MeP I	EtPh ₃ P I	168

5.3 BET- Brunauer-Emmett-Teller isotherm

BET measurements allow for surface area and pore volumes of samples to be measured. This is facilitated by the absorption and desorption of N₂ molecules from the sample surface.

For measurement of SILPs this procedure is particularly handy. It is also important as it allows for the accurate measurement of the pore volume of the support. This value is important when calculating the pore volume filled by the IL in the sample. It is important to study both fresh and used catalysts to see what, if any affect, can be observed on the measured pore volumes. Such measurements of pore volume are common place and give a guide to which pores and how completely are filled with IL.

Table 5.6: BET Measurements

Catalyst	Pore Volume cm ³ /g
[Rh(CO) ₂ Cl] ₂ -30vol% Ph3MePI fresh	0.318
[Rh(CO) ₂ Cl] ₂ -30vol% Ph3MePI used	0.319

5.4 FT-IR - Fourier Transform Infra Red Spectroscopy

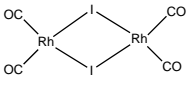
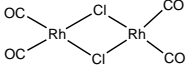
In the original study the [Rh(CO)₂I₂]⁻ SILP catalyst¹¹⁶ was only analysed by FT-IR. This was used to measure the C=O stretching frequencies of the carbonyl ligands. In our first synthesis we used the same method to confirm if our SILP synthesis was successful. Table 5.7. After changing to the [Rh(CO)₂Cl]₂ precursor. FT-IR measurement were also performed and showed the same CO stretching bands shift to slightly higher/lower frequencies.

Table 5.7: Measured C=O Stretches

Sample	Stretches (ν_{CO})
Original	2076, 2006
Expt 1	2077, 2006

Once the precursor was changed, we felt it would be interesting to see if any of the active [Rh(CO)₂I₂]⁻ was formed when an I⁻ containing IL was added to the [Rh(CO)₂Cl]₂. To do this a study of [Rh(CO)₂I]₂ and [Rh(CO)₂Cl]₂ complexes in Bmim I were undertaken. A selection of three Rh containing complexes, [Rh(CO)₂I]₂, [Rh(CO)₂Cl]₂ and RhCl₃ · xH₂O were mixed with either Bmim I or Bmim Cl as shown in Table 5.8 and Fig 5.8.

Table 5.8: IR Experiments performed

Experiment	1	2	3	4	5	6
	Bmim I				Bmim Cl	
		Bmim I			Bmim Cl	
$\text{RhCl}_3 \cdot x\text{H}_2\text{O}$			Bmim I			Bmim Cl

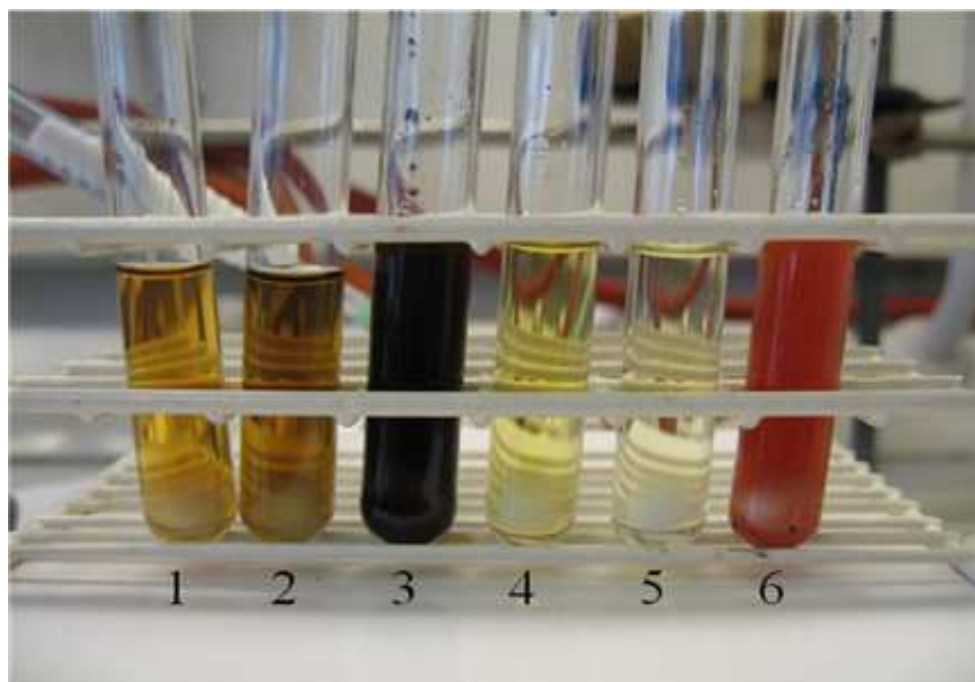


Figure 5.8: Samples used for FT-IR Study

Unfortunately difficulties with the $\text{RhCl}_3 \cdot x\text{H}_2\text{O}$ experiments made it impossible to carry out FT-IR measurements on them, but the other four samples were dried under vacuum and the residue analysed. Fig 5.9 shows the FT-IR spectra of the four experiments with pure $[\text{Rh}(\text{CO})_2\text{I}]_2$ and $[\text{Rh}(\text{CO})_2\text{Cl}]_2$ for comparison. Experiment 5 shows two distinct peaks, indicating that there is only one species of C=O present, this is sensible as there is only Cl^- present in the system. Experiments 1, 2 and 4 all show a more confused picture, with more than two distinct peaks visible. Experiments 2 and 4 show a peak similar to that shown in 5 at 2067cm^{-1} , which would indicate some similarity with the Cl^- containing system, however experiments 1 and 2 show a peak at 1934cm^{-1} which must be indicative of I^- . In order to explain this, it is likely that a mixed species, Fig 5.10, is formed.

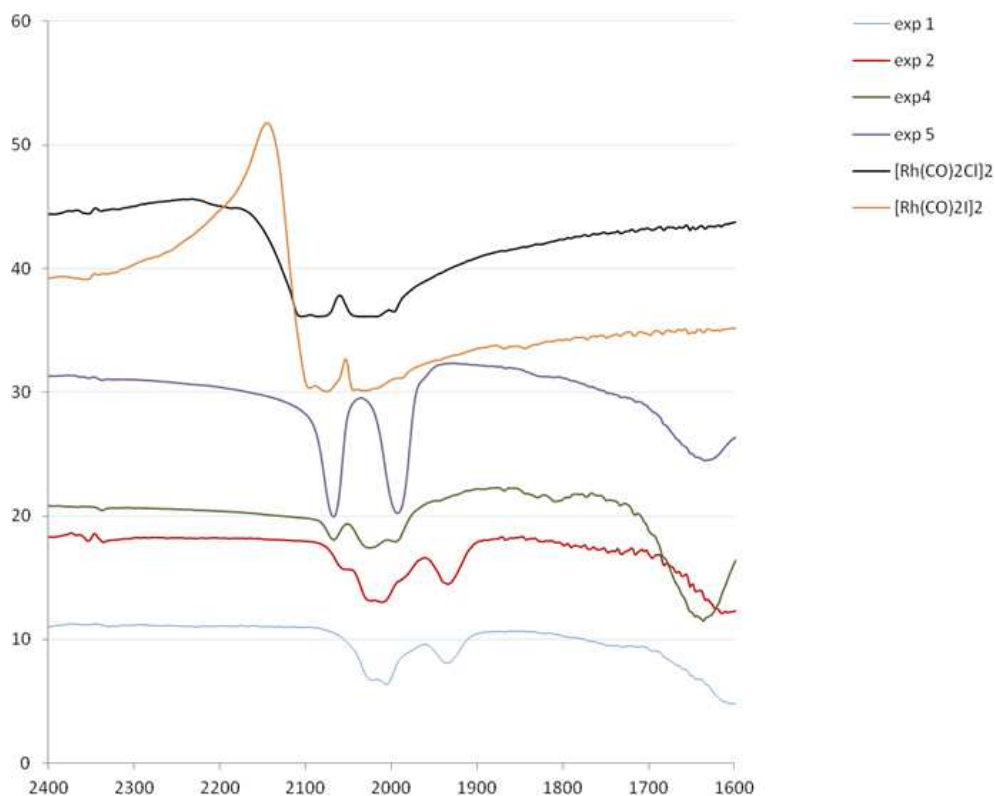


Figure 5.9: Spectra of CO stretching in mixed I/Cl systems

The degradation of $[\text{Rh}(\text{CO})_2\text{I}]_2$ in air was also followed via FT-IR. Degradation of $[\text{Rh}(\text{CO})_2\text{I}]_2$ begins with the loss of CO ligands from the complex,

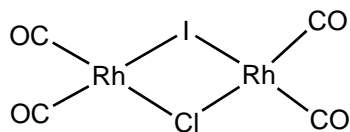


Figure 5.10: The mixed chlorine/iodine complex formed

this loss can be shown by FT-IR by following the disappearance of the C=O stretching bands. As can be seen in Fig 5.11, the two distinct C=O peaks gradually decrease over time as C=O ligands are liberated from the complex. After 20 hours, no remains of the C=O peaks are visible, only a new peak in between where they had been. The cause of this new peak is not known.

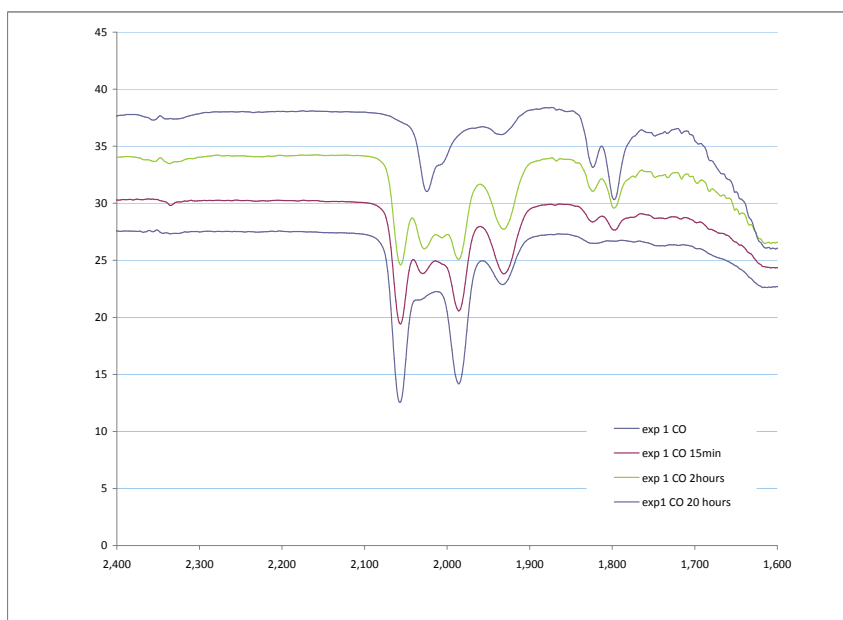


Figure 5.11: Loss of CO from the complex over time

Chapter 6

Experimental

All the catalysts tested were used in the reactor system described in 2.15. The reaction conditions used were kept as similar as possible for all experiments.

6.1 Reactors

The reactors are constructed of a stainless steel-titanium alloy tubing (316Ti). They are 35 cm long, containing a fixed bed 17.5 cm down its length. When loading the catalyst a layer of glass wool is added to retain the catalyst on the fixed bed. Approximately 0.5 g of catalyst was then loaded into the reactor, which was connected to the test-rig. Entering the bottom of the reactor is a sealed 1/8 inch diameter 316Ti tube. Into this tube the thermocouple used for computer control of the ovens is inserted prior to the start of reaction. Initially glass beads were also used at the catalyst bed to ensure suitable distribution of the feeds (particularly MeI) over the whole catalyst bed, unfortunately it was quickly discovered that the glass beads were not stable under the reaction conditions either dissolving or cracking. Thereafter we discontinued their use.

The reactor is connected to the test rig via two fittings. This is to reduce disturbing the pressure integrity of other components. As a result of this, it is not able to pressure test the reactor before it is attached to the system. This usage of only two fittings when connecting the reactor allows us to try

and limit where any leaks may occur. Fittings are at top of reactor and at exit of reactor. This is for practical reasons, mainly to do with MeI inlet tube at top and thermocouple at bottom.

6.2 Flow Controllers

Addition of the CO and MeOH into the system are controlled by the CEM, GMFC and LMFC all of which are in turn are controlled via the Bronkhorst control box. Outside of a reaction flows of CO and MeOH to the system are reduced or stopped.

In general the CEM is constantly maintained at both during and outside of reactions for convenience.

The standard reaction conditions for the gas and liquid flows are:

$\text{CO}/\text{CH}_4 = 100 \text{ ml/min}$ and $\text{MeOH} = 1 \text{ g/hour}$.

Since the gas flow is not a pure gas, this flow is the equivalent of:

92.4 ml/min CO and 7.6 ml/min CH_4

At a flow rate of 1g/h , the MeOH in the tank can last for two months at a continuous flow rate.

Control of the flows is real-time so in general fluctuations observed in the displayed flow (particularly the CO/CH_4 due to the higher flow rate) are often indicative of a problem further downstream in the system.

6.3 Heating

Heating of the reactors is automated via a LabView programme. The programme allows for a set point to be chosen and via control of the oven in reference to an external thermocouple, a constant temperature is maintained. For our experiments the standard reaction temperature was 190°C , mirroring the temperature used industrially. By using LabView we were also able to log all of our heating data.

All of the heating cables to heat the reactor system are set at 180°C . The temperature is regulated by the Bronkhorst control box and is measured by

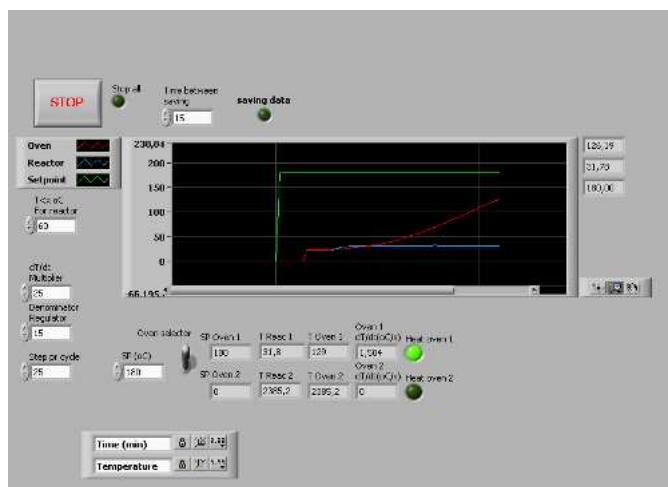


Figure 6.1: Labview Screen for Oven Control

thermocouples linked with each individual heating cable.

It is possible to set each of the heating cables to heat to a specific temperature, allowing different temperature zones, however this is not appropriate in our case and so all of the cables are isothermal.

In addition to the heating of the reactor system, a supplementary system is also in use. Following on from problems related to condensation inside of the pressure regulating valve, it was decided to supply additional heating to the valve housing. To do this a short heating cable is used and set to heat to a maximum possible temperature of 250°C. Although in practice the cable cannot reach this high temperature due to difficulties in getting it sufficiently tightly wound round the valve box, combined with difficulties in securing the thermocouple so as to get an accurate temperature reading.

6.4 Pressure

The standard reaction pressure of the system is 20 bar. This is maintained through the use of a pressure transducer and back pressure regulating valve.

The controller, Fig 6.2, can be used manually or automatically. The main display has 2 lines. The upper line shows the pressure of the system being measured by the transducer. The lower line can be used to show the set

pressure, valve open %age and standard deviation from the set point.

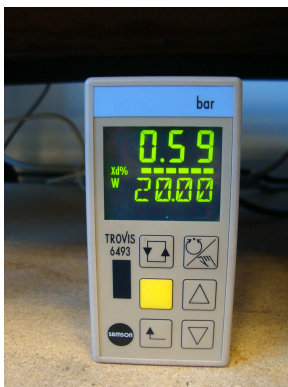


Figure 6.2: Pressure Valve Control Box

The valve needs to be kept heated at all times; this is to stop the condensation of chemicals onto the valve plug and blocking/corroding it. When stopping the system for any prolonged period of time it is important to make sure the valve is 100% open to stop the pin becoming jammed, this must be done manually via the controller. The valve is independently heated to try and reduce any such corrosion. The heating is wired independently of the rest of the reactor heating system, in order to avoid it being switched off by accident.

6.5 MeI Addition

The addition of MeI into the system is what initiates the reaction.

The MeI is added via a HPLC pump into the top of the reactor. Prior to addition the tubing is flushed with MeI to remove any air pockets and to flush out any degraded MeI (in the presence of water MeI can hydrolyse to MeOH, I₂ and HI). The MeI feed is pumped against a closed valve until it reaches an internal pressure slightly above that of the reactor. This stops the MeI being pushed back down the tubing when it is introduced into the system. Once the valve is opened, the pressure measured by the HPLC pump equalises with that of the system.

The requirement to have this over pressure in the MeI line results in a

“spike” in the GC area detected. This spike peaks one or two GC runs after addition of the MeI is begun, before returning to a more stable level. With this initial MeI spike, it is already possible to see a peak indicating formation of MeOAc.

Occasionally, the peak area corresponding to MeI can be seen to decrease. This is generally as a result of bubbles in the tubing. To correct this there are two options employed 1) Increase the MeI flow into the system in an attempt to “kick start” the MeI flow again or 2) Close the valve and allow an overpressure to build up in the tubing before opening the valve to the system again. In most cases either solution will work. If neither option works, the MeI tubing should be flushed to atmosphere before being re-pressurised again

6.6 Product Isolation

Initially condensation of products was possible prior to GC analysis, but following the removal of the dead space outlined in Section 2.8.2, condensation was only possible after the GC.

Reaction products are collected in a condenser cooled by an external cryostat. It is important to remember that the condenser also contains CO gas. It is important therefore to close the valve after a sample has been removed from the condenser so as not to leak CO into the lab. Samples are initially a colourless liquid, but if left to stand on the bench will slowly begin to turn brown as MeI slowly oxidises to give MeOH and I₂.

6.7 Methanol Tank

All of the liquid feed for the reaction comes from a single pressurised stainless steel tank, Fig 6.3. Due to the relatively low flow of MeOH used in our reactions, the tank does not often need to be refilled. If it does need to be refilled and/or the MeOH level checked, it is *very* important to release the pressure from the system before attempting to open the tank. The pressure in the tank is generally between 25 - 30 bar in order to provide a sufficient

back pressure for the MFCs.



Figure 6.3: MeOH tank used

When depressurising the MeOH tank it is very important to close the valves to the MFCs in to avoid problems when restarting the system

6.8 After a Reaction

To stop the reaction, first the flow of MeI is stopped and the valve closed. Once the addition of MeI has stopped, the reaction itself will stop once all of the MeI in the system passes through the reactor. To make sure all of the products are removed from the system, it is run under flows of CO and MeOH for some time to “flush out” any remaining compounds in the reactor.

After approximately 30 mins, the MeOH flow is stopped and only the CO flow remains. After a further 30 mins, the flow is directed via the reactor bypass and the oven turned off.

Once the oven has been turned off, it can be removed carefully wearing gloves. The heating blocks can also be removed carefully, with appropriate protection. Once the oven and heating blocks are removed from the reactor, it takes about 45 - 60 minutes for it cool down completely. When the reactor has cooled down to a manageable temperature, the remaining pressure is slowly released via the exhaust valve before the reactor itself is removed. It is important to release the pressure slowly so as not to damage the reactor bed during depressurisation. Once the reactor is depressurised it should be removed from the system via the two specific joints used for this.

Once the reactor is removed from the system, the spend catalyst should be collected from the reactor and the glass wool used for the catalyst bed recovered. The reactor should then be dismantled and cleaned thoroughly to remove all traces of contamination before the next reaction. The components should be cleaned using acetone and the connectors at the bottom of the react should be soaked in acetone for a period to make sure that all traces of contamination is removed. All other components should be cleaned by washing. The initial waste acetone will have a black/dark brown colour, washing should be continued until the waste acetone is clear once more. Once the components have been cleaned they should be checked for signs of corrosion and seriously corroded components should be replaced.

6.9 GC Sequence

Analysis of the product stream is carried out using the GC system described in Chapter 3. A sequence has been created that will run the analysis method on a loop, thus creating, in theory, a maximum of 999 sets of results for each reaction.

When starting a new sequence the date of commencement, details of the catalyst being tested and any other pertinent information are noted. Once the sequence is begun, it will begin online analysis of the reactor output

stream.

The sequence may be stopped at any point. In general this is done once a reaction is completed and the reactor removed from the system. By allowing the GC to continue running after the reaction we can observe how the product composition of the exhaust gas is distributed.

All of the GC data generated is accessed and analysed using the supplied Agilent Chemstation software. The data collected from each sequence may be accessed one run at a time and peak data is presented for each detector. Due to software issues, initially all peak data had to be transcribed manually from here to a “results” spreadsheet. This spreadsheet was set up to take the peak areas and generate conversion, yield, selectivity, STY and TOF data. Eventually we were able to obtain a macro from Wacker Chemie AG that was able to extract the data from all of runs into a format that we were able to work with. This allowed us to very quickly collect and use all of the peak data obtained for each experiment.

Chapter 7

Conclusion

The work presented here has focused on the application of SILP specifically for the catalytic carbonylation of MeOH to AcOH.

This carbonylation reaction is highly important as it is the major industrial route for the synthesis of AcOH. AcOH is an important precursor to a variety of products mainly in the field of plastics. Whilst the work carried out was initially based on the original patent of Rasmus Fehrmann and Anders Riisager, it has taken the knowledge of SILP carbonylation further and has resulted in the filing of patent applications related to the work carried out.

The work overall took two distinct approaches.

Initially an engineering/chemical engineering strand, that took precedence in the initial stages and then dropped off to a more background role related to the maintenance of the test-rig. This involved the construction of the test rig including relevant modifications to improve system performance. This process also included the wiring of all external components and calibration of the GC that would be used for analysis.

The second stand that began slowly, but came to take a more prominent role was the chemistry strand. This began with simple catalyst screening an optimisation before moving on to encompass a degree of catalyst characterisation.

Overall the work presented here vindicates the applicability of the SILP

concept for reactions allowing them to be converted from standard batch reactions to more environmentally and economically beneficial continuous flow reactions. Currently this has only been shown on a larger scale for gas phase reactions, but it is not unreasonable to assume extension to slurry phase systems.

The two major discoveries of the work are the ability to activate a catalytically inactive Rh source into the active catalytic species of $[\text{Rh}(\text{CO})_2\text{I}_2]^-$ in-situ and the efficaciousness of phosphonium based salts over the standard ionic liquid based imidazolium and other N^+ based salts. This last indicates an important departure from SILP systems as the phosphonium salts used all had melting points above the 100°C standard definition of ILs, thus creating Supported Molten Salt Phase (SMSP) systems.

The importance of the iodide anion was emphasised by trials of IL using alternative anions. These results were poor and seems to validate the improvements shown by the industrially applied Celanese system with the addition of further iodide salts. The saturation of the reaction medium with free I^- seems beneficial to the system.

In a departure from the standard system, we have shown that addition of H_2O is not required for the reaction, either to stabilise the catalyst or to facilitate the established mechanism.

Overall the results of the work have shown the successful application of a SILP system to a major industrial reaction. This is borne out by the construction and operation of a pilot plant by our collaborators Wacker Chemie AG.

Bibliography

- [1] “Definitions of vinegar.,” *The Lancet*, vol. 179, p. 109, Jan. 1912.
- [2] F. S. Wagner, “Acetic Acid,” in *Kirk-Othmer Encyclopedia of Chemical Technology*, John Wiley & Sons, Inc., 2000.
- [3] N. Yoneda, “Recent advances in processes and catalysts for the production of acetic acid,” *Applied Catalysis A: General*, vol. 221, pp. 253–265, Nov. 2001.
- [4] A. Haynes, “Catalytic Methanol Carbonylation,” in *Advances in Catalysis*, vol. 53, pp. 1–45, Elsevier Inc., 1 ed., 2010.
- [5] H. Cheung, R. S. Tanke, and G. P. Torrence, “Acetic Acid,” in *Ullmann’s Encyclopedia of Industrial Chemistry*, Wiley-VCH, Weinheim, 2000.
- [6] H. Ebner, H. Follmann, and S. Sellmer, “Vinegar,” in *Ullmann’s Encyclopedia of Industrial Chemistry*, Wiley-VCH Verlag GmbH & Co. KGaA, 2000.
- [7] Vinyl Acetate Council, “What is Vinyl Acetate?,” <http://www.vinylacetate.org/what.cfm>.
- [8] G. Roscher, “Vinyl esters,” in *Ullmann’s Encyclopedia of Industrial Chemistry*, Wiley-VCH Verlag GmbH & Co. KGaA.
- [9] H. Rinno, “Poly(vinyl esters),” in *Ullmann’s Encyclopedia of Industrial Chemistry*, Wiley-VCH Verlag GmbH & Co. KGaA, 2000.

- [10] Dow Chemical, “Product Safety Assessment: Vinyl Acetate,” <http://www.dow.com/productsafety/finder/vinyl.htm>.
- [11] Global Industry and Analysts, Inc., “Growth in Tow Consumption to Drive Global Demand for Cellulose Acetate,”
- [12] ICIS, “Acetic Acid Uses and Market Data,” <http://www.icis.com/Articles/2007/10/31/9074779/acetic-acid-uses-and-market-data.html>.
- [13] Oxford English Dictionary, “Vinegar, noun.”
- [14] H. Ebner, H. Follmann, and S. Sellmer, “Vinegar,” in *Encyclopedia of Inorganic Chemistry*, 2005.
- [15] United States Food and Drug Administration, “Federal Food And Drugs Act,” 1906.
- [16] United States Food and Drug Administration, “Vinegar Origin Requirements,” 2010.
- [17] Frings Homepage <http://www.frings.com/>.
- [18] Food and Agriculture Organisation of the United Nations, *Industrial charcoal making*. 1985.
- [19] United States Geological Society, “Pyroligneous Acid Definition,” http://toxics.usgs.gov/definitions/pyroligneous_acid.html.
- [20] K.-i. Sano, H. Uchida, and S. Wakabayashi, “A new process for acetic acid production by direct oxidation of ethylene,” *Catalysis Surveys from Japan*, vol. 3, pp. 55–60, 1999.
- [21] J. R. Zoeller, V. H. Agreda, S. L. Cook, N. L. Lafferty, S. W. Polichnowski, and D. M. Pond, “Eastman chemical company acetic anhydride process,” *Catalysis Today*, vol. 13, pp. 73–91, Mar. 1992.
- [22] British Zeolite Association, “What are Zeolites?,” <http://www.bza.org/>.

- [23] D. Tomczak, "Chemistry of rhodium in zeolite Y," *Microporous Materials*, vol. 5, pp. 263–278, Jan. 1996.
- [24] H.-E. Maneck, D. Gutschick, I. Burkhardt, B. Luecke, H. Miessner, and U. Wolf, "Heterogeneous carbonylation of methanol on rhodium introduced into faujasite-type zeolites," *Catalysis Today*, vol. 3, pp. 421–429, Sept. 1988.
- [25] T. Yashima, Y. Orikasa, N. Takahashi, and N. Hara, "Vapor phase carbonylation of methanol over RhY zeolite," *Journal of Catalysis*, vol. 59, pp. 53–60, Aug. 1979.
- [26] P. Gelin, C. Naccache, and Y. B. Taarit, "Coordination chemistry of rhodium and iridium in constrained zeolite cavities: methanol carbonylation," *Pure and Applied Chemistry*, vol. 60, no. 8, pp. 1315–1320, 1988.
- [27] T. Blasco, M. Boronat, P. Concepción, A. Corma, D. Law, and J. A. Vidal-Moya, "Carbonylation of methanol on metal-acid zeolites: evidence for a mechanism involving a multisite active center.," *Angewandte Chemie (International ed. in English)*, vol. 46, pp. 3938–3941, Jan. 2007.
- [28] N. Takahashi, Y. Orikasa, and T. Yashima, "Kinetics and mechanism of methanol carbonylation over RhY zeolite," *Journal of Catalysis*, vol. 59, pp. 61–66, Aug. 1979.
- [29] J. Knifton and J. J. Lin, "Syngas reactions XII. The selective preparation of acetaldehyde, alkanols, esters and acetic acid from synthesis gas," *Applied Organometallic Chemistry*, vol. 3, no. 6, pp. 557–562, 1989.
- [30] W. Chen, Y. Ding, D. Jiang, T. Wang, and H. Luo, "A selective synthesis of acetic acid from syngas over a novel Rh nanoparticles/nanosized SiO₂ catalysts," *Catalysis Communications*, vol. 7, pp. 559–562, Aug. 2006.

- [31] T. P. Wilson, P. H. Kasai, and P. C. Ellgen, "The State of Manganese Promoter in Rhodium-Silica Gel Catalysts," *Journal of Catalysis*, vol. 201, pp. 193–201, 1981.
- [32] H. Yin, Y. Ding, H. Luo, H. Zhu, D. He, J. Xiong, and L. Lin, "Influence of iron promoter on catalytic properties of Rh-Mn-Li / SiO₂ for CO hydrogenation," *Applied Catalysis*, vol. 243, pp. 155–164, 2003.
- [33] H. Yin, Y. Ding, H. Luo, L. Yan, T. Wang, and L. Lin, "The Performance of C₂ Oxygenates Synthesis from Syngas over Rh-Mn-Li-Fe / SiO₂ Catalysts with Various," *Energy*, vol. 17, no. 6, pp. 161–166, 2003.
- [34] W. Partenheimer, "Characterization of the reaction of cobalt (II) acetate, dioxygen and acetic acid, and its significance in autoxidation reactions," *Journal of molecular catalysis*, vol. 67, pp. 35–46, 1991.
- [35] A. Onopchenko, "Oxidation of butane with cobalt salts and oxygen via electron transfer," *The Journal of Organic Chemistry*, vol. 5473, no. 1966, 1973.
- [36] W. Slink and P. DeGroot, "Vanadium-titanium oxide catalysts for oxidation of butene to acetic acid," *Journal of Catalysis*, vol. 68, no. 2, pp. 423–432, 1981.
- [37] Y. Taniguchi, T. Hayashida, H. Shibasaki, D. Piao, T. Kitamura, T. Yamaji, and Y. Fujiwara, "Highly Efficient Vanadium-Catalyzed Transformation of CH₄ and CO to Acetic Acid," *Organic Letters*, vol. 1, pp. 557–560, Aug. 1999.
- [38] A. E. Shilov and B. Shul'pin, Georgiy, "Chapter IX: Homogeneous Catalytic Oxidation of Hydrocarbons by Molecular Oxygen," in *Activation and Catalytic Reactions of Saturated Hydrocarbons in the Presence of Metal Complexes*, 2000.
- [39] W. Suprun, E. M. Sadovskaya, C. Rüdinger, H.-J. Eberle, M. Lutecki, and H. Papp, "Effect of water on oxidative scission of 1-butene to acetic

- acid over V_2O_5 - TiO_2 catalyst. Transient isotopic and kinetic study,” *Applied Catalysis A: General*, vol. 391, pp. 125–136, Jan. 2011.
- [40] T. Takei, N. Iguchi, and M. Haruta, “Synthesis of Acetaldehyde, Acetic Acid, and Others by the Dehydrogenation and Oxidation of Ethanol,” *Catalysis Surveys from Asia*, pp. 80–88, Mar. 2011.
- [41] J. Rass-Hansen, H. Falsig, B. Jørgensen, and C. H. Christensen, “Bioethanol: fuel or feedstock?,” *Journal of Chemical Technology & Biotechnology*, vol. 82, pp. 329–333, Apr. 2007.
- [42] C. H. Christensen, B. Jørgensen, J. Rass-Hansen, K. Egeblad, R. Madsen, S. K. Klitgaard, S. M. Hansen, M. R. Hansen, H. C. Andersen, and A. Riisager, “Formation of acetic acid by aqueous-phase oxidation of ethanol with air in the presence of a heterogeneous gold catalyst.,” *Angewandte Chemie (International ed. in English)*, vol. 45, pp. 4648–51, July 2006.
- [43] D. Linke, “Catalytic Partial Oxidation of Ethane to Acetic Acid over $Mo_1V_{0.25}Nb_{0.12}Pd_{0.0005}O_x$ I. Catalyst Performance and Reaction Mechanism,” *Journal of Catalysis*, vol. 205, pp. 16–31, Jan. 2002.
- [44] C. E. H. Bawn, T. P. Hobin, and L. Raphael, “The Metal-Salt-Catalyzed Oxidation of Acetaldehyde,” *Proceedings of the Royal Society A: Mathematical, Physical and Engineering Sciences*, vol. 237, pp. 313–324, Nov. 1956.
- [45] J. Smidt, W. Hafner, R. Jira, J. Sedlmeier, R. Sieber, R. Rüttinger, and H. Kojer, “Katalytische Umsetzungen von Olefinen an Platinmetall-Verbindungen Das Consortium-Verfahren zur Herstellung von Acetaldehyd,” *Angewandte Chemie*, vol. 71, pp. 176–182, Mar. 1959.
- [46] M. Renz, “100 years of Baeyer-Villiger oxidations,” *European journal of organic chemistry*, pp. 737–750, 1999.

- [47] B. H. Carpenter, "Oxidation of Acetaldehyde to Acetic Anhydride," *Industrial & Engineering Chemistry Process Design and Development*, vol. 4, pp. 105–111, Jan. 1965.
- [48] C. E. H. Bawn and J. B. Williamson, "The oxidation of acetaldehyde in solution. Part I. The chemistry of the intermediate stages," *Transactions of the Faraday Society*, vol. 47, p. 721, 1951.
- [49] M. J. Kagan and G. D. Lubarsky, "The Intermediate Stages of Aldehyde Oxidation. I. The Catalytic Action of Manganese Catalyst in the Various Stages of the Process of Acetaldehyde Oxidation," *The Journal of Physical Chemistry*, vol. 39, no. 6, pp. 847–858, 1935.
- [50] D. R. Larkin, "The role of catalysts in the air oxidation of aliphatic aldehydes," *The Journal of Organic Chemistry*, vol. 55, pp. 1563–1568, Mar. 1990.
- [51] M. Eckert, G. Fleischmann, R. Jira, H. M. Bolt, and K. Golka, "Acetaldehyde," in *Ullmann's Encyclopedia of Industrial Chemistry*, Sept. 2006.
- [52] A. Haynes, P. M. Maitlis, G. E. Morris, G. J. Sunley, H. Adams, P. W. Badger, C. M. Bowers, D. B. Cook, P. I. P. Elliott, T. Ghaffar, H. Green, T. R. Griffin, M. Payne, J. M. Pearson, M. J. Taylor, P. W. Vickers, and R. J. Watt, "Promotion of iridium-catalyzed methanol carbonylation: mechanistic studies of the cativa process," *Journal of the American Chemical Society*, vol. 126, pp. 2847–61, Mar. 2004.
- [53] BASF, "German Patent DRP 293 787," *Chemisches Zentralblatt*, vol. 11, p. 530, 1916.
- [54] N. Von Kutepow, W. Himmele, and H. Hohenschutz, "Die Synthese von Essigsäure aus Methanol und Kohlenoxyd," *Chemie Ingenieur Technik - CIT*, vol. 37, pp. 383–388, Apr. 1965.

- [55] C. Thomas, "Ligand effects in the rhodium-catalyzed carbonylation of methanol," *Coordination Chemistry Reviews*, vol. 243, pp. 125–142, Aug. 2003.
- [56] S. Bhaduri and D. Mukesh, "Carbonylation," in *Homogeneous Catalysis: Mechanisms and Industrial Applications*, pp. 55–83, John Wiley & Sons, Inc.
- [57] F. E. Paulik and J. F. Roth, "Novel catalysts for the low-pressure carbonylation of methanol to acetic acid," *Chemical Communications (London)*, vol. 11, no. 24, p. 1578a, 1968.
- [58] S. L. M. Frank E. Paulik, F. M. Arnold Hershman, T. . C. M. Walter R. Knox, and A. P. James F. Roth, "Rhodium-containing carbonylation catalysts with halogen-containing promoter," *US 4690912*, 1987.
- [59] J. H. Jones, "The Cativa process for the manufacture of acetic acid," *Platinum Metals Review*, vol. 44, no. 3, pp. 94–105, 2000.
- [60] G. Sunley, "High productivity methanol carbonylation catalysis using iridium The Cativa process for the manufacture of acetic acid," *Catalysis Today*, vol. 58, pp. 293–307, May 2000.
- [61] N. Yoneda, S. Kusano, M. Yasui, P. Pujado, and S. Wilcher, "Recent advances in processes and catalysts for the production of acetic acid," *Applied Catalysis A: General*, vol. 221, pp. 253–265, Nov. 2001.
- [62] S. Zhang, Q. Qian, and G. Yuan, "Promoting effect of transition metal salts on rhodium catalyzed methanol carbonylation," *Catalysis Communications*, vol. 7, pp. 885–888, Nov. 2006.
- [63] B. L. Smith, G. P. Torrence, A. Aguilo, and J. S. Alder, "Methanol carbonylation process," *EP 0161874 B2*, 1992.
- [64] B. L. Smith, G. P. Torrence, A. Aguilo, and J. S. Alder, "Methanol carbonylation process," *US5001259*, 1991.

- [65] A. Fulford, C. E. Hickey, and P. M. Maitlis, "Factors influencing the oxidative addition of iodomethane to $[\text{Rh}(\text{CO})_2\text{I}_2]^-$, the key step in methanol and methyl acetate carbonylation," *Journal of Organometallic Chemistry*, vol. 398, pp. 311–323, Nov. 1990.
- [66] B. Smith, G. Torrence, M. Murphy, and A. Aguiló, "The Rhodium-Catalyzed Methanol Carbonylation to Acetic Acid at Low Water Concentrations: The Effect of Iodide and Acetate on Catalyst Activity and Stability," *Journal of molecular catalysis*, vol. 39, pp. 115–136, Jan. 1987.
- [67] W. L. Armarego and C. L. L. Chai, *Purification of Laboratory Chemicals*. Elsevier, 6th ed., 2009.
- [68] C. Thomas, "Ligand effects in the rhodium-catalyzed carbonylation of methanol," *Coordination Chemistry Reviews*, vol. 243, pp. 125–142, Aug. 2003.
- [69] US Geological Survey, "Platinum-group metals statistics and information," *Mineral Commodity Summaries*.
- [70] D. Forster and T. Singleton, "Homogeneous catalytic reactions of methanol with carbon monoxide," *Journal of Molecular Catalysis*, vol. 17, pp. 299–314, Nov. 1982.
- [71] P. M. Maitlis, A. Haynes, G. J. Sunley, and M. J. Howard, "Methanol carbonylation revisited: thirty years on," *Journal of the Chemical Society, Dalton Transactions*, no. 11, p. 2187, 1996.
- [72] M. Howard, M. Jones, M. Roberts, and S. Taylor, "C1 to acetyls: catalysis and process," *Catalysis Today*, vol. 18, pp. 325–354, Dec. 1993.
- [73] N. V. Plechkova and K. R. Seddon, "Applications of ionic liquids in the chemical industry," *Chemical Society reviews*, vol. 37, pp. 123–150, Jan. 2008.

- [74] H. Weingärtner, "Understanding ionic liquids at the molecular level: facts, problems, and controversies.," *Angewandte Chemie (International ed. in English)*, vol. 47, pp. 654–70, Jan. 2008.
- [75] P. Wasserscheid and W. Keim, "Ionic Liquids - New "Solutions" for Transition Metal Catalysis.," *Angewandte Chemie (International ed. in English)*, vol. 39, pp. 3772–3789, Nov. 2000.
- [76] J. P. Hallett and T. Welton, "Room-temperature ionic liquids: solvents for synthesis and catalysis," *Chemical reviews*, vol. 111, pp. 3508–76, May 2011.
- [77] M. J. Earle and K. R. Seddon, "Ionic liquids. Green solvents for the future," *Pure and Applied Chemistry*, vol. 72, no. 7, pp. 1391–1398, 2000.
- [78] I. Newington, J. M. Perez-Arlandis, and T. Welton, "Ionic liquids as designer solvents for nucleophilic aromatic substitutions," *Organic Letters*, vol. 9, pp. 5247–5250, Dec. 2007.
- [79] P. Wasserscheid, "Ionic liquids in heterogeneous catalysis," in *Green Solvents for Synthesis, Berchtesgarden, 2010*.
- [80] M. Alvarez-Guerra and A. Irabien, "Design of ionic liquids: an ecotoxicity (*Vibrio fischeri*) discrimination approach," *Green Chemistry*, vol. 13, no. 6, p. 1507, 2011.
- [81] J. R. Harjani, R. D. Singer, M. T. Garcia, and P. J. Scammells, "Biodegradable pyridinium ionic liquids: design, synthesis and evaluation," *Green Chemistry*, vol. 11, no. 1, p. 83, 2009.
- [82] J. R. Harjani, J. Farrell, M. T. Garcia, R. D. Singer, and P. J. Scammells, "Further investigation of the biodegradability of imidazolium ionic liquids," *Green Chemistry*, vol. 11, no. 6, p. 821, 2009.
- [83] L. Ford, J. R. Harjani, F. Atefi, M. T. Garcia, R. D. Singer, and P. J. Scammells, "Further studies on the biodegradation of ionic liquids," *Green Chemistry*, vol. 12, no. 10, p. 1783, 2010.

- [84] T. P. T. Pham, C.-W. Cho, and Y.-S. Yun, "Environmental fate and toxicity of ionic liquids: a review.," *Water research*, vol. 44, pp. 352–72, Jan. 2010.
- [85] D. Coleman and N. Gathergood, "Biodegradation studies of ionic liquids.," *Chemical Society reviews*, vol. 39, pp. 600–637, Mar. 2010.
- [86] C. D. Hubbard, P. Illner, and R. van Eldik, "Understanding chemical reaction mechanisms in ionic liquids: successes and challenges.," *Chemical Society reviews*, vol. 40, pp. 272–90, Nov. 2010.
- [87] R. Sheldon, "Catalytic reactions in ionic liquids," *Chem. Commun.*, pp. 2399–2407, 2001.
- [88] H. Olivier-Bourbigou, L. Magna, and D. Morvan, "Ionic liquids and catalysis: Recent progress from knowledge to applications," *Applied Catalysis A: General*, vol. 373, pp. 1–56, Jan. 2010.
- [89] Y. Gu and G. Li, "Ionic Liquids-Based Catalysis with Solids: State of the Art," *Advanced Synthesis & Catalysis*, vol. 351, pp. 817–847, Apr. 2009.
- [90] J. Wilkes, "Properties of ionic liquid solvents for catalysis," *Journal of Molecular Catalysis A: Chemical*, vol. 214, pp. 11–17, May 2004.
- [91] C. M. Gordon, "New developments in catalysis using ionic liquids," *Applied Catalysis A: General*, vol. 222, pp. 101–117, Dec. 2001.
- [92] D. Zhao, M. Wu, Y. Kou, and E. Min, "Ionic liquids: applications in catalysis," *Catalysis Today*, vol. 74, pp. 157–189, May 2002.
- [93] J. Dupont, R. F. de Souza, and P. a. Z. Suarez, "Ionic liquid (molten salt) phase organometallic catalysis.," *Chemical reviews*, vol. 102, pp. 3667–3692, Oct. 2002.
- [94] K. Sahandzhieva and G. Maurer, "Phase equilibrium in systems with ionic liquids: An example for the downstream process of the Biphasic

- Acid Scavenging utilizing Ionic Liquids (BASIL) process. Part I: Experimental data,” *The Journal of Chemical Thermodynamics*, vol. 46, pp. 29–41, Mar. 2012.
- [95] G. Charles and R. Michelle, “Continuous carbonylation process,” *US 2003/0212295 A1*, 2003.
- [96] G. Tustin, “High Efficiency Methanol Carbonylation Process Utilising a Gas Stripped Reactor and Ionic Liquid Catalyst System,” in *EuChem: Conference on Molten Salts & Ionic Liquids, Copenhagen*, 2008.
- [97] J. Villadsen and H. Livejerg, “Supported Liquid-Phase Catalysts,” *Catalysis Reviews*, vol. 17, no. 1, pp. 203–272, 1978.
- [98] F. G. Sherif and L.-J. Shyu, “Alkylation Reaction Using Supported Ionic Liquid Catalyst Composition and Catalyst Composition,” 1999.
- [99] C. P. Mehnert, R. a. Cook, N. C. Dispenziere, and M. Afeworki, “Supported ionic liquid catalysis—a new concept for homogeneous hydroformylation catalysis,” *Journal of the American Chemical Society*, vol. 124, pp. 12932–12933, Nov. 2002.
- [100] M. H. Valkenberg, C. DeCastro, and W. F. Hölderich, “Friedel-Crafts acylation of aromatics catalysed by supported ionic liquids,” *Applied Catalysis A: General*, vol. 215, pp. 185–190, July 2001.
- [101] A. Riisager, K. M. Eriksen, P. Wasserscheid, and R. Fehrmann, “Propene and 1-Octene Hydroformylation with Silica-Supported, Ionic Liquid-Phase (SILP) Rh-Phosphine Catalysts in Continuous Fixed-Bed Mode,” *Catalysis Letters*, vol. 90, pp. 149–153, Oct. 2003.
- [102] M. Saffari Jourshari, M. Mamaghani, K. Tabatabaeian, and F. Shirini, “A convenient synthesis of novel 5-arylidene-2-imino-4-thiazolidinones using base supported ionic liquid-like phase (SILLP) as efficient green catalyst,” *Journal of the Iranian Chemical Society*, vol. 9, no. 1, pp. 75–80, 2012.

- [103] P. Lozano, E. Garcia-Verdugo, N. Karbass, K. Montague, T. De Diego, M. I. Burguete, and S. V. Luis, "Supported Ionic Liquid-Like Phases (SILLPs) for enzymatic processes: Continuous KR and DKR in SILLP-scCO₂ systems," *Green Chem.*, vol. 12, no. 10, pp. 1803–1810, 2010.
- [104] M. I. Burguete, H. Erythropel, E. Garcia-Verdugo, S. V. Luis, and V. Sans, "Base supported ionic liquid-like phases as catalysts for the batch and continuous-flow Henry reaction," *Green Chem.*, vol. 10, no. 4, pp. 401–407, 2008.
- [105] U. Kernchen, B. Etzold, W. Korth, and A. Jess, "Solid Catalyst with Ionic Liquid Layer (SCILL): A New Concept to Improve Selectivity Illustrated by Hydrogenation of Cyclooctadiene," *Chemical Engineering & Technology*, vol. 30, no. 8, pp. 985–994, 2007.
- [106] E. Paki, C. Roth, M. Lucas, and P. Claus, "How a Supported Metal Is Influenced by an Ionic Liquid : In-Depth Characterization of SCILL-Type Palladium Catalysts and Their Hydrogen Adsorption," *Journal of Physical Chemistry C*, vol. 114, pp. 10520–10526, 2010.
- [107] Y.-Y. Jiang, Z. Zhou, Z. Jiao, L. Li, Y.-T. Wu, and Z.-B. Zhang, "SO₂ Gas Separation Using Supported Ionic Liquid Membranes," *The Journal of Physical Chemistry B*, vol. 111, no. 19, pp. 5058–5061, 2007.
- [108] P. Scovazzo, A. E. Visser, J. H. Davis Jr., R. D. Rogers, C. A. Koval, D. L. DuBois, and R. D. Noble, *Supported Ionic Liquid Membranes and Facilitated Ionic Liquid Membranes*, ch. 7, pp. 69–87.
- [109] M. Sobota, M. Happel, M. Amende, N. Paape, P. Wasserscheid, M. Laurin, and J. Libuda, "Ligand Effects in SCILL Model Systems: Site-Specific Interactions with Pt and Pd Nanoparticles," *Advanced Materials*, vol. 23, no. 22-23, pp. 2617–2621, 2011.
- [110] J.-P. T. Mikkola, P. P. Virtanen, K. Kordás, H. Karhu, and T. O. Salmi, "SILCA: Supported ionic liquid catalysts for fine chemicals," *Applied Catalysis A: General*, vol. 328, pp. 68–76, Aug. 2007.

- [111] P. Virtanen, H. Karhu, K. Kordas, and J.-P. Mikkola, “The effect of ionic liquid in supported ionic liquid catalysts (SILCA) in the hydrogenation of α -unsaturated aldehydes,” *Chemical Engineering Science*, vol. 62, pp. 3660–3671, July 2007.
- [112] C. Van Doorslaer, J. Wahlen, P. Mertens, K. Binnemans, and D. De Vos, “Immobilization of molecular catalysts in supported ionic liquid phases,” *Dalton transactions (Cambridge, England : 2003)*, vol. 39, pp. 8377–90, Sept. 2010.
- [113] S. Werner, N. Szesni, A. Bittermann, M. J. Schneider, and P. H. “Screening of supported ionic liquid phase (silp) catalysts for the very low temperature water-gas-shift reaction,” *Applied Catalysis A: General*, vol. 377, no. 1-2, pp. 70 – 75, 2010.
- [114] J. Scholz, S. Loekman, N. Szesni, W. Hieringer, A. Görling, M. Haumann, and P. Wasserscheid, “Ethene-Induced Temporary Inhibition of Grubbs Metathesis Catalysts,” *Advanced Synthesis & Catalysis*, vol. 353, pp. 2701–2707, Oct. 2011.
- [115] S. Werner, N. Szesni, R. W. Fischer, M. Haumann, and P. Wasserscheid, “Homogeneous ruthenium-based water-gas shift catalysts via supported ionic liquid phase (SILP) technology at low temperature and ambient pressure,” *Physical chemistry chemical physics : PCCP*, vol. 11, pp. 10817–10819, Dec. 2009.
- [116] A. Riisager, R. Fehrmann, M. Haumann, and P. Wasserscheid, “Supported Ionic Liquid Phase (SILP) Catalysis : An Innovative Concept for Homogeneous Catalysis in Continuous Fixed-Bed Reactors,” *Topics in Catalysis*, vol. 40, no. November, pp. 91–102, 2006.
- [117] A. Chrobok, S. Baj, W. Pudo, and A. Jarzabski, “Supported ionic liquid phase catalysis for aerobic oxidation of primary alcohols,” *Applied Catalysis A: General*, vol. 389, pp. 179–185, Dec. 2010.
- [118] J. Joni, M. Haumann, and P. Wasserscheid, “Continuous gas-phase isopropylation of toluene and cumene using highly acidic Supported

- Ionic Liquid Phase (SILP) catalysts,” *Applied Catalysis A: General*, vol. 372, pp. 8–15, Jan. 2010.
- [119] M. Jakuttis, A. Schönweiz, S. Werner, R. Franke, K.-D. Wiese, M. Haumann, and P. Wasserscheid, “Rhodium-Phosphite SILP Catalysis for the Highly Selective Hydroformylation of Mixed C(4) Feedstocks.,” *Angewandte Chemie (International ed. in English)*, pp. 4492–4495, Apr. 2011.
- [120] M. Haumann, M. Jakuttis, R. Franke, A. Schönweiz, and P. Wasserscheid, “Continuous Gas-Phase Hydroformylation of a Highly Diluted Technical C4 Feed using Supported Ionic Liquid Phase Catalysts,” *ChemCatChem*, Oct. 2011.
- [121] E. Öchsner, M. J. Schneider, C. Meyer, M. Haumann, and P. Wasserscheid, “Challenging the scope of continuous, gas-phase reactions with supported ionic liquid phase (SILP) catalysts: Asymmetric hydrogenation of methyl acetoacetate,” *Applied Catalysis A: General*, vol. 399, pp. 35–41, Mar. 2011.
- [122] F. Kohler, D. Roth, E. Kuhlmann, P. Wasserscheid, and M. Haumann, “Continuous gas-phase desulfurisation using supported ionic liquid phase (SILP) materials,” *Green Chemistry*, vol. 12, no. 6, p. 979, 2010.
- [123] R. Lowry and A. Aguilo, “Acetic acid today,” *Hydrocarbon processing*, vol. 53, no. 11, pp. 103–113, 1974.
- [124] R. Schultz, “Vapor phase carbonylation of methanol to acetic acid,” *Journal of Catalysis*, vol. 13, pp. 105–106, Jan. 1969.
- [125] G. C. Tustin, “Carbonylation process,” *US 7253304*, 2007.
- [126] J. L. Anthony, J. L. Anderson, E. J. Maginn, and J. F. Brennecke, “Anion effects on gas solubility in ionic liquids.,” *The journal of physical chemistry. B*, vol. 109, pp. 6366–6374, Apr. 2005.

- [127] J. K. Shah and E. J. Maginn, "Monte Carlo simulations of gas solubility in the ionic liquid 1-n-butyl-3-methylimidazolium hexafluorophosphate.," *The journal of physical chemistry. B*, vol. 109, pp. 10395–10405, May 2005.
- [128] A. a. Oliferenko, P. V. Oliferenko, K. R. Seddon, and J. S. Torrecilla, "Prediction of gas solubilities in ionic liquids.," *Physical chemistry chemical physics : PCCP*, vol. 13, pp. 17262–17272, Oct. 2011.
- [129] L. F. Vega, O. Vilaseca, F. Llovel, and J. S. Andreu, "Modeling ionic liquids and the solubility of gases in them: Recent advances and perspectives," *Fluid Phase Equilibria*, vol. 294, pp. 15–30, July 2010.
- [130] U. Domanska and U. Domanska, "Solubilities and thermophysical properties of ionic liquids," *Pure and Applied Chemistry*, vol. 77, no. 3, pp. 543–557, 2005.
- [131] S. Ren, Y. Hou, W. Wu, and W. Liu, "Purification of Ionic Liquids: Sweeping Solvents by Nitrogen," *Journal of Chemical & Engineering Data*, pp. 0–3.
- [132] D. Camper, P. Scovazzo, C. Koval, and R. Noble, "Gas Solubilities in Room-Temperature Ionic Liquids," *Industrial & Engineering Chemistry Research*, vol. 43, pp. 3049–3054, June 2004.
- [133] A. W. Taylor, P. Licence, and A. P. Abbott, "Non-classical diffusion in ionic liquids.," *Physical chemistry chemical physics : PCCP*, vol. 13, pp. 10147–10154, June 2011.

Appendix A

Experimental Synthesis

All of the catalysts used during this project were synthesised in house. All syntheses were carried out using standard schlenk techniques.

The original synthesis as published by Riisager *et. al.*¹¹⁶ was the basis for all catalyst syntheses. This procedure was then adapted in line with the catalyst being prepared.

A.1 The basic procedure

For preparation of a 0.65 wt% Rh and 42 vol% IL catalyst.

16.5 mg $[\text{Rh}(\text{CO})_2\text{I}]_2$ (0.029 mmol) and 0.3025 g Bmim I (1.137 mmol) are dissolved in 8 mL degassed anhydrous methanol (Aldrich, 99.8%) in a 30 mL Schlenk tube under argon atmosphere and stirred for 24 h at room temperature. 0.600 g calcined (500°C, 15 h, air) silica support (silica gel 100, Merck) was added (under argon). The suspension was left with slow stirring for another 4 h. The methanol was then removed under reduced pressure at room temperature, leaving the SILP catalyst behind as a red-brownish crystal powder which is further dried under vacuum at 60°C for 24 h. Yield approximately 0.9 g.

The prepared SILP remained stable when stored under CO atmosphere at room temperature. Under Ar atmosphere, the catalyst did not degrade

immediately, but after one week a significant darkening of the catalyst could be observed.

A.2 Variations

Drying

Initially after noticing the colour change during the loading of a fresh catalyst, we reduced the final drying period from 24 h to the time taken to visibly dry the catalyst. This change did not result in any differences in catalyst performance and allowed us to significantly reduce the synthesis time for each new catalyst from just over 1 day to a few hours.

CO atmosphere

Once it was decided to try and carry out the synthesis under a CO atmosphere, a number of safety precautions were required to be implemented. Installation of a permanent CO detector was carried out in the room combined with usage of hand-held CO detectors. Initially the flow of CO was controlled by the regulator on the gas flask, but it was quickly discovered that this was highly impractical. It was then decided to make use of an excess GMFC and control box to better control the CO flow and make the system safer. By this usage of the GMFC it became possible to feed a controlled flow of CO into the schlenk lines instead of having to alter the tubing from the more commonly used Ar to CO and back again whenever catalyst synthesis was required.

Rh source and loading

Once it was decided to explore the effect of Rh loading and rhodium source, the mass of Rh given in the procedure was no longer relevant. Initially variation in the Rh loading was defined in terms of the original procedure, such that 1.3 wt% was in fact 2x Rh loading. This was used in order to make it easier to determine the relevant mass of the Rh precursor that was needed

to prepare the catalyst. When the Rh source was altered, it was important to incorporate the new molecular weight into calculations when preparing the catalyst.

Alternative Supports

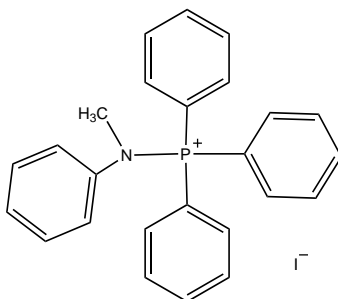
Initially Merk silica was used, but it was decided to switch to support materials supplied by Wacker Chemie AG. This would allow us to synthesis SILPs closer to those that would be used in the Wacker Chemie AG test reactor. The supplied supports were powdered and sieved to obtain particles of a uniform size. The material was then calcined (500°C, 15 h, air) and used as previously described.

Ionic Liquid Loading

All of the ILs tested were used gravimetrically. As such the mass of the ILs used was constant (with the exception of those experiments looking at IL loading). Volume % loadings were calculated on the assumption of the ILs having a standard density, $\rho = 1.2$ g/ml and the silica having a pore volume of $1\text{cm}^3/\text{g}$.

A.3 Ionic Liquids

All imidazolium, pyridinium and guanidinium based ILs were synthesised in house according to the procedures published in literature.



(N-Methyl-N-phenylamino)triphenylphosphonium iodide structure

PPh_3MeI was synthesised by the author and all other phosphonium salts were purchased as listed below.

Cytec: PBu_4I , PPr_3MeI , PBu_4Br

TCI: EtPh_3PI , Ph_4PI , $i\text{-PrPh}_3\text{PI}$, (N-Methyl-N-phenylamino)triphenylphosphonium iodide, above.

PPh_3MeI Synthesis:

PPh_3 (1g) was added to 1ml of MeI in dichloromethane. The solution was then stirred at room temperature for 24 h. After this the dichloromethane was removed under vacuum.

Appendix B

Components Listing

The following components were used during the construction of the system.

Flow Control System

GMFC: High-Tech El-Flow from Bronkhorst. Model:
F-211CV-500-AAD-22V. Supplied by Insatech.

LMFC: High-Tech Liqui-Flow from Bronkhorst. Model:
L13-AAD-22-K/10S Supplied by Insatech.

CEM: High-Tech CEM System from Bronkhorst. Model: W-202A-222-K.
Supplied by Insatech.

Control Box: High-Tech E-7000 flow-bus system from Bronkhorst. Model:
E-7300-04-01-34-AAA. Supplied by Insatech.

Pressure Regulation System

Pressure valve: Samson back pressure regulating valve composed of the
following components.

Actuator type 3277-5

I/P Positioner type 3730-2

Connection plate 1400-7462 for a 3730-positioner on a rotary actuator

Fitting 1400-7452 for a 3730-positioner on 2775-5/20cm²

Regulator pin fitting: Initially $Kvs = 0.001$, later changed to $Kvs = 0.00063$

Pressure Regulator: Samson PID regulator 6493 Trovis. Model: EB 6493-1 EN

Pressure Transducer: Wikia general purpose pressure transducer. Model: S-10

Check valve: Hoke right angle relief valve. Model: R6000. Cracking pressure set to 30 bars

Manometers: 0 - 40 bars range from Stewart Buchanan, UK

Heating Components

Heating Tapes: IT-G25 models from Isopad. Supplied by Teknordic ApS

Heating Cables: HSTD models from Horst GmbH. Supplied by Lund and Sørensen.

Real time temperature readout: DP460 model readout from Omega Ltd.

Set-Up heating Control: Six-zone PID Controller from Omega Ltd. Model: CN616

Thermocouples: All thermocouples were K-type and used quick-disconnect mini-connectors.

Cooling:

Fixed -20°C cryostat: Haake model EK20

Variable cryostat with pump: Julabo F12

Assorted

Labview controller: National Instruments USB-6008/6009 USB to component connector

HPLC Pump: Knauer pump 100. Fitted with 10ml ceramic pump heads.

CO/CH₄ supply: Linde Gas AGA. 10vol% CH₄ in CO. Max uncertainty $\pm 2.0\%$

Rh source - from various sources, collected by AR

MeI: CAS: 74-88-4 ReagentPlus 99% Sigma

MeOH: CAS: 67-56-1 puriss \geq 99.7%

2-methoxyethanol (initial ITSD) 109-86-4 ReagentPlus \geq 99.0%

GC Columns Analysis:

Component list: GC model: Agilent 7890A Series GC (G3440A)

Columns: HayeSep Q XX (7890-0182)

MolSieve 5A XX (7890-0197)

DB-FFAP 30m, 0.53mm, 1.00 μ m (125-3232)

HP-PLOT-Q 30m, 0.53mm, 40 μ m (19095P-QO4)

Gas supply: N₂ 5.0

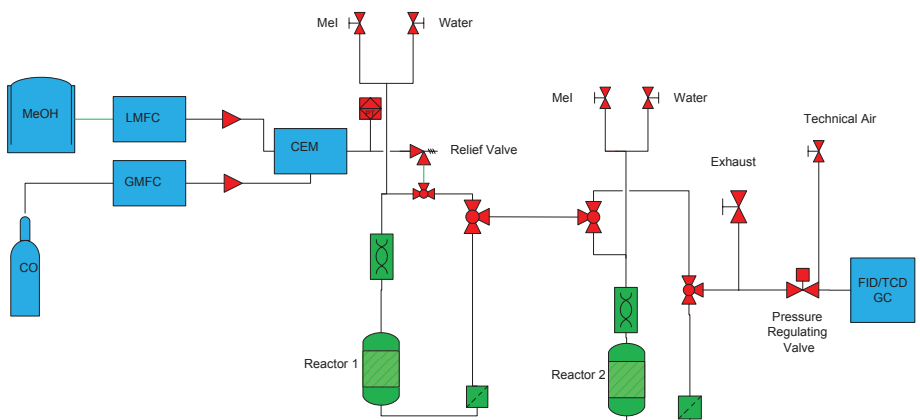
He 5.0

Technical air

H₂ 3.7

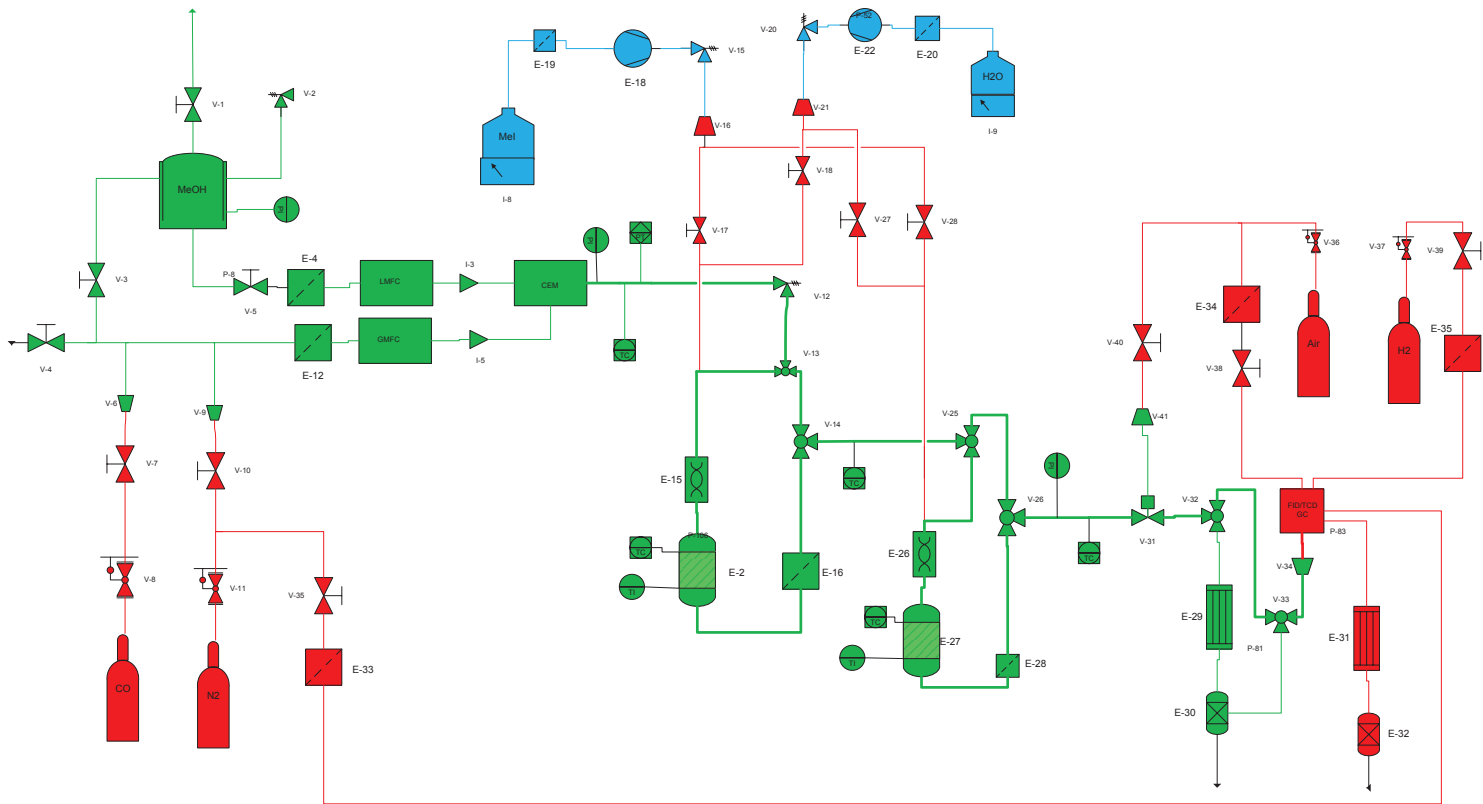
Appendix C

Evolution of the test rig over the course of the Project

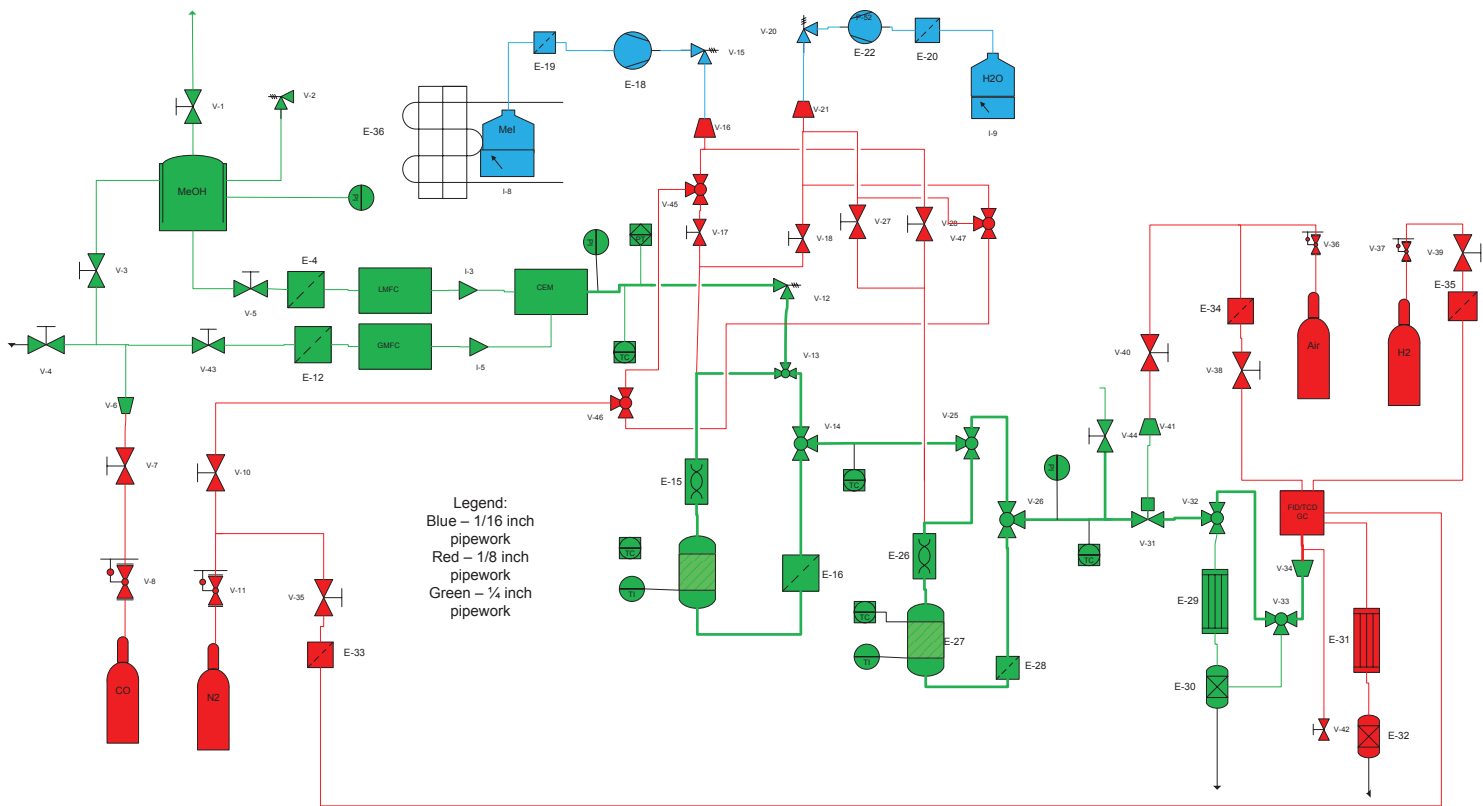


Simplified Process Flow Sheet for System

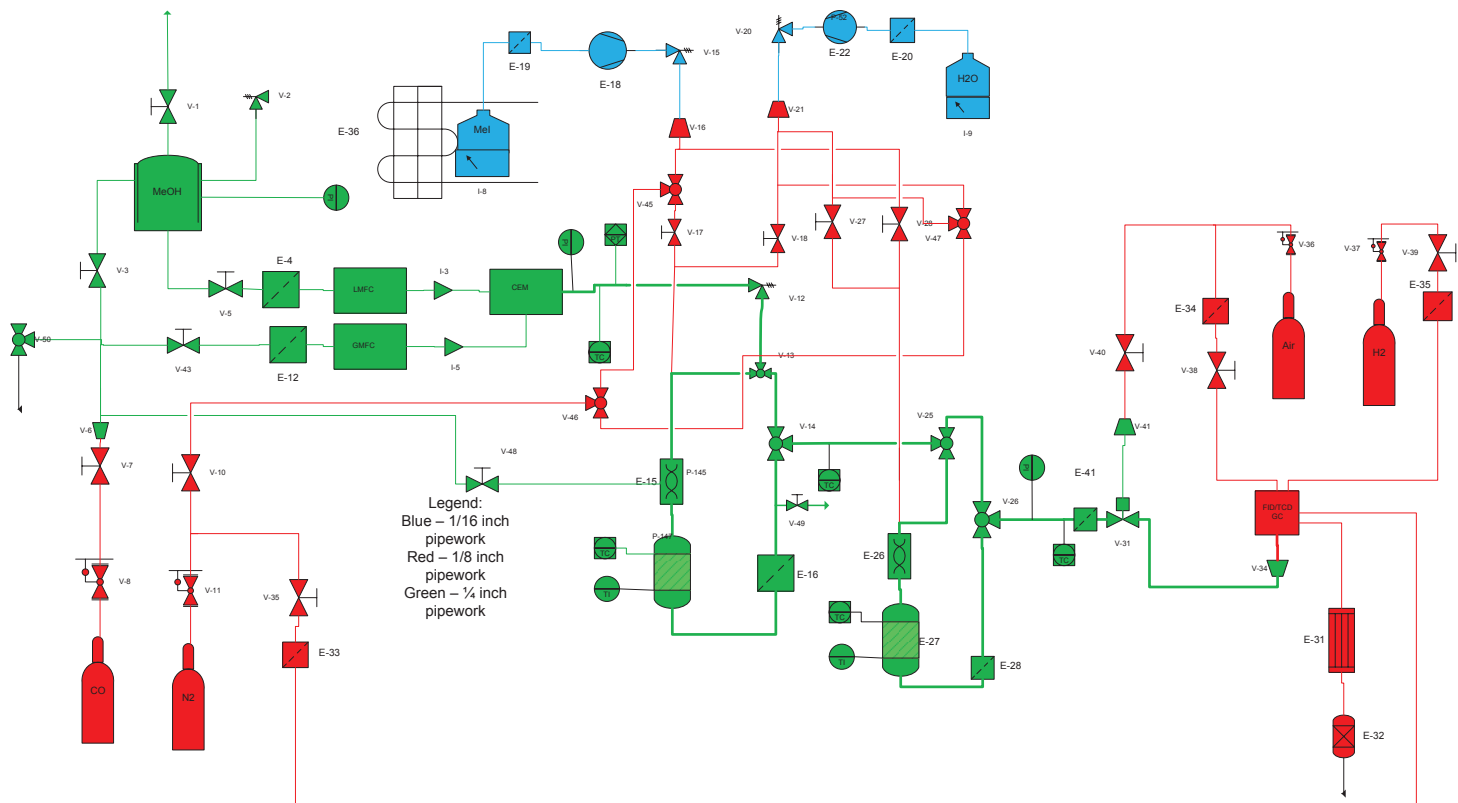
Original Process Flow Sheet



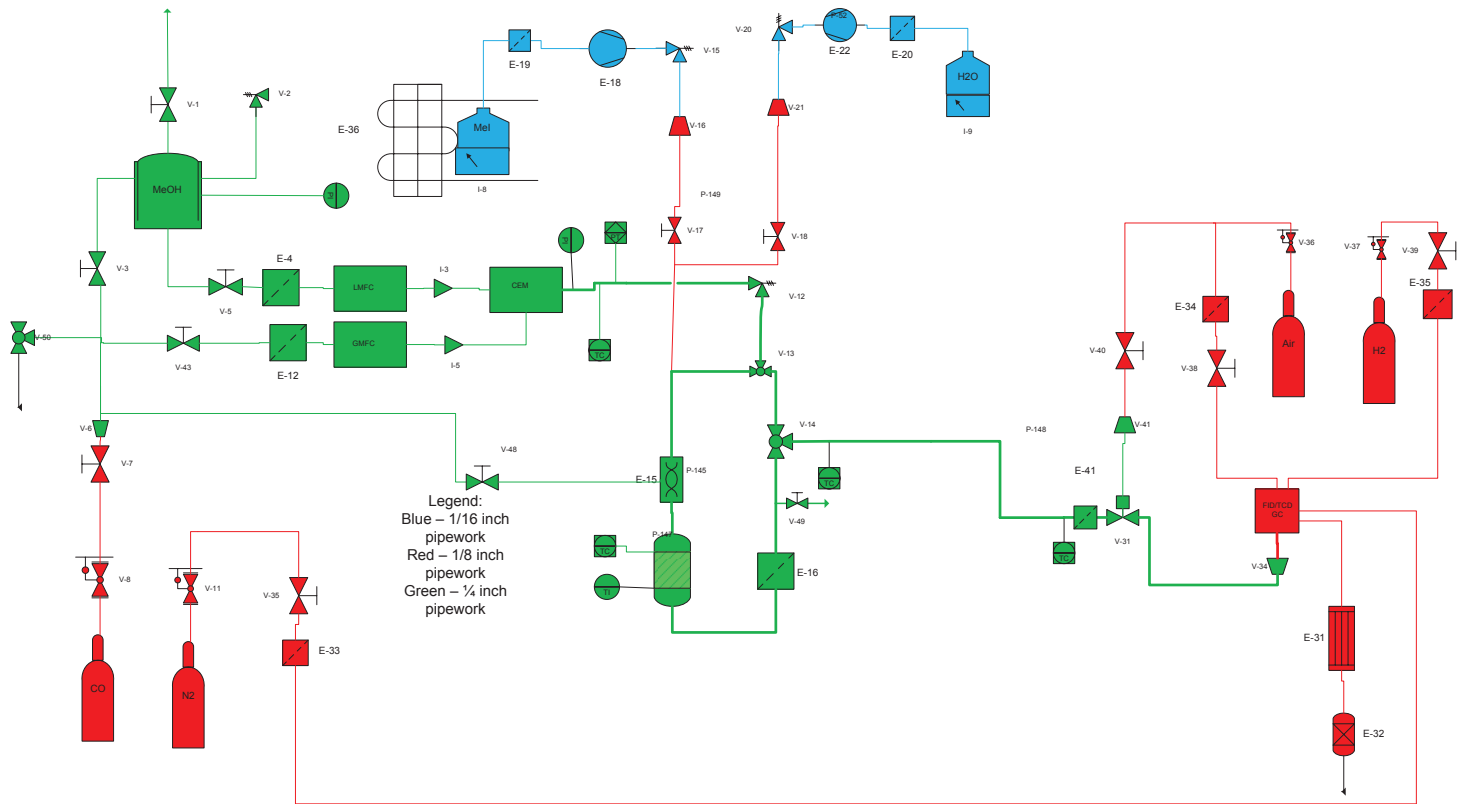
Second Iteration of Process Flow Sheet



Third Iteration of the Process Flow Sheet

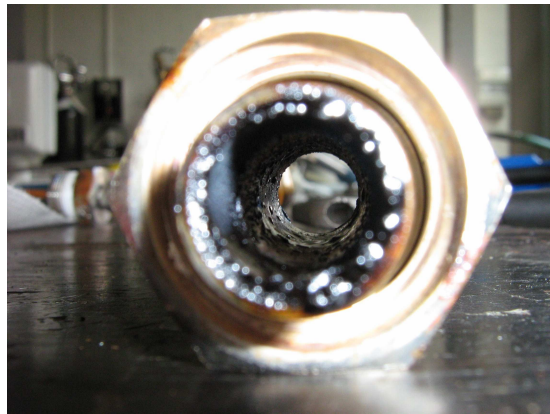


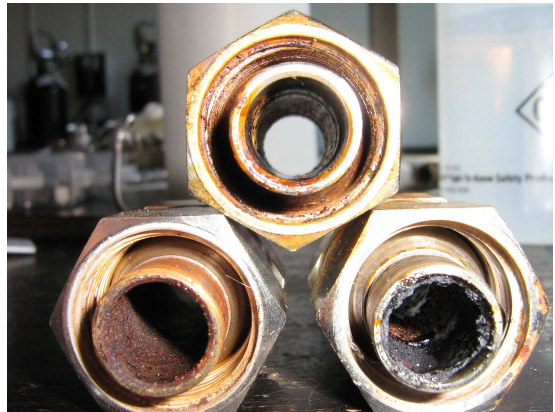
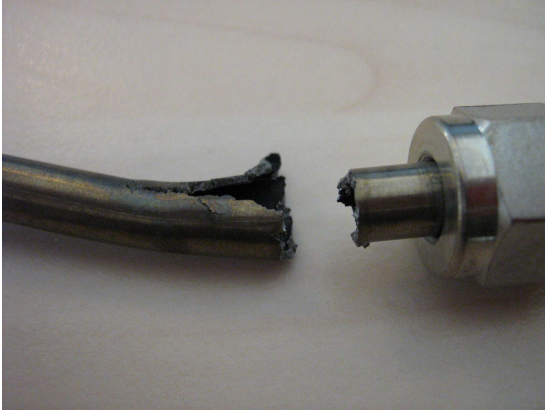
Final Version of the Process Flow Sheet

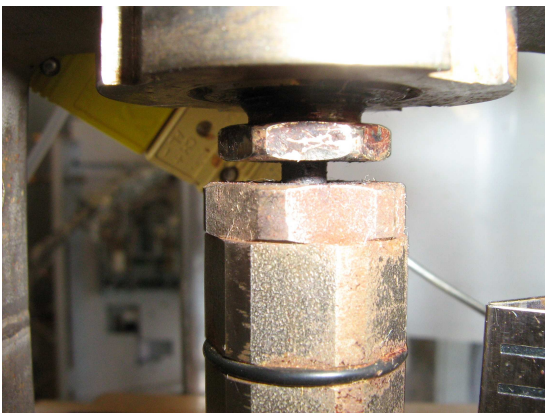
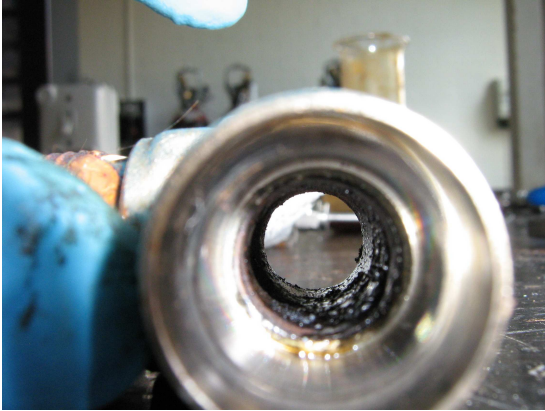


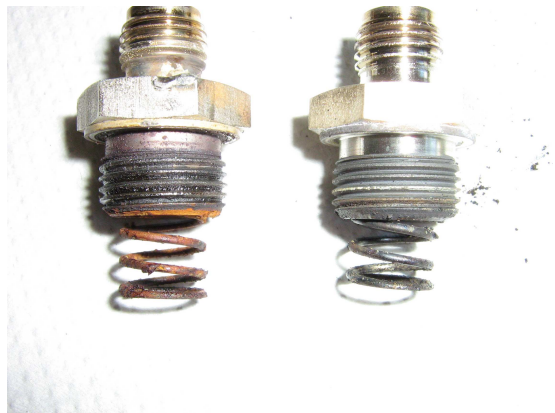
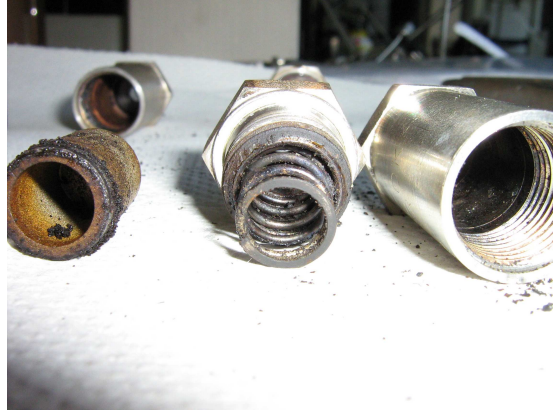
Appendix D

Examples of Corrosion Experienced











Appendix E

Comparison of Various Steel Types

Metal	316 SS	316 Ti	Hasteloy C-22	Alloy 400	2RK65
Carbon	0.08 max	0.0-0.08	0.010 max	0.3 max	0.020 max
Manganese	2.00 max		0.50 max	2.0 max	1.8
Phosphorus	0.045 max	0.00-0.05			0.025 max
Sulphur	0.030 max	0-0.03		0.024 max	0.015 max
Silicon	0.75 max			0.50 max	0.5
Chromium	16.00-18.00	16.00-18.00	22		20
Nickel	10.00-14.00	10.00-14.00	56-balance	63.0 min	25
Molybdenum	2.00-3.00	2.00-3.00	13		4.5
Nitrogen	0.10 max				0.06
Iron	balance	balance	3		
Titanium		0.0-0.70			
Tungsten			3		
Copper				28-34	1.5
Density (g/cm ³)	8	8	8.69	8.8	8
Tensile Strength (MPa)	515	485	690	482-586	520-720

Appendix F

Exposure of a MeOH wetted,
Bmim I/[Rh(CO)₂I₂]⁻ SILP to
air over a period of 1 hour



T = 1min 07s



T = 1min 43s



T = 2min 14s



T = 5min 35s



T = 5min 45s



T = 6min 29s



T = 11min 42s



T = 12min 47s



T = 14min 11s



T = 14min 51s



T = 15min 39s



T = 15min 41s



T = 23min 22s



T = 30min 03s



T = 30min 05s



T = 31min 31s



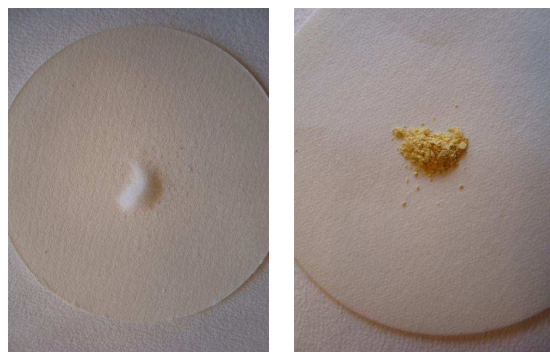
T = 35min 39s



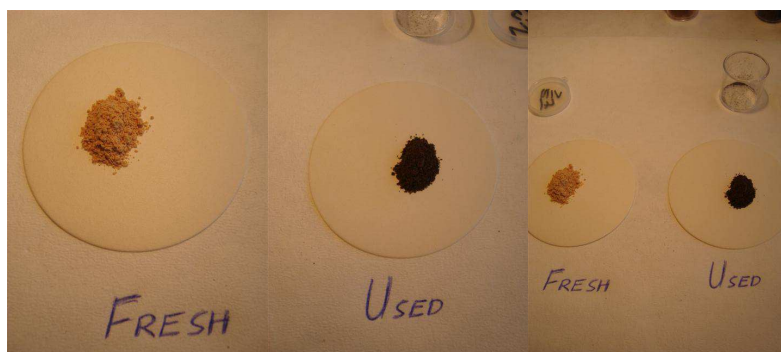
T = 54min 34s

Appendix G

Fresh and Used Examples of SILP Catalysts



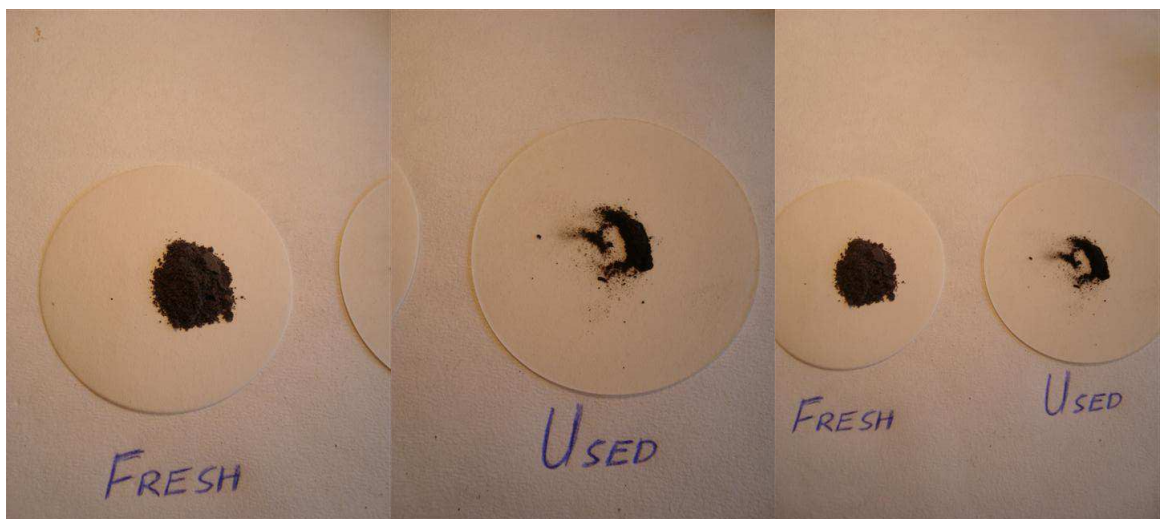
Pure Silica and Silica coated in 30 vol% BmimI



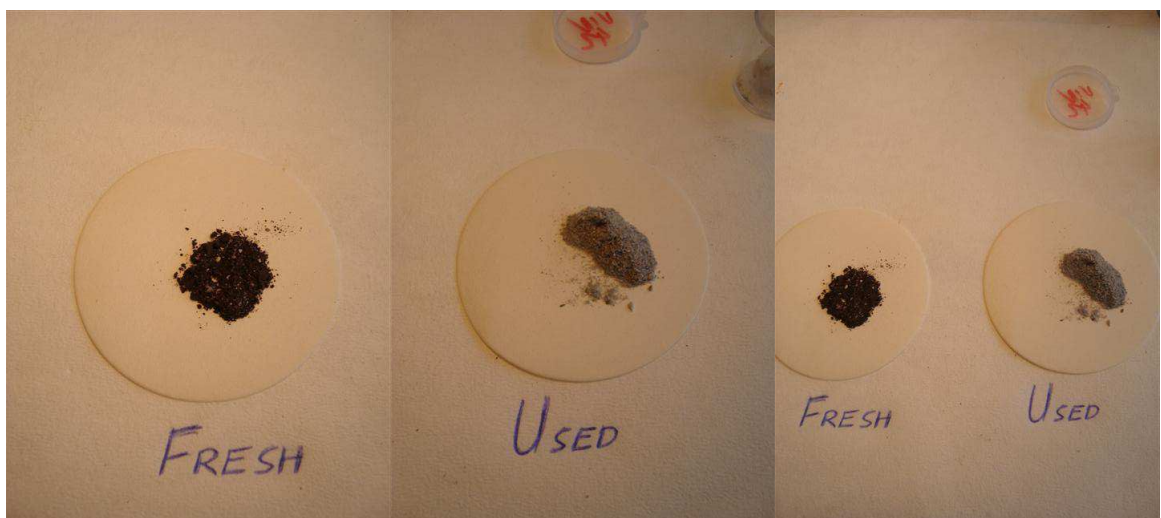
$[\text{Rh}(\text{CO})_2\text{Cl}]_2$ (2.5 wt%) on Silica with no Ionic Liquid



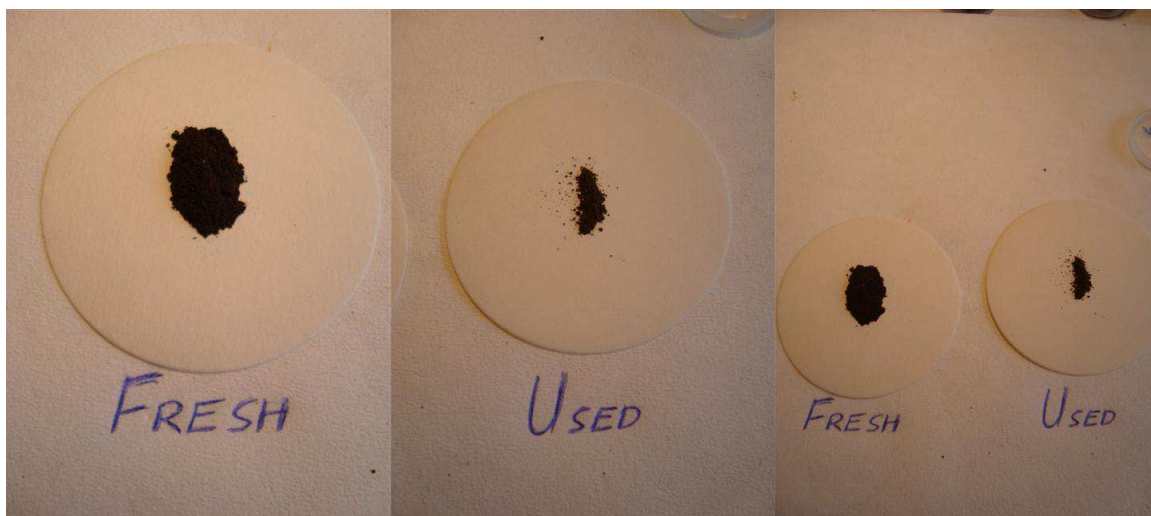
2.5 wt% $[\text{Rh}(\text{CO})_2\text{Cl}]_2$ with 30 vol% Bmim OH



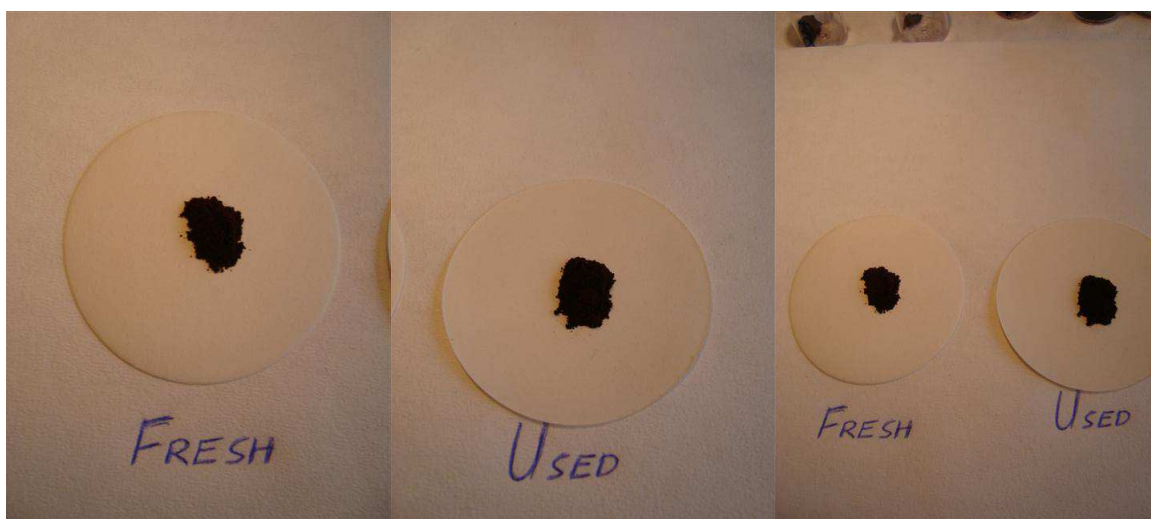
3.3 wt% $[\text{Rh}(\text{CO})_2\text{Cl}]_2$ with 30 vol% Bmim I



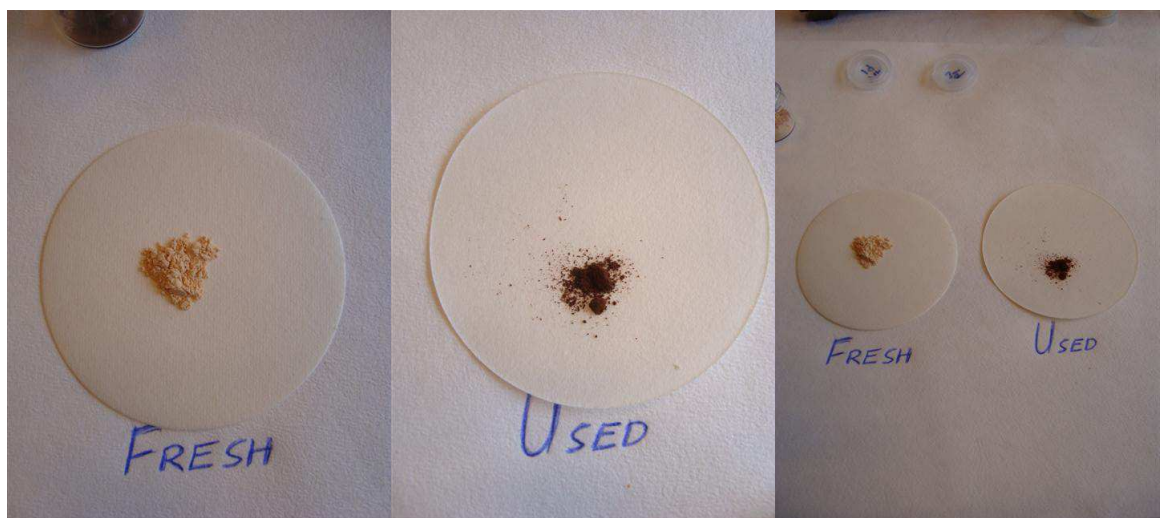
2.5 wt% $[\text{Rh}(\text{CO})_2\text{Cl}]_2$ with 30 vol% $\text{Ph}_3\text{MeP I}$



2.5 wt% $[\text{Rh}(\text{CO})_2\text{Cl}]_2$ with 7.5 vol% $\text{Bu}_3\text{MeP I}$



2.5 wt% $[\text{Rh}(\text{CO})_2\text{Cl}]_2$ with 15 vol% $\text{Bu}_3\text{MeP I}$



4.4 wt% IrI₄ with 30 vol% Bmim I